

P I S T O N - R I N G L U B R I C A N T
F A I L U R E I N
D I E S E L E N G I N E S

Robert D. Wing, M.Sc., B.Sc., D.I.C., A.C.G.I.

Thesis submitted for the degree of
Doctor of Philosophy in the Faculty of Engineering,
University of London.

Department of Mechanical Engineering
Imperial College of Science and Technology
London.

May 1969

ABSTRACT

This work reports on a study made of lubrication problems of the piston rings in diesel engines. Designs of piston rings even today tend to be based on the accumulation of "rule of thumb" guides collected over many years of engine usage. The upper and lower temperature limits of piston ring operation are well known from such practical experience, but it was considered that close inspection of the thermal and vibrational behaviour of piston rings using sophisticated instrumentation would greatly increase our understanding of the mechanism of ring lubrication and the causes of its breakdown.

The results, taken from a variety of miniature temperature and proximity transducers, show that the lubricant in the region of the uppermost ring is cyclicly subjected to large temperature transients on the expansion stroke of the diesel cycle. From these results a postulation is drawn of the probable causes of piston ring failure from 'gumming' of the lubricant, and some conclusions made concerning the variation of oil-film thickness between ring and liner during the working cycle.

ACKNOWLEDGMENTS

The author wishes to express sincere thanks to -

- The Admiralty, who generously supported this work, and their representatives Miss E.J. Macnair, Mr. S. Bolshaw and Mr. W.E. Elford whose technical direction was of enormous assistance.
- Professor Sir O.A. Saunders, whose direction of the project has ensured its satisfactory progress, and to the following members of the staff of Imperial College whose experience and guidance have been invaluable ...
Mr. N.P.W. Moore, Mr. J.C. Lewis, Professor W. Murgatroyd, Dr. A. Cameron, Dr. G. Karim, Dr. P.H.G. Allen and the many technicians who have assisted in the construction and operation of the apparatus.
- The following representatives from industry, whose generous co-operation has given much impetus to the work ...
Mr. V. O'Donoghue of Analog Devices Ltd., Richmond, Surrey.
Mr. H. Strauch of Associated Engineering Ltd., Rugby.
Mr. J. Hempson of Ricardo and Co. Ltd., Shoreham-by-Sea.
Mr. M. Hillier of Services Electronics Research Lab., Baldock.
Mr. R. Chapple of Comark Electronics, Littlehampton.
- Dr. Ing. Carl Englisch, whose comprehensive assistance in surveying Continental developments was exceptionally kind.
- Mrs. R. Cook for patient assistance in translation of the many German texts, and to Mrs. P. Hills for typing the final result.

TABLE OF CONTENTS

	<u>Page</u>
Abstract	2.
Acknowledgements	3.
Contents	4.
Nomenclature	5.
List of figures	6.
List of plates	8.
List of tables	9.
Introduction	10.
Theoretical considerations	19.
Experimental apparatus	31.
i. Engine rig	
ii. Piston linkage	
iii. Electronic instrumentation	
iv. Recording system	
Experimental results	56.
Analysis and discussion	64.
Conclusions	77.
References	79.
Appendix I - Design and construction of thin film thermocouples	84.
Appendix II - Amplifier design for thin film thermocouples	91.
Appendix III - Design of piston linkage	96.
Appendix IV - Supplementary instrumentation for engine rig	101.
Tables	113.
Figures	115.
Plates	146.

NOMENCLATURE

A	-	piston-ring face area
B	-	axial width of piston-ring = 2b.
D	-	diameter
F	-	viscous friction force
h	-	oil film thickness (ring to liner)
k	-	thermal conductivity
L	-	length of connecting rod
N	-	crankshaft speed
p	-	mean pressure on ring face
R	-	electrical resistance
R_c	-	crankshaft radius
R_r	-	radius of curvature of parabolic ring face
T	-	temperature
U	-	linear velocity / piston speed
V	-	velocity
x,y,z	-	co-ordinate directions
τ	-	time constant
η	-	viscosity coefficient
θ	-	crankshaft angle
ρ	-	density
μ	-	lubricant viscosity
ω	-	frequency

LIST OF FIGURES

1. Variation of top piston ring temperature with fuel delivery rate for a variety of diesel engine types and sizes.
2. Cyclic variations in piston ring temperature as measured by Eichelberg.
3. Theoretical surface temperatures (after Nepodog'ev & Podvalnyi).
4. Factors affecting oil film temperature fluctuations.
5. Fuel, Oil, and Water circuits of test-bed.
6. Overload protection circuits.
7. Compressed-air loaded piston contacts.
8. Thin-film and bead thermocouple circuits.
9. Vibration transducers and associated circuitry.
10. Vibration transducer positioning and calibration markings for measurement of oil-film thicknesses.
11. Piston instrumentation layout.
12. Data recording layout.
13. Symbols used in the following oscilloscope records.
14. Bead thermocouple results.
15. Multiple exposures of temperature peaks for statistical analysis.
16. Records showing repeatability of results, and typical film thermocouple recordings.
17. Steady temperature levels as recorded over full range of engine power.
18. Subtraction of vibration signals to estimate oil-film thickness.

LIST OF FIGURES (CONT'D)

19. Oil film thickness variation with engine crank angle.
20. Amplitude of temperature transients as function of b.m.e.p.
21. Calibration curve of nickel-iron thermocouples.
22. Thermocouple amplifier, System I.
23. Thermocouple amplifier, System II.
24. Thermocouple amplifier, System II, circuit layout.
25. Piston linkage - sectional view through piston strut.
26. Piston linkage - connections to outer arms.
27. Piston linkage - outer connection box and tensioning mechanism.
28. Dynamometer load cell circuit.
29. Thermocouple reference oven circuit.
30. Typical calibration curves of A.E. miniature inductive transducers.
31. Thermal and drift stability of A.E. vibration measuring system.

LIST OF PLATES

- Plate 1. - General view of engine test-bed
2. - Front view of test-bed showing rotary switchgear and linkage attachment boxes.
 3. - Test-bed services and dynamometer with gas supply connected.
 4. - Instrumentation and data recording facility.
 5. - Linkage attachment box, modified injector pump bracket, and gas supply regulator.
 6. - Photoelectric disc for crank-angle degree marker.
 7. - Complete piston linkage before attachment.
 8. - Partially wired piston and linkage showing one patchboard uncovered.
 9. - Flexible printed circuit for piston wiring.
 10. - Partially wired piston with flexible circuit and some wiring in position.
 11. - Displacement transducers shown against segment of piston.
 12. - Plating rig for Nickel coating of thin-film thermocouples.
 13. - Enlargement of Nickel coated thermocouple front surface.
 14. - Thin-film and bead thermocouples shown against segment of piston.
 15. - Thermocouple reference oven before assembly into piston.
 16. - Reference thermocouple capsule before assembly into reference oven.

LIST OF TABLES

- Table 1. - List of engine trials and their main features.
2. - Temperature transient and oil-film thickness measurements.

INTRODUCTION

As technological advances are now giving us the benefits of increased output from a given size of diesel engine, it is inevitable that certain internal parts of the engine are being strained to their limits. Piston rings, the mechanical and thermal loadings of which become greatly increased by techniques such as supercharging, are amongst the more important engine components which are causing serious difficulties.

High wear rates, scuffing, poor sealing, and even breakages are becoming all too common phenomena of the contemporary diesel engine.

The research programme undertaken was organised and supported by the British Admiralty, who have been actively concerned with piston ring lubrication as a result of many difficulties with the rings of certain of their highly rated diesel engines.

The experimental complexities in making quantitative measurements of the behaviour of piston rings are so involved that even today we know surprisingly little about the basic behaviour and properties of piston rings under operating conditions. Marine applications of diesel

engines represent one of the most arduous load cycles, in their requirement for sustained use of the engines full output. An especially common problem encountered with this type of operation is the 'gumming' of the upper rings in their grooves, the apparent result of a gradual build-up of decomposed fuel and lubricant particles. Hot products of combustion and unburned fuel particles are presumably carried down the side walls of the piston during each expansion stroke and the resultant effects of such temperature and contamination transients were considered to be a possible key to the mechanism of ring 'gumming'.

The literature covering this aspect of engine lubrication is sparse, and largely of a conjectural nature. Despite the scarcity of experimental data taken from engines whilst in operation, much information has been collected from the examination of dismantled engines that have failed or proved unsatisfactory in service. The greatest volume of work, and perhaps the most authoritative, appears in the publications of Englisch. (1,2,3,4,5,6,7)*

* A list of references is given on pages 79 - 83.

Current knowledge of the operating temperature limits in the ring region of Diesel pistons taken from service records has been presented by a number of investigators, as for example in the following condensed quotation from Englisch (1)

'It is generally advised that the metal parts in contact with the piston rings must not exceed 190°C . In marine usage, from the experience of engines under continuous loading, the temperatures must not exceed 180°C . In the case of discontinuous loads, such as in locomotives and auxiliary power units, 200°C may be permitted.

If the temperature rises above these limits the oil loses its lubricating ability and the oil film breaks down.

If the temperature of the parts in contact with the rings is too low when operating with poor fuel the sulphuric acid contained in the products of combustion will condense. In this case corrosion results, the reaction between the acid condensate and the alkalies contained in the lubricating oil bringing about cumulative corrosion of the rings.

The result of these observations is that there are definite upper and lower temperatures between which the parts in contact with the rings must be operated.' *

It may be seen from these remarks that the temperature limits are critical, and in highly rated machines the closeness to which the upper limits may be approached is a decisive factor in the overall performance of the engine.

Temperatures in engine pistons and their rings have been measured by many previous workers, using a variety of experimental techniques. Due to the inherent inaccuracies

* Translated and condensed from the original French.

of the types of temperature sensors generally used, and various experimental problems involving data recovery from within operating engines, these have only given an outline of the temperature conditions in the ring regions of pistons.

Janota⁽⁸⁾, Ip⁽⁹⁾, Keig⁽¹⁰⁾, Fitzgeorge⁽¹¹⁾, and Britain⁽¹²⁾ have successfully used fusible plug and hardness-recovery techniques to measure running temperatures in pistons, and their methods are in general use for analysis of operating temperatures. The main objection to such results is that they show only time-integrated mean temperatures for the hottest running condition attained during any engine trial. Restricting our attention to the ring-belt of diesel pistons, it was considered that the thermal conditions of the lubricant around the piston rings would be far from steady when considered on a cyclic basis. The quantities of gas passing through the ring belt should be small, but the upper ring will certainly be exposed to pressure and temperature changes due to the combustion process. Englisch⁽²⁾ speaks of a "fire-ray" passing down the side of the piston,

but any combustion would certainly be quenched in this relatively cool restricted space. However, it seems probable that hot products of combustion will be driven by the combustion pressure down into the clearance between piston and cylinder, and depending on the magnitude of this effect, cyclic variations in the lubricant and component-surface temperatures will result.

Eichelberg⁽¹³⁾, and more recently Whitehouse⁽¹⁴⁾ and Fujita⁽¹⁷⁾ using thermocouples have measured the cyclic variations of piston surface temperatures, but restricted the measurements to the crowns of pistons. Their main objective was to determine the fluctuating stresses superimposed on piston crowns by the heat transfer from the combustion process. Results of these experimenters all indicate that the temperature fluctuations during each engine stroke are confined to a depth of only a few millimetres below the piston surface, also that the positive variation (during the firing stroke) is of greater amplitude than the negative variation. This effect is the result of the higher coefficient of heat transfer between the gases and the piston during the combustion period when the pressures and temperatures are high and when there is considerable

turbulence. In the case examined by Whitehouse⁽¹⁴⁾, in which the fatigue strength of a cast aluminium alloy piston was marginal, it appeared that the stresses brought about by temperature fluctuations on the piston crown could explain service failures.

The fact that transient temperatures in the region of the top piston ring have never been measured prompted this research work, in an effort to discover whether temperature transients such as those recorded in the main combustion region exist in the region of the piston rings, and whether they are of sufficient magnitude to explain failure of the lubricant in service.

Contemporary work in assessing upper piston-ring operating temperatures has led to some confusion, in that the slow response or mean-temperature indicating methods have in many cases indicated that the lubricant around the upper rings is operating at a safe temperature, whereas 'gumming' of these pistons in service suggests that higher temperatures than those measured have been experienced in these regions. Such results, and in particular those collected from "Deltic"* pistons in Admiralty

* a highly rated opposed piston two-stroke engine originally designed for marine propulsion.

service led to the supposition that the oil in the region of the upper rings is subjected to rapid cyclic peaks of high temperature, thus causing its gradual decomposition. The cyclic variations, having durations of far less than one engine cycle, would give no indication on slow-response temperature indicating instruments.

As may be seen, precise knowledge of the mechanism of piston ring 'gumming' and a number of other phenomena associated with ring lubrication is slight. Another point, which has been a topic of great academic and practical interest for many years, is the assessment of the thickness of the oil film between piston ring and liner and its variation during the engine cycle. Estimates of this oil film thickness vary greatly, being based on several differing theoretical presumptions. Fogg⁽¹⁹⁾, using the variable density or 'thermal wedge' theory of parallel surface thrust bearings predicts ring-to-liner oil film thicknesses of the order of 1-2 microns. Den Besten⁽²⁰⁾, using Fogg's analysis points out that the mechanism of lubrication of the piston ring - bore assembly varies through the piston stroke. Normally we can expect boundary lubrication at the outer dead centres, and a form of hydrodynamic lubrication through

the centre of the stroke. Considerably thicker mean oil-film thicknesses were arrived at by Eilon and Saunders ⁽²¹⁾ from their ring friction measurements. The theoretical basis of this work follows the parabolic-faced ring theory of hydrodynamic lubrication, which, like the thermal wedge proposition of Fogg is another possible explanation of there being an oil film between two parallel load bearing surfaces, even though classical hydrodynamic theory precludes its existence.

In the literature of a more conjectural nature we find authors who claim that the ring probably does run in the absence of any oil film at the upper dead centre, and the interesting theory of de Malherbe ⁽²²⁾ where the oil film is considered never to be continuous, but to consist of an oil - gas froth under most conditions.

From the start of this research programme it was intended that any instrumentation used to investigate the causes of ring 'sticking' should be used to its full potential in order to throw as much light as possible on the whole subject of piston ring lubrication. Two types of transducer were used, fast response thermocouples and vibration pick-ups, the whole ring belt of the piston being scattered with a profusion of various

of these detectors in order to measure as far as possible the vibrational and thermal behaviour of the rings under operating conditions. As will be explained later, the vibration detectors were employed in a fashion that attempted to monitor the variation in oil-film thickness between the top ring and liner during operation. A special type of lead-wire linkage was designed to extract data from the transducers within the piston. The design of this reciprocating linkage, with which it was possible to maintain continuous contact with 30 transducers was a 'project' in itself and is fully described later. The engine employed was a Petter type AV-1 of standard build using the "Specialloid" piston as normally supplied with the machine.

THEORETICAL CONSIDERATIONSFactors affecting the temperature of rings in operation

The temperature of piston rings in operation will lie somewhere between the temperatures of the adjacent parts of the piston and the cylinder walls, although exact values will depend on a great many factors included amongst which are the material of the piston, its design and type of cooling, as well as the material and cooling arrangements of the liner, the type of lubricant, the engine size, its design, its operating cycle, its type of loading, its speed, its compression ratio, and the super-charge pressure. Clearly, the determination of the operating temperatures of the piston rings is likely to be a subject for experimental measurement rather than theoretical prediction, and the most useful academic approach will be to examine the effect of each of the factors mentioned above by analysis of data accumulated from temperature measurements on a variety of engines.

Whatever the factors affecting the operating temperatures of the piston rings, only one major requirement determines their permitted upper temperature limit, this being that the lubricant must retain its lubricating capability even on the uppermost ring until it is replaced

by a fresh supply of lubricant. It is therefore - next to the quality of the oil and fuel - a question of what quantity of oil remains in the ring belt of the piston as to what ring temperatures can be allowed. In order to allow high ring temperatures it is important that the ring grooves are well swilled with oil so that "gum" and "coke" deposits are satisfactorily removed.

The bulk of experimental work on ring temperature measurement has, as mentioned in the introduction, been carried out using the fusible plug type of transducers. Despite their wide margin of uncertainty (approx. $20^{\circ}\text{C}.$), useful comparative work has been carried out using this technique, and Englisch⁽⁴⁾, who has collected and summarised the results of many authors, has arrived at a number of general conclusions:

- i. There appears to be a direct proportionality between ring temperatures and the fuel delivery rate.
- ii. The relation between ring temperature and engine speed is difficult to establish, as other factors such as the engine size and type of injection system seem to predominate.

The effects of both i. and ii. are illustrated in Fig.1, from (23), where the top ring temperature (measured

in the ring-groove) is given on a basis of fuelling rate and shows the effect of speed for several engine types.

iii. Englisch⁽⁴⁾ attempts to find a correlation between b.m.e.p. and ring temperature, but again the over-riding effects of the many other factors affecting the temperature prevented him from finding any sort of trend with the data he had available.

iv. Englisch⁽⁴⁾ establishes that the general effect of engine size is for the ring temperatures to decrease with increase in piston diameter for similar engines.

Variation of piston-ring temperatures during the engine cycle

As the piston-ring travels across the surface of the liner and is intermittently exposed to combustion transients, the outer faces of the ring show fluctuations of temperature. Whilst these are only surface effects, they can have serious consequences on the performance of the lubricant in contact with the rings and in severe conditions - such as "scuffing" - become of great importance. Perhaps the most dramatic measurements of these fluctuations were made by Eichelberg⁽¹³⁾, who embedded thermocouples in the top ring of his engine at depths of $\frac{1}{2}$, 2, and 5 mm. from the outer surface. These results are reproduced in Fig.2,

together with the calculated variation of the ring surface temperature and heat flow through the ring as found from Fourier analysis. The diminution in amplitude of the transients and the high rate of heat transfer as indicated by the change in mean temperature level through the thickness of the ring is well shown in these results.

Nepogod'ev and Polval'nyi ⁽²⁴⁾ have examined a theoretical model of oil films on cylinder walls using a simple model of a two-layered barrier exposed on one side to gas with cyclic temperature and pressure variations.

With T as temperature and x measured radially,

$$\left| \frac{\partial T}{\partial x} \right| \gg \left\{ \left| \frac{\partial T}{\partial y} \right| \right. ; \text{ and if circumferential and} \\ \left. \left| \frac{\partial T}{\partial z} \right| \right\}$$

longitudinal thermal diffusions are neglected on this basis, the heat flow can be considered to be unidirectional along the radius. After this simplification, approximate solutions for the heat flow equations are found using a finite difference method. For this the oil film and liner surface are subdivided into a large number of thin layers, and with a time interval suitably chosen to keep the length of the calculation within reason an iterative procedure is carried out using an

electronic computer. The heat transfer coefficient from gas to cylinder wall was computed from the simple empirical formula of Eichelberg⁽¹³⁾, and the temperatures and pressures were obtained from indicator diagrams taken from engine tests.

This publication is extremely significant in the field of cylinder lubrication because of its extremely comprehensive nature. The authors have performed these calculations for an enormous range of conditions covering various engine speeds, oil film thicknesses, supercharge pressures, compression ratios, and excess air ratios. In each instance they have computed, to a base of engine crank-angle degrees, the following quantities:-

- (i) - Oil film surface temperature in liner where not covered by piston.
- (ii) - Metal surface temperature of liner at same point as (i).
- (iii) - Mean oil temperature at point (i).
- (iv) - Oil film surface temperature at portion of liner swept by piston surface at 120° of crankshaft revolution.

Fig. 3 is a reproduction of a typical result from Nepogod'ev and Podval'nyi's analysis, and from this three outstanding features are evident:

- (a) - the temperature rise of the oil film surface where it is exposed to the combustion radiation is of considerable magnitude.

- (b) - the temperature rise of the adjacent metal surface is negligible in comparison to (a).
- (c) - the temperature rise of the oil film surface where it is for the mostpart covered by the piston is of almost half the magnitude of (a).

The last point is of great interest to our own investigation, as it concerns a part of the liner that is in contact with the piston rings at some stages of the cycle, and also like the rings, is not subjected to the full radiative effects of combustion.

In the absence of any suitable theory describing the thermal behaviour of the piston rings, it was considered that it would be advisable to use the results of Nepogod'ev and Podval'nyi's theory for the parts of the cylinder liner covered by the piston as a background to this practical investigation. Whilst this would not seem to provide a fully satisfactory theoretical basis for this work, it was expected that there would be important similarities in the phenomena encountered in these two regions and that at least some of the trends of the theoretical work would be evident in our own experimental results.

It remains to summarise briefly the results of Nepogod'ev and Podval'nyi, and these are listed below in

conjunction with Fig.4. :-

- i. - the amplitude of the temperature fluctuations at the surface of the oil film increases sharply with increasing film thickness.(Fig.4,trace 1).
- ii. - the amplitude of the oil film temperature fluctuation decreases approximately linearly with distance from the surface.
- iii. - at constant brake mean effective pressure, the temperature fluctuations increase with increase in engine speed. (Fig.4, trace 2)
- iv. - the amplitude of the oil film temperature fluctuations increase with reduction in the excess air ratio and with increase in compression ratio. (Fig.4, traces 5 and 6).
- v. - temperature variations of the cylinder liner wall within the limits of operational practicability (20° - 150° C.) have little effect on the amplitude of the temperature fluctuations in the oil film.

The vibration of diesel engine piston rings

During the working cycle, lifting of the piston rings from their lower sides occurs, a fact that has been theoretically predicted and also experimentally demonstrated by Dykes⁽²⁵⁾ and Steinbrenner⁽²⁶⁾. The radial movement of the rings is less predictable, and the consequences that the variation in radial clearance might have on the transient temperature measurements led to serious consideration of this aspect of piston ring behaviour. Blow-by conditions caused by the inward radial

collapse of rings has been well covered in the brilliant experimental work of Dykes⁽²⁵⁾, but the radial ring motion under normal conditions requires examination of the mechanics of its lubrication.

According to conventional hydrodynamic lubrication theory, the only piston ring configuration that will permit existence of a lubricating oil film is one that forms a 'wedge' between ring and bore in the direction of motion. Two theories are in common use to explain the lubrication of parallel surfaces, (i) the 'thermal wedge' theory due to Fogg⁽¹⁹⁾, and (ii) the parabolic ring profile theory as presented by Eilon and Saunders⁽²¹⁾. The results of both theories are summarised below in order to examine and compare the different variables involved and their effects on the predicted oil film thicknesses, whilst, as these theories do not represent original work as far as this presentation is concerned, the reader is referred to the above mentioned works for detailed derivations.

(i).. the 'thermal wedge' theory:

The load bearing capacity, P, of a parallel surface thrust bearing, as derived from Reynolds' equation for hydrodynamic flow, is given by Fogg as

$$P = \frac{6 \mu U B}{h^2} \left[\frac{1}{2} + \frac{e' - 1}{1 - e'} + \frac{1}{\ln e'} \right]$$

where P = Unit load, μ = Lubricant viscosity,
 U = Linear velocity, B = Width of thrust surface,
 h = oil film thickness, and $\rho' =$ Density ratio, i.e.
 across wedge.

Considering a segment of piston ring of unit length, the temperature rise of the oil film in the axial direction from upper to lower face of the ring - the 'thermal wedge' - can be expressed in terms of the density ratio, and determined from the viscous friction, F , between ring face and bore using -

$$F = \frac{\mu U B}{h}$$

Eventually, h , the oil film thickness can be reduced to basic engine parameters only, yielding:

$$h = 0.01354 \frac{(\mu B R_c N)^{\frac{1}{2}}}{P^{\frac{1}{4}}} \left[\sin \theta \cdot \frac{\sin 2\theta}{2 \left[\frac{L}{R}^2 - \sin^2 \theta \right]^{\frac{1}{2}}} \right]^{\frac{1}{2}}$$

where h = Oil film thickness, in. μ = Oil viscosity, lb.sec/in²
 B = Width of thrust surface, in. R_c = Crankshaft radius, in.
 N = Crankshaft speed, r.p.m. P = Unit load on ring, lb/in.²
 θ = Crankshaft angle, degrees. L = Connecting rod length, in.

The following are among the major disadvantages of this approach -

- (a) - the oil film between ring and bore is treated as adiabatic, which is an unrealistic assumption.
- (b) - the ring loading, P (in the radial direction), is difficult to determine, especially during the firing stroke where the gas load on the back of the ring predominates. (The authors give additional equations to cover this instance, and also the cases of $\theta = 0$, 180° , or 360° where the film thickness would otherwise become zero).

(c) - the instantaneous state (physical and chemical) of the lubricant in the ring region cannot be precisely established throughout the operating cycle, and hence the true transport properties of the oil can never be determined.

(ii).. the parabolic ring profile theory:

The experimental work of Eilon and Saunders was carried out on a reciprocating rig, with which instantaneous friction forces from the piston rings were directly measured. Using equations of the form -

$$F = \frac{\eta U A}{h}$$

where F = frictional force ; η = viscosity coefficient;

A = piston ring face area; and h = ring-to-liner oil film thickness.

- these authors calculated values for the oil-film thickness, h. The derived results were then compared to estimates of the film thickness made from the following theoretical treatment of the ring/liner lubrication.

Again using Reynold's equation as a starting point, this theory takes account of the worn profile of the piston ring, the pressure build-up on the converging wedge between the worn ring face and the cylinder liner providing the necessary boundary conditions for solution of the equation.

Three dimensionless groups, H , r , and P_m , are used to express the final results which are as follows:-

For the upward stroke of the piston:

$$P_m \cdot r^{3/2} \left[1 - \frac{P_1}{2 \cdot P_m} \cdot f(H) \right] = 0.3536 \left[\left(\frac{H}{1+H^2} + \tan^{-1} H \right) \cdot f(H) - \tan^{-1} H \right]$$

and for the downward piston stroke:

$$(P_m - P_1) \cdot r^{3/2} \left[1 + \frac{1}{2} \cdot \frac{P_1}{P_m - P_1} \cdot f(H) \right] = 0.3536 \left[\left(\frac{H}{1+H^2} + \tan^{-1} H \right) \cdot f(H) - \tan^{-1} H \right]$$

where $H = b / (2R_r \cdot h_r)^{1/2}$, $r = h / R_r$, $P_m = p_m \cdot R_r / 6 \cdot \eta \cdot U$.

$$f(H) = [H + 3(1+H^2) \tan^{-1} H][1+H^2] / [5H + 3H^3 + 3(1+H^2)^2 \tan^{-1} H].$$

and $2b$ = axial width of ring, p_m = mean pressure on ring face,

R_r = radius of parabolic face, η = coefficient of viscosity,

h = oil film thickness, U = piston velocity,

$r = h / R_r$.

Curves of the above equations are given in Ref.21, but as a convenient indication of the general trend of the variables involved the approximation :-

$$h \propto b \left[\frac{\eta \cdot U}{P_m \cdot R_r} \right]^{1/3}$$

for the upward piston stroke when $H < 0.8$ is of value.

It is apparent that the two theories presented here bear few similarities in their final results, and will in general predict oil-film thicknesses of greatly differing magnitude. As will be clear later, the difficulties of measuring oil film thicknesses of only a few microns are considerable, and it was expected that the experimental results would only indicate an order of magnitude of the film thickness. The objective therefore was to establish which theory might be nearer the truth, rather than to attempt an exact correlation between either theory and these experiments. For this reason, comprehensive solutions to the above equations are not given at this stage.

EXPERIMENTAL APPARATUSIntroduction

The experimental section of this investigation was carried out on a small single cylinder diesel engine, mounted on a standard test-bed with an electrical dynamometer.

Instrumentation to monitor the metal surface and lubricant temperatures under operating conditions was developed and installed in the ring belt region of the piston, and an elaborate linkage mechanism constructed to extract the electrical signals from the transducers within the piston. An advanced type of data recording facility was installed which permitted the simultaneous recording of a great number of channels of information from these transducers to a very high degree of fidelity.

The engine rig, linkage mechanism, electronic instrumentation, and the recording system are each considered in turn below, and complete details of much of the apparatus presented in the Appendices.

i. The engine rig.

The diesel engine employed was a Petter type AV-1, this being a small 4-stroke single cylinder machine of 80 mm. (3.15") bore and 110 mm. (4.33") stroke. Other important

details and specified ratings are summarised below:

Compression ratio = 16.5 : 1
 Capacity = 553 cc.
 Compression pressure = 535 p.s.i.
 Power rating - 3 b.h.p. at 1000 r.p.m.
 5 " at 1500 "
 6 " at 1800 "
 Lubricant - Shell 'Rotella' T30.
 Fuel - Shell Diesel to B.S. 2869/1957, Class A.

The Petter machine was mounted onto a substantial test-bed together with a B.K.B. (Birmingham) electrical dynamometer of 7 kW. capacity. A strain-gauged element was attached to one of the dynamometer radius arms, and, suitably amplified, displayed the brake load on a dial instrument on the engine control panel. (Appendix IV (i) gives full details of this load measuring device).

Fuel, water, and oil circuits followed standard test-bed practice, heat exchangers and electrical circulating pumps being employed in the oil and water systems to achieve steady conditions. These systems were completely self-operating by the use of temperature sensors directly controlling magnetic valves in the heat exchanger feed water supplies. Outline diagrams of these systems are given in Figure 5.

An engine operating panel was constructed, as is shown in the left foreground of Plate 1, the engine being located immediately behind the panel. Engine conditions

displayed on this panel were :-

- i. Engine speed.
- ii. Brake load.
- iii. Oil pressure.
- iv. Oil temperature.
- v. Water inlet temperature.
- vi. Water outlet temperature.
- vii. Fuel delivery rate (using a graduated pipette tube in the delivery line).

For safety of operation, overload protection circuits were fitted to the following :-

Oil pressure - minimum 20 p.s.i.
Oil temperature - maximum 70°C.
Water outlet temperature - maximum 70°C.
Engine speed - maximum 1800 r.p.m.
Emergency stop button.

Overload of any of the above caused immediate closure of a magnetic valve in the fuel supply line, and effected complete shut-down of the engine within 20 seconds. Details of the circuitry for the over-speed trip are given in Appendix IV (ii), and wiring details of all the overload protection circuits are given in Figure 6.

Engine speed was measured by a "Hasler" electrical tachometer directly coupled to the output shaft, and degrees of crank-angle could be measured from a photo-electric disc attached to the same shaft. Both instruments are shown in Plates 2 and 6, and full details of the crank-angle degree indicator given in Appendix IV (iii).

Only one modification was made to the engine as

supplied by the manufacturers, this being the injector pump mounting bracket, which had to be re-designed to permit assembly of the lead-wire linkage. No changes in the engine's characteristics were expected from this minor modification.

An additional facility was provided to enable the engine to be run on methane gas. As shown in Plates 3 and 5, a bottled gas supply was connected via a low pressure regulating valve to a spray nozzle in the air intake, and the system was completed with contact-breaker points, ignition coil, and a miniature sparking plug inserted through the diesel injector-nozzle holder.

ii. The piston linkage

The means whereby electrical signals may be extracted from the pistons of engines whilst in operation has a long, and generally unsuccessful history. In this instance, the requirements were particularly difficult, as a capability of maintaining contact with a minimum of 22 information channels from a piston of only 80 mm. diameter was expected.

Multiple channel connections to thermocouples have been achieved successfully in the past by early experimenters such as Eichelberg ⁽¹³⁾, who used direct connections

to the underside of the piston. This technique was only possible by virtue of the very low engine speeds used (400 r.p.m. maximum), and subsequent workers have almost invariably had to use non-continuous connections. Flynn and Thompson ⁽²⁷⁾ used wiper strips on the lower rim of the piston skirt to provide contact at B.D.C. (bottom dead centre) with spring pins attached to the crankcase. Speeds up to 1800 r.p.m. have been used with this device, but trouble was experienced with the high fatigue rate of the long cantilever wiper strips and electrical noise from the sliding contacts.

French and Hartles ⁽¹⁵⁾, and the B.I.C.E.R.I. organisation ⁽²⁸⁾ have also run successful versions of the instantaneous B.D.C. contact methods in their research works.

F.M. telemetry (or the "radio link") has been favoured in recent years as the result of advances in the miniaturisation of electronic circuitry. ⁽²⁹⁾ This system employs a miniature F.M. transmitter fixed within the piston skirt, having its aerial extended down the side of the connecting-rod. A receiver with its aerial inside one of the crankcase doors and suitable F.M. receiving/demodulating equipment complete the system. A servo-controlled

automatic frequency loop is necessary to ensure that the receiver is always tuned to the transmitter frequency, as considerable drifting is likely to be experienced in the fluctuating temperature environment of the engine crankcase. Where space within the piston is limited, very few data channels can be accommodated and this is certainly the major disadvantage of the technique. For high speed engines, however, this method is superior to any mechanical system as the electronic components in the transmitter are capable of withstanding acceleration loads of several hundred 'g'.

Early attempts to establish contact with the piston for the purposes of our own experimental work started with the instantaneous B.D.C. contact method. After much trouble with electrical noise and 'oiling-up' of the contact surfaces, a method was developed whereby the most troublesome components, the spring contacts, were replaced by miniature compressed-air loaded pistons. The fatigue life of the device was greatly extended by cutting off the air pressure to withdraw the contacts when not required, and the optimum spring pressure for minimum contact noise could be achieved by varying the air pressure behind the pistons. The final form of this

device is shown in Figure 7. Ten such contacts could be accommodated in the space available in the Petter engine crankcase, and satisfactory contact was maintained at speeds up to 2200 r.p.m.

Later requirements derived from the development of fast response transducers made it necessary to seek a device which could maintain continuous electrical contact throughout the engine cycle and also accommodate many more channels of information. At this time there were developments in the ideas as pioneered by Steinbrenner⁽²⁶⁾, of elbow linkage continuous contact devices from the Admiralty (A.R.L., Teddington) and Messrs. Associated Engineering Ltd. (Group Research and Development Unit, Rugby). With these techniques in mind a linkage was developed for the Petter engine which could be run at 2000 r.p.m. whilst maintaining continuous contact with 48 lead-wires. This device is shown in Plates 7 and 8, and may be seen to consist of a rigid strut attached to the piston skirt and a pair of reciprocating tubes which carry the wiring across to attachment boxes in the crankcase doors of the engine. This linkage was used in all the tests described herein, and full details of the construction may be found in Appendix III.

iii. Electronic instrumentation

The specialised thermocouples and vibration transducers required for the research work are described below, and details are given of the chains of electronics which back-up each transducer type - wiring, switching, amplification, recording, storage, and display systems.

Temperature transducers :

It was required to measure the fluctuations in the oil-film and metal surface temperatures in and around the ring belt region of the piston with extreme accuracy and with a frequency response much faster than that associated with conventional temperature transducers.

Three types of sensor are in common use for the measurement of piston and ring temperatures:

- (a) Fusible calorimetric plugs.
- (b) Hardness recovery plugs.
- (c) Thermocouples.

The calorimetric method (a) uses plugs of selected metals and their eutectics peened into small holes(1/16"dia.) in the piston surface. At the finish of an engine test, a survey of those plugs which have melted indicates the highest temperature attained at each test point to an accuracy of approximately $\pm 10^{\circ}\text{C}$. This poor accuracy and

the fact that there are some gaps in the range of suitable eutectic plugs has led to preference of the hardness recovery technique during recent years.

This method (b) uses small plugs of hardened steel which indicate the maximum temperature to which they have been exposed during testing by changes in the surface hardness of the steel. A proprietary brand of these plugs ("Templugs" - Shell Thornton Research Centre) claims measurement accuracy of $\pm 5^{\circ}\text{C}$., and this technique gives a further gain over the calorimetric method in that only one plug is required at each measuring station thereby permitting steeper temperature gradients to be plotted.

Methods (a) and (b) are in general use for plotting the steady temperature levels at various points in engine pistons, and have been used by Janota ⁽⁸⁾, Ip ⁽⁹⁾, Fitzgeorge ⁽¹¹⁾, and Britain ⁽¹²⁾ in engine heat transfer analyses.

Electrical methods of measurement (c) have three distinct advantages over (a) and (b), these being the increased accuracy of measurement, the more precise location of the point of measurement, and, most important from the point of view of the work being considered here,

the potential of reading transient temperatures. The use of thermocouples in engines research dates back to the work of Eichelberg⁽¹³⁾, and they are used today in the most sophisticated work, for example, the research of Whitehouse et al⁽¹⁴⁾, French and Hartles⁽¹⁵⁾, Steiger and Aue⁽¹⁶⁾, Fujita⁽¹⁷⁾, and Brock and Glasspoole⁽¹⁸⁾. Of these, only Eichelberg, Whitehouse, and Fujita have been concerned with fluctuations in temperatures within the engine cycle, and little attention has been paid to this topic in the literature since Eichelberg's⁽¹³⁾ conclusion that the temperature fluctuations on piston crown surfaces are usually small enough to be negligible. Subsequent research workers, concerned with possible fluctuating stress levels on the piston crown surface have confirmed Eichelberg's findings, but make the point that for certain piston materials such as steel - as compared with Eichelberg's cast-iron - stress levels can become significant.

Results of the various experimenters all indicate that the temperature fluctuations during each engine stroke are confined to a few millimetres depth below the piston surface, and also that the positive variation (during the

firing stroke) is of greater amplitude than the negative variation. This latter effect is the result of the higher coefficient of heat transfer between the gases and the piston during the combustion period when the pressures and temperatures are high and there is considerable turbulence. In the case examined by Whitehouse et al⁽¹⁴⁾ in which the fatigue strength of a cast aluminium alloy piston was marginal, it appeared that the stresses brought about by temperature fluctuations on the piston crown would explain service failures.

Since the publication of the works outlined above there have been a number of interesting developments in temperature transducers, and a survey of these together with experiments to determine their suitability were made. Only fast response types were considered, and the response times quoted below were arrived at by plunging specimen transducers into a bath of heated lubricating oil and deriving the value of the transducer time constant from the rate of rise of its output waveform.

The time constant, τ , of a transducer is an indication of its response to a step function, and is defined as the time taken for the output to reach $(e-1)/e$ of its final value, i.e. 63.2% of the amplitude of the step

function. A suitable value of the time constant required for these experiments may be estimated as follows:-

An engine at speed 1800 r.p.m., regarding one cycle as one revolution of the crankshaft, is operating at a cyclic frequency of 30 Hz.

Assuming that a sample is required every ten degrees of crank-angle, and that the temperature fluctuations will be of a sinusoidal nature, the minimum acceptable frequency response will be $30 \times 360/10 = 1080$ Hz.

For a sinusoidal input at frequency ω , the frequency response and time constant are related by

$$R_f = \left[\frac{1}{1 + \omega^2 \cdot \tau^2} \right]^{\frac{1}{2}}$$

where $R_f = \frac{\text{temperature fluctuations of the thermocouple}}{\text{" " " " environment}}$

For the minimum acceptable frequency response, $R_f = 3$ db.down
 $= 0.707$ giving $\tau = 0.15$ ms.

The choice of transducers capable of response times of this order is limited to four types:

- (1) thermocouples.
- (2) thermistors.
- (3) thin-film thermometers.
- (4) thin-film thermocouples.

(1) thermocouples

The time constant of a bead thermocouple is governed by two factors; the dimension of the thermocouple bead, and the surface heat transfer coefficient between the bead and its environment. Considering the thermocouple and its attachment wires as a single wire in cross-flow it may be shown that:

$$\tau \propto D^{3/2}$$

$$\tau \propto 1/k$$

$$\tau \propto 1/V^2$$

where D =diameter of the thermocouple junction.
 k =thermal conductivity of the environment.
 V =flow velocity of the environment.

From experiments on the smallest bead type of thermocouple commercially available (Baldwin-Lima-Hamilton Corp. type TCA-ES-200), this being a chromel-alumel couple having a junction diameter of only 0.001", a time constant of 35 ms. in oil was arrived at. This compares well with the value of 30 ms. which may be derived from the manufacturers' quoted value for water and the relationship between τ and k quoted above.

(2) thermistors

Thermistors are thermally sensitive resistors whose

temperature coefficient of resistance is negative and many times greater than that of ordinary metals. The change in resistance is approximately exponential with temperature, following the law :

$$R = c \cdot e^{B/T}$$

where R = thermistor resistance at reference temperature
(usually 20°C.)

T = absolute temperature
c and B = "constants" which vary only slightly with temperature.

The smallest thermistor available in this country is a naked bead type of 0.01" diameter, and its time constant does not compare favourably with the bead thermocouple described above. However, a new type of silicon thermistor (or silistor) is available from the United States in much smaller sizes. The silistor is a considerable improvement on the conventional ferric oxide thermistor in that it has a positive temperature coefficient of resistance and a linear response to temperature. The smallest available silistor is in the form of a flat disc of 0.0005" thickness and has a time constant of 15 ms. in oil. Unfortunately the overall disc dimensions and mounting difficulties made it unsuitable for this application.

(3) thin-film thermometers

Laderman, Hecht, and Oppenheim⁽³¹⁾ describe the manufacture of a temperature gauge using a 0.15 micron film of platinum as the sensing element. The platinum strip was deposited in a thin strip between two electrodes on a lava backing, thus forming a minute platinum resistance thermometer.

The response rate is probably well within our range of interest, but the delicacy of the platinum film and the considerable disturbance to the piston heat flow that would be caused by the lava backing material precluded this device from further consideration.

(4) thin-film thermocouples

This final type of temperature sensor has a slightly different application to those described above, in that the active element is in thermal contact with its backing material. Thus the device is suitable for measurement of surface temperatures, providing the backing material has a similar thermal conductivity to that of the surface being studied.

Bendersky⁽³²⁾ describes a thermocouple in which the active element is deposited by a vacuum coating technique so that the transducer's effective thickness is only of the

order of 1.0 microns, and its time constant approximately 0.25 ms. in air.

- - - -

In the instrumentation of the Petter piston, two of the above transducers types were employed for measurement of the transient temperatures - the miniature bead thermocouples for the oil temperatures, and thin-film thermocouples for the metal surface temperatures. Appendix I gives full details of the construction of the thin-film devices, and the layout of the various transducers in the ring belt region of the piston is given later in this chapter.

Before leaving the subject of thermocouples, mention must be made of some further problems concerning their use in this particular application.

Firstly, the conveyance of the thermocouple voltages from the piston through the linkage, and out through the engine casing to the amplifiers was not a straightforward matter. As the linkage was wired with pure copper wires, it was necessary to provide a region of constant and precisely known temperature within the piston where the Chromel/Alumel and Iron/Nickel thermocouple leads could be changed to copper outlet wires. A miniature electric oven was designed and constructed (Plate 15) into which

a capsule containing the terminations of all the thermocouple leads and outlet wires could be inserted (Plate 16). The oven was electronically controlled by transistor switching circuits and could maintain a pre-set temperature to within $\pm 0.1^{\circ}\text{C}$. provided that its 15 volt power supply was stabilised to within 0.5%. The oven was fitted to the inside of the piston skirt on the side opposite to the strut and, to avoid control difficulties, was operated at temperatures slightly above that of the lubricant, i.e. in the region of 60°C . (Appendix IV) (iv)).

Using Moffat's method ⁽³³⁾ for plotting multiple thermocouple circuits, the complete electrical circuits for the bead and film thermocouples are shown in Figure 8. (Moffat's method plots the gradients of all the constituent metals in the circuit to the base of pure platinum, and plots the composite circuit to this common base.)

Amplification of the signals from the fast response thermocouples presented further problems, as it was necessary to provide the unusual requirement (for thermocouples) of high accuracy, low drift amplification over a bandwidth of d.c. to at least 1 kHz. Specification of a measurement accuracy of $\pm 1^{\circ}\text{C}$. resolution over the range 0 - 200°C .

determined the remaining amplifier requirements, which may be summarised as follows:

Voltage gain - X 100 to 1000, adjustable.
Bandwidth - d.c. to 1 kHz. \pm 1 db.
Zero drift - \pm 1 μ V/ $^{\circ}$ C. referred to input.
Voltage noise - 1 μ V. referred to input.
Common mode rejection ratio - at least 80 db.

The output voltages from the thermocouples were expected to be in the form of a large d.c. (or fixed value) component onto which a.c. components (or fluctuations) would be superimposed. The above amplifier requirements being difficult to satisfy, two methods of approach were available - (i) to accurately back-off the d.c. component of the signal and use a relatively simple amplifier to handle the fluctuating component, - or (ii) to pursue the latest advances in transistor microcircuitry, whereby amplifiers to the specifications quoted above were just approaching the realm of feasibility. Such amplifiers would greatly simplify the whole electronics and data handling systems which, if handling multi-channel operation of method (i) would be formidable.

In the early stages of the project the second method was not in a satisfactory state of development and consequently during the course of the work both of the above methods were used for thermocouple amplification. Full details of these amplifier systems are given in Appendix II.

Vibration transducers:

Measurements of the motion of engine piston rings present an intriguing experimental problem. As with any electrical measurements made within the piston there are difficulties of extracting the data, but with the vibration measurements there are the additional problems of providing suitably small transducers which can withstand the arduous conditions imposed within the engine cylinder.

In the work of Dykes ⁽²⁵⁾ which was concerned with the radial collapse of piston rings, strain-wire transducers were employed, the ends of the wire elements being actually attached to the rings. Steinbrenner ⁽²⁶⁾ and some early work by the author ⁽³⁴⁾ have examined the possibilities of using inductive transducers for these measurements, thus avoiding the possibility of disturbing the pattern of the ring motion by direct contact between transducer and ring. In the inductive type of transducer the piston ring is made to form part of the armature circuit of a small pick-up coil which is excited by an a.c. voltage. Any movement between the coil and the piston ring then produces an inductance change in the coil, which, after suitable electronic processing can be directly related to the amplitude of the movement.

Major problems in the design of such transducers are the size requirements for measurements in small engines, and the difficulties of temperature compensation. The transducers used by Steinbrenner were too large for use in the Petter piston, which employs rings of only 0.1" height, and those developed by the author had previously only been used in a non-firing engine rig and had poor temperature stability beyond 110°C. To avoid further development work a proprietary system was used in this work (manufactured by Messrs. Associated Engineering Ltd., Rugby - hereafter referred to as A.E.), which employs a transducer of 0.090" diameter having an upper temperature limit of 180°C. The complete A.E. system is shown diagrammatically in Figure 9, and it may be seen that a "dummy" transducer is used in bridge configuration to provide temperature compensation.

Although measurements of piston to ring and piston to liner movements are relatively simple by this technique, the most interesting measurement - that of the clearance between the piston ring and the liner - remained impossible by a single direct measurement, as the vibration transducer was too large to accommodate within the piston ring itself.

However, as shown diagrammatically in Figure 10, a subtraction of the clearances measured from piston to ring and from piston to liner would, in theory, give a measure of the ring to liner clearance.

Lubrication theory predicts that this clearance may only be of the order of a few microns if filled with a continuous lubricant film, and it remained to be seen whether the system was capable of such a high degree of resolution from a signal derived from two independent measurements. In fact the accuracy of measurement could not be relied upon without an independent check on the calibration, and this was provided by engraving small slots in the cylinder liner so that a continuous check of the calibration and zero-drift would appear on all recordings. These calibration marks are also depicted in Figure 10, and full details of the A.E. transducers and their associated electronics are given in Appendix IV (v).

Location of transducers:

The three transducer types having been chosen, it was necessary to select their positions with great care, bearing in mind the very limited space available, the difficulty of fixing the transducers into place, the points at which measurement would be most advantageous, and the

temperature problems likely to be encountered by any transducers sited above the top piston-ring. The final layout consisted of two identical instrument clusters, one oriented on the thrust axis and the other on one of the gudgeon-pin axes, as shown in Figure 11.

Fast response thermocouples were located on the outer piston face immediately above each piston-ring groove.

Miniature bead thermocouples were placed behind both upper rings and below the third ring, the thermocouple mountings being slightly recessed (as shown in the insert of Figure 11.) in order to measure the oil film temperature whilst providing some protection for the thermocouple bead.

The vibration transducers and their "dummy" compensators were set into the back of the top ring groove and immediately below the same groove in order to measure piston to ring and piston to liner vibrations respectively.

This scheme, including the compensating transducers, involved a total of 20 instruments in the ring belt of the piston. Thus 40 lead-wires had to be brought through the inside of the piston to the connection tags at the top of the linkage strut. In order to alleviate the

bulkiness of such extensive wiring a flexible printed circuit was made up which fitted inside the piston skirt and around the gudgeon-pin in order to provide terminations for the transducer wiring on the underside of the piston crown. This flexible circuit, shown in Plate 9, consisted of 0.002" etched copper on 0.003" Mylar film and successfully simplified the intricate internal wiring problems.

iv. The recording system

The recording requirements for phenomena varying during the engine cycle are particularly severe if several such wide bandwidth information channels must be recorded simultaneously. An Ampex FR1300 instrumentation tape recorder was used as the basis of the recording system, providing 14 independent recording channels with adequate frequency bandwidth.

With a total of 12 thermocouples installed in the piston it was not possible to simultaneously record all necessary information on a 14 channel machine, and therefore a rotary switching unit was made up in order to consecutively sample the thermocouple outputs. The switching unit was driven through reduction gearing from the engine output shaft, and using two banks of magnetic reed-switches

the data from the 12 thermocouples was reduced to two channels, each thermocouple being sampled once in every six engine cycles.

Further recording channels were required for the crank-angle degree marker (as described in section i.), for trigger pulses to synchronise the oscilloscope sweep-rate with the cyclic frequency of the engine, and for the recorded voice-log. This latter facility proved to be of great value in the storage of data from the slowly changing variables (e.g. brake load, inlet air conditions, fuel-flow timings) as well as providing a means of permanently identifying unusual features of any test with the actual recording. The above channels were all recorded on a.c. record-amplifier channels (direct-record, D.R., system), these having a bandwidth of 100 Hz. to 75 kHz. \pm 3 db.

The outputs from the vibration transducers all had to be recorded simultaneously, thus occupying a total of 4 tape tracks. As with the thermocouple records, the recording system employed was a frequency-modulated type (F.M.), this providing - at a tape speed of 15 inch/s. - a bandwidth of d.c. to 5 kHz. \pm 1 db.

Use of the thermocouple switching unit together with

the FR1300 tape recorder made up a complete recording system as follows :

4 vibration transducer outputs	- - - -	4 F.M. channels.
6 thin film thermocouples	- 6 channel switch unit	- 1 F.M. channel
6 bead thermocouples	- 6 " " " "	- 1 F.M. channel
Crank angle degree marker	- - - -	- 1 D.R. channel.
Oscilloscope trigger	- - - -	- 1 D.R. channel.
Voice log	- - - -	- 1 D.R. channel.

Analysis of the recordings obtained were carried out by play-back of selected tape tracks into a Tektronix type 564 storage oscilloscope. Selected stored images were then photographed with a Polaroid oscilloscope camera to produce permanent records.

Figure 12. shows the layout of the complete recording system in diagrammatic form, and Plate 4 shows the majority of the recording equipment as installed adjacent to the engine. Full specifications of all the above mentioned recording equipment are given in Appendix IV (vi).

EXPERIMENTAL RESULTS

Introduction

The engine test schedule was planned to provide the maximum retrieval of data before the instrumentation and linkage mechanism would begin to give trouble. A relatively short life was anticipated for the delicate film thermometers, and it was expected that the epoxy resin mountings of the displacement transducers would soften at the highest engine temperatures. Further, the high 'g' loadings at maximum power would inevitably shorten the life of the linkage and its lead wires.

The frequency response of the film thermocouples is seriously affected by soot deposits on their working surfaces, and the bead thermocouples would, to a lesser extent, be similarly affected. The first consideration in planning the test schedule, therefore, was to arrange for all the "setting-up" runs to be completed with the minimum of damage to the transducers. To this end it was decided to initially operate the engine on methane gas, which leaves virtually no soot deposits and, in addition, gives a slower rate of pressure rise on the expansion stroke. As a means of expediting the "warm-up" time for each test,

the cylinder block was pre-heated by circulating the cooling water via an immersion heater tank at 70°C. for 30 minutes before starting the engine. The test schedule was therefore arranged as follows:-

1. Methane operation - medium load, medium speed conditions only - pre-heated cylinder block. (Details of the operating conditions for the methane trials are given in the final paragraph of this section).
2. Diesel operation - low load, low speed runs, working towards high load, high speed conditions - pre-heated cylinder block.

Table 1 lists the tests carried out, and the main features of each of these.

During engine tests, virtually all data was transferred immediately to the magnetic tape storage system. The few remaining variables that changed only slowly with time were recorded on the voice channel at frequent intervals, these being:

- Air intake temperature.
- Thermistor temperature.
- Brake load.
- Engine speed.

In practice, the thermistor temperature was found to drift slightly during most runs, and a chart recorder was installed to ensure that a complete check could be kept of any variations.

Figure 12. shows, in block diagram form, the complete

instrumentation and data recording scheme as used in all tests.

Methane operation: Methane gas was fed from a bottled supply at a regulated low pressure (0 to 10 p.s.i.) to a simple spray nozzle in the engine air intake. The ignition system consisted of a 10 mm. sparking plug fitted into the diesel injector casing, driven by a high performance coil using contact-breaker points coupled to the camshaft. As engines running on methane have approximately twice the output power potential as compared with diesel operation, it was necessary to instal a throttle plate for safety reasons. The throttle plate was fitted across the air intake, and provided a maximum of 1/3 of normal full throttle. The sparking plug gap was set at 0.010", and the spark advance was 15° before T.D.C.

Results

A few recordings were made of the initial runs using methane as fuel, but these only served their purpose of setting up the various instrumentation systems and of providing experience with the recording techniques. In addition, electrical interference from the spark ignition source rendered the majority of the low-voltage output signals unintelligible.

The diesel trials provided a total of more than two hours of recorded data, covering as wide a range of conditions as the delicate instruments permitted. By the end of the final test - at full power output - only four

bead thermocouples, three film thermocouples, one vibration transducer, and the thermistor were giving reliable output signals, and further trials were abandoned at this stage. However, the recordings already obtained provided a wealth of information, and were considered to fulfil all the aims of the experimental programme.

Results obtained from the various transducers are outlined briefly below, and discussed in the following chapter.

i. Bead thermocouples

Reliable results were obtained from the six bead thermocouples through almost the entire test programme. The mean temperature levels of each thermocouple were monitored continuously, and many recordings made of the temperature transients that were encountered by some of the transducers. The transients were in every case associated with the expansion stroke of the combustion cycle, and were apparent at all engine operating conditions.

Transducer A1, located on the thrust face behind the top ring, showed the greatest amplitude of these transients, and a typical trace from this transducer is shown in Figure 14 (upper frame)* The steady temperature level ($184^{\circ}\text{C}.$)

* Please refer to Figure 13 for explanation of the presentation of all oscilloscope records.

can be seen to be interrupted by a temperature transient of approximately 20°C . coinciding with the diesel combustion process. Some problems were encountered with voltage pick-up from the 50 Hz. mains power supply, and in order to assess accurately the true amplitude of these transients it was necessary to analyse a series of such peaks on a statistical basis. For this it was necessary to provide a recording of a number of consecutive engine cycles, and the centre frame of Figure 14 shows how this was achieved in practice; the upper trace shows a recording similar to that discussed above, and the lower trace presents the same recording together with records from the next 16 engine cycles displayed on a much compressed time scale.

The lower frame of Figure 14 shows 18 consecutive traces in a similar format, showing the outputs of all six bead thermocouples together, for comparison. The transients are clearly greatest on trace A1, but also apparent on all but the two lowest mounted transducers (A3 and A6).

Figure 15 presents the output waveforms for transducer A1 at three different load/speed conditions, the time scale again being compressed for statistical analysis of the results.

Finally, the upper frame of Figure 16 shows a number of consecutive sweeps of the output waveform of transducer A1. In this instance, however, the time scale is not compressed, but successive engine cycles are displayed beneath each other in order to show the excellent repeatability of the results from one cycle to the next.

ii. Film thermocouples

The majority of information received from the thin-film thermocouples showed steady-state temperatures at the point of measurement. Only at full output power could any transient effects be detected, and these were only of minute amplitude. By the time the full power conditions had reached, the top transducer on the thrust face (TC1) had failed, but its companion on the G.P. axis (TC4) showed transients of approximately 0.5°C . amplitude, as shown in Figure 16 (lower trace). The absence of transients on the other traces, as typified by trace TC3, is also shown on this record.

iii. Overall piston temperatures

Apart from the capability of recording transient temperature phenomena, the transducers described above give an accurate assessment of the mean temperature levels at each measuring station. In Figure 17 mean temperatures

from each transducer are plotted against b.m.e.p. for engine tests which cover the whole range of available output power.

iv. Vibration transducers

The four sets of vibration transducers employed to measure the piston-to-ring and ring-to-liner displacements were, apart from an early failure of one of the temperature compensating transducers, as accurate in their measurements as could be expected from the system. Typical results as recorded directly from the outputs of the detector-filter units are given in the top frame of Figure 18. The signals required considerable electronic processing before they become suitable for analysis, it being necessary to match the amplifier gains, the transducer characteristics, and the zero offset voltages for each channel.

The processing of the signals is shown pictorially in Figure 18 (centre frame). A selected signal of the piston-to-ring displacement was displayed and stored on the oscilloscope at a suitable amplitude (trace 'e'). The corresponding piston-to-liner displacement signal was then taken and its gain, characteristic, and offset voltage matched against the former signal to the maximum possible

degree of compatibility (trace 'g'). Electronic subtraction of the two signals then gave the clearance between ring and liner (trace 'f').

The accuracy of location of the position of the ring in relation to the liner is chiefly determined by a precise knowledge of the zero offset voltages on the two channels, and the slight temperature dependence of these voltages was found to prejudice the accuracy of the measurements. The thermal drifting of the systems was compensated for by taking "zero" reference readings at various known temperatures and then using the adjacent piston thermocouples each reading was adjusted for drift. The lower frame in Figure 18 shows two such reference traces, and also the ring-to-liner clearance at increased amplification.

As a further check on the accuracy of the results, the reference marks in the cylinder liner were used to provide a secondary means of measurement. This was considered necessary as the high levels of amplification used on these signals brought the amplitude of the subtracted signals close to the noise levels of the signals. However, it was proved that clearances down to 5 microns (0.0002") could be accurately detected.

ANALYSIS AND DISCUSSION

Results from the various transducers are considered below, the data from each of the instruments types being presented in the same order as in the previous chapter. Subsequent sections deal with correlation of the results, general comments, and suggestions for future work.

i. Bead thermocouples

The durability of the bead thermocouples was well beyond expectations. These 0.001" diameter beads, despite their arduous environment, gave continuous results which were reliable, plausible, and above all, repeatable. After thorough examination, including statistical analysis, of many such readings the results could be given with a high degree of confidence.

Six widely differing engine operating conditions gave the results presented in Table 2, which are plotted to a base of b.m.e.p. in Figure 20. As presented here, the results display the peak amplitude of the temperature rise at the time of combustion as measured by the transducer A1 (thrust face-behind top ring). These transients give weight to the hypothesis presented in the theoretical discussion of this work, namely that the oil remains at a steady temperature during the majority of the engine

cycle, and is subjected to a rapid thermal shock at the instant of combustion. With the piston ring seated on the lower face of the ring groove - as it would be on the expansion stroke - there exists a narrow but direct passage between the combustion chamber and the region behind the uppermost ring.

The results show that the duration of the temperature transient is sufficiently short to be completely disregarded by slow-response temperature indicators, thus any measurements from these types of transducer would give a completely false impression of the maximum temperature to which the lubricant behind the top ring is subjected during each cycle.

At full load conditions, where the steady temperature of the oil in the region of the top ring is already likely to be close to the temperature at which rapid oxidation takes place, it is clear that the transients could bring about a gradual deterioration of the oil. Obvious remedies are identical to those already in use for cases of "gummed" rings, that is either to improve the cooling of that area of the piston, or to locally improve the oil circulation so that oxidised particles are washed away before they

have a chance to accumulate. Therefore, although the results do not provide new remedies for the problems of ring gumming, they do explain why piston rings that are thought, from the results of slow-response temperature indicators, to be operating at "safe" temperatures can still suffer from gumming.

The last statement promotes the question of how it might be possible to predict the amplitude of the transients at any prescribed engine condition. This proved to be beyond the scope of the available data for, as may be seen in Figure 20, apart from the indicated trend in the relationship between transient amplitude and b.m.e.p., there appeared to be no simple correlation between amplitude and the engine operating parameters. It would be expected that any such relationships would be complex, as it would be necessary to take into account such effects as oil viscosity/temperature relationships and the closure effect on the space between piston and liner when the piston geometry changes at high load conditions. It was unfortunate that the delicacy of the instrumentation allowed too short a test programme to permit comparison of these results with those of Nepogod'ev and Podval'nyi⁽²⁴⁾, which were summarised in

the theoretical section. These Russian workers were, however, primarily concerned with the effects of radiative heat transfer to the oil films, and it is clear that the phenomena occurring in the ring-packing region of diesel engines are more suited to experimental than theoretical treatment.

Records from the transducers situated below the uppermost ring (e.g. Figure 14, bottom frame) show no temperature transients, thus indicating the excellent sealing of the top ring and concurring with the results of Englisch⁽⁴⁾ who showed that this ring supports the majority of the pressure drop through the ring packing.

A further point indicated by the results is the almost uncanny repeatability of the temperature transients over a series of engine cycles. Figure 16 (upper frame) shows a series of consecutive cycles which, apart from the 50 Hz. pick-up, are identical in all respects. Whilst this could not be regarded as conclusive proof, such repeatability would indicate that the top ring groove remains filled with oil - at least in the region of the transducer - for if there were gas (or an oil/gas froth) present the turbulent nature of its behaviour during the diesel cycle would undoubtedly lead to cyclic irregularities in the temperatures behind the top ring.

ii. Film thermocouples

The absence of temperature transients on the records from the film thermocouples was noted in the previous chapter, but it must be stressed that this "negative" result was expected. In comparison with the lubricating oil the thermal inertia of the piston material is enormous, and only under conditions of direct exposure of the surface to intense radiation or convection would any transient response be possible. Thus the principal purpose of these transducers was as a further indication of the presence or absence of a lubricating oil film. If, for example, the transducer immediately above the top ring became entirely starved of the thin lubricant film with which it would normally be expected to be covered, then the combustion transients would, even through the narrow passage between piston and liner, have sufficient energy to communicate a temperature transient to the transducer. There is slight evidence of such conditions existing in the single result obtained at full engine output power (Figure 16, lower trace), where a transient of 0.5°C . amplitude was detected. Thorough examination of this condition would require operation of the engine at even higher output powers (by supercharging, for example) where

the absence of lubricant could eventually lead to scuffing. However, the test rig was not designed for such operation, and further examination of this aspect of the work could not be undertaken.

iii. Overall piston temperatures

In view of the great volume of work already published on the operating temperatures of diesel pistons, including the detailed isotherm plots produced by such workers as Keig and Bailey⁽¹⁰⁾, Ip⁽⁹⁾, Britain⁽¹²⁾, Steiger and Aue⁽¹⁶⁾, and Whitehouse⁽¹⁴⁾, the steady state temperature records - which were a by-product of the transient temperature measurements - contribute nothing further to present knowledge. It will be noted that the oil temperatures invariably lie some few degrees above the adjacent metal surface temperatures, this being another factor contributing to the inaccuracy of lubricant temperature assessments from measurements made in the piston.

The high mean temperature attained by the oil on the thrust face behind the top ring (transducer A1) at high b.m.e.p., is typical of diesel engine operating practice (Figure 1), and , together with the temperature transients described in the previous section, will always present difficulties of operation in respect of ring "gumming".

iv. Vibration transducers

Having carried out the elaborate calibration and thermal testing of the vibration transducers as described in Appendix IV, the first check on the results was made by comparison of the piston-to-liner clearance measurements with those of other investigators. Such measurements had been made by Elford (unpublished work carried out at A.R.L., Teddington) who found that in the case of a piston running with adequate lubrication, the piston slap occurred between 6° and 8° after T.D.C., All the results show this condition, and are in agreement with those of Elford in many other details. No comparable results were available for the piston-to-ring clearances, but as the ring appeared to be running in close proximity to the liner through most of the engine cycle, the similarity of the results gave sufficient confidence of their probable fidelity.

The results of greatest interest were obtained by electronic subtraction of the two measured clearances, these indicating the clearance between ring and liner and its variation during the engine cycle. As outlined in the previous chapter, the processing necessary to obtain an individual result to the required precision was complex, and could only be used for selected results where the

transducer characteristics could be matched and where their operating temperatures were precisely known. Finally three such results were obtained, these being at low, medium, and high engine loads, and are presented in Figures 18 (lower frame) and 19, and Table 2.

It remains questionable as to whether the clearances shown in these results are completely filled with lubricant, but as (i) the position of the piston-slap, being in

concurrency with Elford's findings, indicates a well oiled piston,

(ii) the cycle to cycle repeatability is excellent, and

(iii) the measured clearances are in the order of only

a few microns,

it is reasonable to assume that the measurements are in fact of the oil-film thickness between ring and liner.

Very thin lubricant films (averaging up to 0.0005" or 12 microns) were recorded at all three test conditions, with a reduction to zero film thickness at the beginning of the expansion stroke.

As with the transient temperature results, the data collected were not of sufficient quantity to permit correlation with engine operating variables, but at least trial comparisons with the two lubrication theories could be attempted.

Den Besten⁽²⁰⁾, in connection with whom the "thermal wedge" theory was presented in the theoretical section of this work, uses three basic premises:

- i. that hydrodynamic lubrication exists during most of the cycle,
- ii. that the gas loading on the back of the ring predominates during firing.
- iii. that the hydrodynamic lubrication follows Fogg's "thermal wedge" theory.

The results obtained show no evidence of the first condition, but favour the second in so far as the gas loading due to firing reduces the oil film thickness to zero during the initial part of the expansion stroke.

For the condition of the result shown in Figure 19, where $N = 950$ r.p.m., b.m.e.p. = 36.1 p.s.i., and the lubricant temperature (taken from the nearest piston surface thermocouple) = 93°C ., the thermal wedge theory yielded the following estimation of the mean oil-film thickness: Using an assumed average ring rail loading, p , of 100 p.s.i., and for the assumption that the mean piston speed will give an estimate of the mean oil-film thickness,

$$h = 0.00417 (\mu \cdot U \cdot B)^{\frac{1}{2}} / p^{\frac{1}{4}}$$

where μ = lubricant viscosity, lb.s./in².
 U = piston speed, in./s.
 B = ring width, in.
 p = unit load on ring, p.s.i. (ring rail loading).
 and h = oil-film thickness, in.

For this particular case, the mean oil-film thickness, $h = 6.1 \times 10^{-6}$ in. Whilst it is only possible to make an assumption of the ring rail loading, and similarly the viscosity is only approximately correct, it is clear that this theory predicts much thinner oil films than those measured.

Eilon and Saunders⁽²¹⁾ used the relationship -

$$F_m = \frac{A \cdot \eta \cdot U}{h_m}$$

where A = ring face area,
 F_m = mean friction force,
 η = viscosity coefficient,
 and U = mean piston velocity.

- to assess the oil-film thickness. Measurements were made of the friction losses in the Petter engine by carrying out motoring tests at hot conditions. This yielded a motoring mean effective pressure of approximately 30 p.s.i. at 1000 r.p.m., from which it may be assumed that approximately 40% is lost to piston ring friction. Knowledge of the piston area leads to the estimate of a friction loss of 24 lb. per ring.

Using the above relationship for the same conditions as in the previous calculation, an oil-film thickness of $h = 0.1 \times 10^{-3}$ in. results.

As the measured film thickness was 0.2×10^{-3} in. for

this case, the correlation with the latter theory is encouraging. Further theoretical treatment cannot be carried out without more precise knowledge of the instantaneous conditions of friction, temperature, and pressure on and around the top piston ring. In the lightest load condition, for example, a thicker oil film (0.0005") was recorded, but the above equation is insensitive to the effect of the reduced ring-rail loading without detailed knowledge of the instantaneous friction forces.

Any improvements in accuracy and response of the measuring system could only come from improved transducer design, where ideally a linear response to displacement and a much improved thermal drift performance is required. The nature of the transducer and the unusually small size requirements unfortunately put such developments beyond the range of present technology. Increase of the system bandwidth (by raising the carrier frequency) would yield better resolution of the calibration marks, but only at the expense of overall sensitivity; in fact there is no doubt that these measurements represent the limit of feasibility of the A.E. instrumentation system.

v. Correlations between results

As mentioned in the introductory chapter, it was

expected that the complete instrumentation system could be used to maximum advantage in the examination of blow-by phenomena, where temperature and vibration transients could be tracked simultaneously as they passed through the ring packing. In fact, despite careful examination of many traces, there was no evidence of the temperature transients below the top ring or the radial inward movement of the rings that would indicate serious blow-by.

The only correlation that can be made concerns the obvious relationship in the timing of the temperature transients behind the top ring and the thinning of the ring-to-liner oil film. Clearly the pressure and temperature transient which communicates from the combustion chamber to the space behind the top ring during the expansion stroke is responsible for both phenomena.

vi. Suggestions for further work

Any extension of this work would probably gain most from pursuit of the oil-film thickness measurements, especially into the "scuffing" regime of engine operation. The means of carrying out such experiments is by no means clear, however, as the instrumentation system used here would not withstand any further increase in piston

temperatures. Alternative methods of measurement of oil-film thicknesses are by optical interference techniques - using a vertical quartz slit in the liner as the viewing section, or by low voltage electrical resistance measurements. Both methods are fraught with experimental difficulties, however, and current experiments using these techniques have so far been fruitless.

CONCLUSIONS

Close examination of the thermal and vibrational performance of the ring-packing region of a diesel engine piston, with particular attention paid to the uppermost ring, has led to the following conclusions.

Conditions which could lead to cyclic thermal overstressing of the lubricant in the region of the top piston ring have been measured at high engine output powers. Such conditions are created by the superposition of cyclic temperature transients, due to passage of hot combustion products down the side of the piston during the expansion stroke, on the steady operating temperature, which, at high loads would already be close to the maximum operating temperature of the lubricant. It is believed that the gradual decomposition of unburned fuel and oil particles by these temperature transients is the true mechanism of piston ring "gumming".

Oil-film thickness measurements have been made of the piston ring/liner combination under diesel operating conditions, these being the first such measurements known to be recorded. Oil-film thicknesses generally were of the order of 5 microns, reducing to zero at the instant of combustion. The results favour Eilon and Saunders' theory of hydrodynamic lubrication, and the effect of the

combustion pressure on the back face of the top piston ring appears to play a greater part in determining the lubricant thickness than was previously supposed.

REFERENCES

1. Englisch, C., "Practical experiences of Diesel engine piston rings for medium and heavy duty", D.A.R.O.S. Conference, April 1966.
2. Englisch, C., "Piston rings for high duty I.C. engines", C.I.M.A.C. Conference, 1965.
3. Englisch, C., "Design, manufacture, and selection of piston rings for Diesel engines", Trans.Inst. Marine Engrs., March 1967.
4. Englisch, C., Kolbenringe, Springer Verlag, Wien. 1958. (2 volumes).
5. Englisch, C., "Einige Kolbenring-Betriebsprobleme bei Mittel-und Grossmotoren", M.T.Z. Jahrg. 18.Nr.11. Nov. 1957.
6. Englisch, C., "Kolbenringe für grosse und mittelgrosse Schiffs-dieselmotoren", M.T.Z. Jahrg. 28. Nr.3. 1967.
7. Englisch, C., "Daros Kolbenringe und Dichtungsprobleme bei Dieselmotoren", Schiffs-Ingenieur Journal 12, Nr. 59. 1965.
8. Janota, M.S., "An experimental survey of component temperatures in small high speed loop scavenged two stroke diesel engine with varying simulated turbo-charging conditions", ** (see below).

** - All papers marked with this symbol are from the 1964 Symposium "Thermal loading of diesel engines", Inst. Mech. Eng. 179, 3c, 1964.

9. Ip, E.S., "Temperature distribution in diesel engine pistons", The Engineer, Nov. 30, 1962. p. 935.
10. Keig, R.J.B. and Bailey, G.L.J., "Heat flow and stresses in pistons for medium speed C.I. engines", Admiralty Eng. Lab. Report 127, 1941.
11. Fitzgeorge, D. and Pope, J.A., "An investigation of the factors contributing to the failure of diesel engine pistons and cylinder covers", Trans.N.E.Coast Inst. Engrs. and Shipbuilders, Vol.71, p. 163, 1955.
12. Britain, E.W.M., "Thermal loading of small high speed two stroke diesel engines", **.
13. Eichelberg, G., "Some investigations on old combustion engine problems", Engineering, Vol. 148. Oct.27, 1939, et. seq.
14. Whitehouse, N.D., Stotter, A. and Gray. C., "Piston thermal loading", **.
15. French, C.C.J. and Hartles, E.R., "Engine temperatures and heat flows under high load conditions", **.
16. Steiger, H.A. and Aue, G.K., "The influence of thermal loading criterion on the design of turbo-charged two-stroke diesel engines". **.

17. Fujita, H., "Service records of Mitsubishi Nagasaki diesel engines and improvements", Trans. Inst. Marine Engrs. Vol. 73, Feb. 1961.
18. Brock, E.K. and Glasspoole, A.J., "The thermal loading of cylinder heads and pistons on medium speed oil engines", **.
19. Shaw, M.C. and Macks, F., Analysis and lubrication of bearings, McGraw-Hill, New York, 1949.
20. Den Besten, J.A., Leverenz, E.G. and Bloom, C.M., "A modern approach to piston ring-bore assembly wear determination", S.A.E. Jan. 10-14, 1966.
21. Eilon, S. and Saunders, O.A., "A study of piston ring lubrication", Proc. Inst. Mech.Eng. Vol. 171, No. II, 1957.
22. Firth, B.W. and de Malherbe, M.C., "The piston problem and the designer", The South African Mechanical Engineer, Oct. 1966.
23. Stillbroer, C. and Wassenaar, H., "Temperatures of pistons and valves of various I.C. engines", Bericht Internat. Kongress für Verbrennungsmotoren, Paris, May 1951.
24. Nepogod'ev, A.V. and Podval'nyi, L.D., "Computed determination of oil-film temperatures at the working surfaces of an I.C. engine cylinder", Energo Mashinostroenie, 1966 (8).

25. Dykes, P. de K., "Piston ring movement during blow-by in high-speed petrol engines", M.I.R.A., R/12, 1947.
26. Steinbrenner, H., "Messungen zur Erfassung des Kolbenringflatterns in schnellaufenden Kolbenmaschinen", M.T.Z. 7.Juli. 1961.
27. Flynn, G. and Thompson, F.D., "Fatigue testing of engine parts for thermal and dynamic loading", **.
28. B.I.C.E.R.A., "A simple intermittent contacting system for thermocouples in an engine piston", B.I.C.E.R.A. Bulletin, March 1961.
29. Associated Engineering Ltd., "Telemetering system for I.C. engines research", Engineering Materials and Design, May, 1962.
30. Baldwin, Lima, Hamilton Corporation, "High temperature micro-miniature thermocouples-basic theory", B.L.H. Data sheet 4336-1.
31. Laderman, A.J., Hecht, G.J., and Oppenheim, A.K., "Thin film thermometry in detonation research", Temperature, its measurement and control, Vol.3, Part 2, 1962.
32. Bendersky, D., "A special thermocouple for measuring transient temperatures", Mechanical Engineering, Vol. 75, 1953, p. 117.

33. Moffat, R.J., "The gradient approach to thermocouple circuitry", Temperature, its measurement and control, March Symposium, 1961.
34. Wing, R.D., "The motion of engine piston rings", Imperial College, D.I.C. dissertation, 1962.

APPENDIX IDESIGN AND CONSTRUCTION OF THIN-FILM THERMOCOUPLES

Eichelberg's⁽¹³⁾ measurements of the surface temperatures of piston rings, as reproduced in Figure 2, were arrived at by extrapolation to zero of temperature records taken at 0.5, 2.0, and 5.0 mm. from the metal surface. The measurements show how rapidly surface transients are damped as they penetrate the surface of the material, and it is clear that the only true picture of the real surface state would be given by a transducer that is either part of the surface, or is close enough to the surface to be regarded as such.

A surface thermocouple which virtually fulfils this condition, having a junction thickness of only a few millionths of an inch, has been reported by Bendersky⁽³²⁾. The application described is for surface temperature measurements in gun-bores, and the design appears to originate from research in Germany dating back to the last war.

It was found that such a thermocouple could be made in very small sizes, suitable in fact for piston instrumentation, and by virtue of the junction dimensions would fulfil the response-time requirements as previously specified.

Plate 13 shows the construction of the thermocouples as designed for this work. The outer casing consists of an iron tube which is shrunk onto a 0.010" diameter nickel wire. The nickel wire is coated with a film of nickel oxide, a semiconductor which in this application acts as an effective insulator between the two thermocouple metals. On the active face of the transducer the surface is coated with a film deposit of nickel, thus completing the thermocouple circuit and creating a surface junction having a thickness only as great as that of the deposited film.

Choice of the metals used was governed by a number of requirements, including:

- i. the thermocouple output e.m.f. should be reasonably large.
- ii. the thermal expansion coefficients of the metals should be very similar in order to avoid damage to the insulating oxide film.
- iii. both metals should have mechanical strength suitable for use in the diesel engine application.
- iv. the thermal conductivities of the metals should be as close as possible to that of the surface being studied, in order that the transducer does not interfere with the overall heat transfer pattern of the surface.

Nickel and iron proved to be a very suitable combination, the iron being chosen for the outer casing on

account of its ready availability in preformed tubes. As shown in Plates 13 and 14, the final transducer was in the form of a slug of 0.090" diameter x 0.25" length, and these were inserted as a light drive fit into the piston surface where required, the output lead-wires being carried through holes drilled from the inside of the piston.

Manufacture of the film thermocouples

The nickel wires were first prepared, approximately 50 ft. being wound onto a former and heated at 1200°C. for one hour in an atmosphere of carbon dioxide. The resulting nickel oxide coated wire was then cut into lengths of approximately 6".

The iron tubing (as supplied by Messrs. Accles and Pollock Ltd.) was of nominal 0.10" O.D. and 0.010" I.D. Short lengths were prepared for assembly by lapping the hole with powdered alumina and machining a feed taper on one end. The nickel wire was carefully inserted into the lapped hole, the tube inserted into a die and drawn down to 0.090" O.D., this producing the necessary "squeeze" on the nickel wire to generate clamping pressure without damaging the oxide film.

Discarding the tapered end of the drawn tube, the remainder was trimmed to $\frac{1}{4}$ " length and the face polished

to a $\frac{1}{4}$ micron surface finish. The specimens in this stage were then stored in "Chloroethene" (a solvent having very low water content) for the final plating process.

The nickel film deposition was carried out on equipment loaned by courtesy of the Services Electronics Research Laboratories, Baldock. An "Edwards" high vacuum coating unit (Model 12EA/838) was used, this essentially consisting of a large bell-jar within which vaporisation of metals could be carried out at very low pressures.

It was found that in order to achieve satisfactory adhesion of the metal film to the specimen surface it was necessary to pre-heat the specimen to approximately 650°C ., and the final arrangement within the bell-jar was therefore as shown in Plate 12. The upper copper beam clamps six specimens, these hanging vertically downwards by their lead-wires. A heater coil of 0.040" diameter tantalum is coiled around the charges and connected to the input current terminal posts, a Chromel/Alumel thermocouple also being installed close to the specimens to check their pre-heating temperatures. Below the

specimens and the heater coil may be seen the charge-wire, which consists of a 0.030" diameter tungsten rod, the centre 2" being wound with a 10 cm. length of 0.010" diameter nickel wire which, in turn, is overwound with 0.010" diameter tungsten wire (see lower frame of Plate 12).

In operation the bell-jar was evacuated to 5×10^{-5} mm.Hg., and the tantalum heater operated at 20 Amperes for 15 minutes, this providing the required 650°C . specimen preheat temperature. The nickel was then evaporated by passing 20 A. through the tungsten charge-wire, which produced the temperature of some 1500°C . necessary to vaporise the nickel.

The film thickness of deposited nickel was determined by precision weighing of the specimens before and after the evaporation, a weight increase of 36 μgm . producing a 1.0 micron nickel film. Specimens were also tested for adhesion of the film, the test being simply whether or not "Scotch-tape" pressed onto the surface could peel off the film. Plate 13 shows a microphotograph of the front surface of a typical thermocouple, and it can clearly be seen how the plated film bridges the nickel oxide annular gap between the nickel and iron surfaces,

so producing the thermojunction.

With so complex a manufacturing process, the failure rate of the specimens was high, and it is of interest to note the following table which lists the failures and their causes:

Initial number of specimens prepared.....	80
Damaged in polishing process.....	12
Lead-wires broken in handling.....	4
Short-circuit.....	26
Low resistance	3
Unsatisfactory adhesion of plating	10
	<hr/>
Usable remainder.....	25
	<hr/>

The most common cause of failure was the short-circuit or partial short-circuit (low resistance) caused by breakdown of the nickel oxide insulating film during the drawing process.

Calibration

A selection of thermocouples was calibrated to determine the output e.m.f. versus temperature relationship. Consistency between the various thermocouples was excellent, and a single calibration curve could be used for all the transducers (Figure 21). The calibration was carried out in a mechanically stirred silicon

oil bath, measurements being taken on the cooling cycle, working to an accuracy of $\pm 0.1^{\circ}\text{C}$. against a standardised Chromel/Alumel thermocouple.

The dynamic response of the thermocouple was carried out in a shock-tube, the facilities being kindly made available by the Aeronautics Department of Imperial College. With the transducer mounted in the endwall of the shock-tube, its output response was recorded on an oscilloscope and the time constant evaluated. The response proved to be much faster than expected, and presented some difficulties in recording. However, it was estimated that the time-constant, τ , lay somewhere between 1 and 5 μs .

Installation

The finished thermocouples were fitted into precision-drilled holes in the piston surface at the points indicated in Figure 11. A micro-reamer was used to provide seating for the back-face of the transducers, and "Loctite" adhesive sealed the transducers securely into place. Output lead-wires were insulated and led through narrow holes drilled through from within the piston, and these were terminated on the flexible printed circuit shown in Plate 9.

APPENDIX IIAMPLIFIER DESIGN FOR THIN-FILM THERMOCOUPLES

The problems of high accuracy, low drift amplification of very low voltage signals, such as are received from thermocouples, were briefly outlined in the chapter on experimental apparatus. The film thermocouple described in Appendix I gives an output of approximately 5 mV. for 200°C. junction temperature, and therefore to achieve a resolution of 0.5°C., it is necessary for the amplifier to be able to resolve 12 μ V. signal levels.

Such low voltages are below the normal noise and drift levels of conventional amplifiers, and it was necessary to use very sophisticated devices for this work. In the initial stages of the project no such high performance amplifiers were available, and the system shown in Figure 22 was built up. Although this amplifier - referred to here as System I - was not adequate for the work, it is worth brief description as it highlights many of the problems of low voltage amplification.

System I uses a technique whereby the majority of the thermocouple output (its d.c. component) is backed-off, and the remaining voltage, comprising mostly a.c. components,

is amplified for display. Referring to Figure 22, a thermojunction is shown, which feeds into the 60°C . transistor controlled oven within the piston, and then into the voltage back-off circuit, where a precision multi-turn potentiometer injects a known voltage into a $0.5\ \Omega$ high stability series resistor. A second voltage injection circuit is bridged across the amplifier input leads to provide a calibration checking voltage, and by use of contact breaker points A and B, the zero and calibration voltages are superimposed onto the signal. In practise, the contact points used were miniature magnetic reed switches, driven by the engine camshaft, each closed for 5 degrees of crank-angle once every engine cycle.

The amplifier employed was an S.G.S.-Fairchild type $\mu\text{A}702\text{C}$ transistor microcircuit, operated at a gain level of 60 db. By virtue of its extremely small size - the amplifier case was 9 mm. diameter by 5 mm. high - the whole microcircuit could be operated within a controlled temperature environment, thus minimising thermal drift.

As shown in the inset of Figure 22, the gain curve of the amplifier rolls off at about 60°C , and choosing this as the amplifier operating temperature, gain stability was further improved. A transistor-controlled oven was

used to contain the amplifier at a regulated temperature of $60^{\circ}\text{C.} \pm 1^{\circ}\text{C.}$

Various problems were encountered with this system, including insufficient common mode voltage rejection, high frequency transistor noise, drift of the offset voltage, and instability when the "zero input" contact breaker points were closed. Before improvements were made to this system, however, new developments in precision instrumentation amplifiers made further pursuit of System I pointless.

The basic circuitry of System II, as was used in all final test runs, is shown in Figure 23. The amplifiers were manufactured by Messrs. Analog Devices Ltd., Kingston, Surrey, (Model 180B), and these are representative of the best that is currently available in high performance instrumentation amplifiers. Exceptionally low drift performance is achieved by use of selected dual-transistors for the long-tailed-pair input stage (see insert of Figure 23). In this application it seemed advisable from previous experience with the System I amplifier to seek the highest possible common mode rejection ratio (C.M.R.R.), as stray "pick-up" seemed to be very high on this rig. To this end a differential input/differential

output circuit was employed, as shown in Figure 23, which, by careful selection of R1 and R2 gave a C.M.R.R. of 120 db., although at the expense of having to use a pair of these amplifiers.

Resistors R3, R4, and R5 determine the overall amplifier gain, which for this application was set to precisely 60 db., resulting in a system frequency response of d.c. to 7 kHz. flat, 3 db. down at 8 kHz. The amplifiers were battery driven, and the complete circuit layout is shown in Figure 24.

Thermocouple switching

To avoid the expense of providing separate amplifiers and data storage channels for all thermocouples, fast switching was employed whereby the six film and six bead thermocouples were consecutively sampled, each for the duration of one engine cycle. The switching speed was beyond the capabilities of mechanical relays, yet not sufficiently fast to justify solid-state switching, and consequently a simple magnetic reed-switch bank was used and found to be adequate at the rotational speeds of the Petter engine.

Basically, the reed-switch unit consisted of a circular array of 12 reeds, six connected to thin-film,

and six to bead thermocouples. A perspex arm carrying magnets at each end was coupled through reduction gearing to the engine output shaft and rotated amongst the reeds, thus selecting different thermocouples once each engine cycle. The entire unit was built into heavy aluminium casing, as the thermocouple voltages were low enough to require extensive shielding, and this may be seen in the centre foreground of Plate 2.

Amplifier for the bead thermocouples

The less stringent bandwidth requirements for the bead thermocouples permitted use of a commercial amplifier system. The model chosen was the type 1602 by Messrs. Comark Electronics Ltd., of Littlehampton, an amplifier with correct compensation for Chromel/Alumel thermocouples which gave an output (suitable for direct recording onto tape) of 10 mV. per $^{\circ}\text{C}$. at 1% accuracy.

APPENDIX IIIDESIGN OF PISTON LINKAGE

Electrical measurements within an engine piston are only of value if a satisfactory means of transmitting the information to the outside world is possible. The various methods available - radio telemetry, B.D.C. contacts, etc. - were described in a previous chapter, where it was shown that for the fast response instrumentation and the nature of the required results only the continuous contact data link would be suitable for this work.

The first design for a linkage mechanism which could carry instrument wiring away from the piston of a high speed engine was by Steinbrenner ⁽²⁶⁾. This used a narrow steel pipe rigidly attached to the inner edge of the piston skirt, positioned vertically with the bore axis. To the lower end of this pipe two long flat spring-steel strips were attached, each terminating in sprung attachment arms at the end of extension boxes built into opposite crankcase doors. The wiring was carried from the piston transducers, through the centre of the pipe, along the surface of the steel strips, and onto further steel strips from the ends of the attachment arms to termination posts on the crank-casing. Tension on the spring-steel

strips permitted vertical movement of the pipe, the opposing tensions producing a balanced system.

Most I.C. engines have insufficient accommodation for this type of linkage, but with the Petter engine it was found that by moving one of the balance weights approximately $\frac{1}{4}$ " further away from its normal position in relation to the connecting rod, a modified form of such a linkage could be used. To improve rigidity a strut of 1" x $\frac{3}{8}$ " cross section was used in place of the pipe described above, and the spring-steel strips replaced by stainless-steel hyperdermic tubing with ball-bearing joints at each end. The hyperdermic tubes were kept under constant tension by coil springs built into special extension boxes on the crankcase doors.

Sectional views through various parts of the linkage are given in Figures 25 to 27, and details may be seen in the photographic Plates 2, 5, 7, 8 and 10.

Referring to Figure 25, and initially examining the piston end of the linkage, the wiring from all thermocouples, vibration transducers, etc., was brought to a pair of 20-way soldered termination patchboards which were incorporated in the top bracket of the piston strut (Plate 8).

The strut, although of substantial cross sectional area, was of laminated construction, consisting of 1/4" thick "Tufnol" sheet sandwiched between a pair of 1/16" outer steel plates, and, as may also be seen in Plate 8, generously perforated for lightness.

The 40 lead-wires (0.010" diameter enamelled copper) were brought through the centre of the strut to the inner spring terminations where they again separated into two groups of 20 wires each. Miniature loops of Bowden cable were used for the inner springs, which performed the function of allowing the electrical wiring to bridge the joints of the linkage with minimum flexure. The lead-wires were wound spirally onto the Bowden cables, bonded into place with shrinkable plastic sleeving, led around the lower joint in a slender arc, and thence into the hyperdermic tubing of the reciprocating linkage arms.

The pair of linkage arms, one of which is shown in Figure 26, were of 0.125" O.D. x 0.100" I.D. stainless steel tube, and were each terminated with ball-bearing carriers. The inner terminations were simple twin ball-bearing joints, fitting onto pins at the bottom end of the piston strut. At the outer ends, however, a more complex mechanism was used whereby the linkage could be kept in

constant spring tension to prevent "whipping" of the reciprocating arms at high engine speeds. The spindles at these outer terminations each carried four ball-bearings, of which the inner pair carried hooks to transmit spring tension, and the outer bearings ran in 3/8" guide slots to permit horizontal movement of the linkage arms. The hook and guide slots are clearly shown in Figure 27, and the attachment boxes which were built into the crankcase doors of the engine in order to accommodate them are shown in Plates 2 and 5. The screwed spring tensioning rods were set to give a tension of 8 lb. on the linkage arms at their outermost position.

The electrical wiring having passed through the linkage arms was brought at the outer ends onto further C - springs of the same Bowden cable construction as the inner springs described above. Figure 27 and Plates 7 and 8 show the outer springs, which were anchored onto the crankcase extension boxes, and all the wiring which was brought out to multi-pin plugs for connection to the various instruments, amplifiers, power supplies, and recorders.

The linkage in this form gave many hours of satisfactory

operation, including some prolonged runs at full engine speed (1800 r.p.m.). In the prototype design the major problems were all associated with the delicate inner and outer springs carrying the electrical wiring. Early designs used piano-wire and Beryllium-copper as the spring material, but both had short fatigue lives. The spiral construction of the Bowden cable with the electrical wiring shrunk onto the outer surface by thin plastic sleeving proved to be sufficiently flexible and durable for use in the final version of the linkage.

APPENDIX IVSUPPLEMENTARY INSTRUMENTATION FOR ENGINE RIGi. Dynamometer load cell

From past experience it was considered that one of the most tedious measurements during engine testing was the reading of brake loads and continuous checking of their consistency. The exceptionally short duration of these engine tests, and consequent shortage of time for taking measurements led to the necessity of a more streamlined version of the usual mechanical brake load meter. This took the form of an electrically amplified load cell with a meter output display on the engine operating panel.

The load cell consisted of a 1" x 0.005" strip of Beryllium - copper attached at one end to the engine test bed, and at the other to a radius arm extending from the dynamometer casting. Thus the engine output torque was directly transformed to tensional strain in the strip, the end terminations of which were fitted with knife edges for certainty of alignment. Strain gauges in half-bridge configurations were bonded to the Beryllium - copper strip and led to a d.c. amplifier to drive the

display meter. The amplifier was an S.G.S. - Fairchild type μ A702C (as described in Appendix II) used in the circuit shown in Figure 28, and powered from a mains operated +14 : 0 : -14 V. d.c. power supply. The variable resistor in series with the amplifier output permitted calibration of the output display meter in lb. units of brake load.

ii. Overspeed trip

The reasons given above for the necessity of a rapid means of brake-load measurement apply equally to the overspeed trip. To avoid use of extra manpower whilst operating the engine rig it was necessary to provide complete protection against overloads with a comprehensive "fail-safe" protection device. The essential components of this device were described in an earlier chapter and illustrated in Figure 6, but one somewhat novel aspect - the overspeed protection - has been left for further explanation.

An electromagnetic coil in the engine-speed indicating device was used as the sensing element for overspeed trip circuit. A "Hasler" type 5.3330.008 tachometer transmitter was fitted to the Petter engine for measurement

of engine speed, this being in the form of a single phase a.c. generator producing an output voltage proportional to rotational speed, and capable of driving an a.c. voltmeter type of indicator. The particular tachometer transmitter used was fitted with two output coils, the second of these providing an optional facility of driving an additional indicating instrument. In this application the output voltage from the second coil was used to drive a voltage overload sensing circuit which, in turn, triggered the engine shut-down relay.

Figure 6 shows the complete overspeed sensing circuit. The output from the second coil on the "Hasler" tachometer was led into a full wave rectifier and the d.c. output voltage backed-off against an 87 Volt Zener diode. Using a trip relay with an operating voltage of 6 Volts it was possible to trigger the engine shut-down circuit when the output from the rectifier reached 93 Volts. A 1 k Ω variable potentiometer permitted limited variation of the rectifier input voltage and consequently of the speed at which the trip operated, the range being 1400 to 2000 r.p.m.

The high voltage Zener diode was made up of a series

of low voltage diodes connected in series. Such connection gives a sharper "knee" in the Zener characteristic and results in a more positive relay action than would be the case with a single high-voltage diode.

The output from the overspeed trip relay was connected in the same manner as the other overload circuits, its operation causing immediate interruption of the fuel supply to the engine.

iii. Crank-angle degree marker

The photoelectric crank-angle marker has been referred to at various stages in the preceding chapters, this unusual method of angular indication having proved extremely satisfactory in this particular application. For reasonable accuracy in presenting the results against a base of engine crank-angle degrees, it was considered necessary to use a fast response electronic indicator which could discriminate fractions of one crank-angle degree.

The method chosen used a photoelectric device which responded to signals from a light source chopped by a prepared disc on the engine output shaft. As may be seen in Plate 6, where the physical layout and electrical circuit is shown, the light source was a low voltage pre-focus bulb with a shield to reduce the beam aperture

to approximately 2 mm. diameter. The beam from this source was directed at an OCP71 phototransistor which was backed up by a simple trigger/output stage using a 2S322 transistor. Any interruption of the light beam produced an output voltage spike of very fast risetime, having positive or negative amplitude dependent on whether the light interruption was on/off or off/on.

An 8" diameter segmented disc mounted on the engine output shaft was used to interrupt the light beam at pre-determined crank-angle degree positions, the segments being at 10° intervals except at the outer dead centres where subdivisions of 5° and $2\frac{1}{2}^{\circ}$ were used. "Perspex" of $\frac{1}{8}$ " thickness was used for the disc, the optically dense segments being cut from black adhesive plastic film. Figure 13 shows the output pattern obtained on rotation of the engine output shaft, this forming the basis of all the oscilloscope records thereafter presented.

The photoelectric device was operated from 12 Volt batteries, and the output led to a "direct record" (a.c. coupled) channel on the Ampex tape recorder, the excellent high frequency response of which (-3 db. at 75 kHz.) permitted accurate preservation of the degree mark pulses and especially of their precise time relationship with the other recordings.

iv. Thermocouple reference oven

The thermocouple junctions within the piston whereby all output lead-wires were converted to copper wiring required an accurate reference temperature zone of size small enough to be contained within the available space in the piston. As may be seen in Plate 16, all the thermocouple junctions were gathered together as a capsule inside a copper sheath of 1/4" I.D. together with a thermistor for temperature measurement and control. Around this capsule the copper block shown in Plate 15 was mounted, the whole assembly being fixed to the inside of the piston skirt on a "Tufnol" mounting bracket.

Within the confines of the outer copper block and the mounting bracket was mounted all the transistor circuitry for heating and accurate temperature control of the thermojunction capsule. The electrical circuit is given in Figure 29, and basically consists of a 15 Ω heating coil controlled by transistor switching from a thermistor sensor within the copper block.

The thermistor, having an electrical resistance governed by its absolute temperature, biased the first

OC200 transistor, the output of which was amplified and compared to a reference voltage level derived from an OAZ203 Zener diode to produce switching bias for the pair of 2N696 power transistors. A heater coil in series with the second power transistor was wound around the thermojunction capsule and generated, together with the self heating of the power transistors, the necessary heat to raise the capsule temperature to 60°C. The stability of the capsule temperature could be held by this control circuit to within 0.1°C, but it was necessary to provide regulation of the d.c. supply voltage to at least ½% for operation at this level of accuracy.

Despite the environment and high acceleration loads imposed on the device, no trouble whatsoever was experienced during engine tests. The well-regulated voltage supply was carried to the oven through the piston linkage wiring from a Wier Electronics "Minireg" mains operated d.c. power supply. To ensure no changes in the reference junction temperature, the output of the thermistor within the thermojunction capsule was brought out - again through the piston linkage - to a chart recorder for continuous monitoring.

v. The A.E. vibration measuring system

This complete system for vibration measurement, comprising miniature inductive transducers and a multi-channel signal processing system is shown in Figure 9 in block diagram form.

The transducers were non-contact devices of 0.090" overall diameter, capable of withstanding high temperatures and vibration loadings, and having a measurement range of 0 to approximately 0.010". The top section of Figure 9 shows the construction of the transducers; a coil wound onto the centre axis of the device senses changes of inductance in the armature coil - a series of iron wires, bundled at the centre axis and forming an annular armature opening on the front surface of the transducer. The magnetic circuit is then completed by any metal surface within 0.010" of the transducer front surface, the proximity of which causes inductance changes in the coils.

For temperature compensation a second transducer was used, this having its armature circuit "short-circuited" by a 0.002" steel shim bonded onto the front surface. The pair of transducers were connected in half bridge configuration, and their physical appearance is shown in Plate 11.

A four channel signal processing unit, shown in the left foreground of Plate 2, was installed for conversion of the inductive signals to displacement amplitudes, and consisted of an oscillator, an oscillator amplifier, four detector/filter units, and the necessary power supplies. The lower diagram of Figure 9 explains the operation of the signal processing unit. A pair of inductive transducers plugged into one of the detector/filter units form the remaining two arms of a full four arm inductance bridge, individual transducers being adjusted for resistance and inductance by bridge balance controls. The bridge and the transducers were driven by a 10 Volt peak-to-peak carrier voltage of 50 kHz. from the oscillator and its amplifier. Inductance changes in the active transducer are sensed as bridge out-of-balance a.c. voltages and via the coupling transformer are amplified, demodulated, filtered to remove the carrier frequency, and appear as voltage changes at the output terminals.

The output voltage change was not linear with armature displacement, and it was necessary to calibrate each pair of transducers before operation of the system. Specimen calibration curves for two of the transducers used in this work are shown in Figure 30. A rig was

constructed for the calibration, and consisted basically of a transducer clamp and a segment of piston ring set on a micrometer screw to permit measurement of the armature gap. This rig could be immersed in a silicon oil-bath for calibration at high temperatures, and by this means the accuracy of the temperature compensation was tested. Over the specified operating range of the transducers, ambient to 150°C , the maximum deviation for a fixed signal level was 2% of the signal output voltage - Figure 31.

The long term drift of the electronics was also tested, and, as shown in the chart record in Figure 31, the worst deviation - 30 minutes after switching-on - was only 0.26% of the output voltage, the long term stability being considerably better.

vi. Specifications of recording equipment

The data recording system, as shown in the block diagram of Figure 12, was described briefly in previous chapters. An Ampex instrumentation recorder was used for collection of all data, and in order to permit assessment of the capabilities of the system, the specification is summarised below:

AMPEX FR 1300 RECORDER

Tape width - 1", permitting 14 channel recording.

Tape speed - 15 i.p.s. was used for all recordings,
and the figures below relate only to this
speed.

Tape speed deviation - 0.25% max.

Tape length - 3600 ft. per reel.

Direct record/reproduce system:

Bandwidth - 100 Hz. to 75 kHz. \pm 3 db.

Signal/Noise ratio - 27 db.

Total harmonic distortion 1.2 % for 1 kHz. signal
recorded at 60 i.p.s.

Input level - 1.0 Volt r.m.s. nominal.

Input impedance - 50 k Ω resistive.

Output - 1.0 Volt r.m.s. nominal across impedance 600 Ω .

F.M. record/reproduce system:

Frequency response - 0 to 5 kHz \pm 1 db.

Signal/Noise ratio - 45 db. r.m.s.

Total harmonic distortion - 1.2 %.

Carrier frequency - 27 kHz.

Input level - \pm 2.0 Volt max.

Input impedance - 20 k Ω resistive.

Output level - 1.0 Volt r.m.s. into impedance 10 k Ω .

A Tektronix storage oscilloscope was used for playback of the recorded data. Stored images were photographed with an oscilloscope camera using 2 $\frac{1}{4}$ " x 3 $\frac{1}{4}$ " Polaroid negative film. A brief specification of the oscilloscope is given below:

TEKTRONIX type No. 564 STORAGE OSCILLOSCOPE

Time base unit 2 B 67 - calibrated sweeptime rates of
1 μ s to 5 s. /div. at 3% accuracy.

Amplifier unit type 3 A 3 - dual trace, differential inputs.

- frequency response, - 3 db. at 500 kHz.
- C.M.R.R. up to 90 db. when d.c. coupled.
- sensitivities, 0.1 mV. to 10 Volt/div. calibrated to 3% and adjustable to 0% using external voltage reference source.

Run No.	Tape log	SPEED	BRAKE LOAD	B.H.P.	Fuel	Features
		r.p.m.	lb.	-		
1	A1740	-	-	-	Methane	Trial run.
2	A.0	950	7.7	1.47	"	Vibration records taken.
3	A300	750	-	-	"	Engine failure before stable condition
4	A540	850	11.8	2.00	"	All systems recording.
5	A825	860	11.8	2.0	"	All systems recording.
6	A1030	-	-	-	Diesel	Trial run on diesel fuel.
7	A1290	1000	14.0	2.80	"	Bead thermocouple records.
7a		600	Motored under compression			
8	B.0	1000	10.5	2.10	Diesel	All systems recording.
9	B1050	850	7.3	1.24	"	" " "
10	B1510	1050	13.5	2.85	"	" " "
11	C.0	1420	0	0	"	" " " (no load)
11a		1330	22.5	6.00	"	" " " (full load)

Table I. - List of engine trials and their main features.

Engine speed (r.p.m.)	b.m.e.p. (p.s.i.)	B.H.P.	Amplitude of temperature transient °C.
1420	0	0	16.5
850	34.1	1.24	19.0
1050	63.2	2.85	32.0
1330	106.0	6.00	36.0
1000	49.3	2.10	40.0
1000	65.5	2.80	44.0

Engine speed (r.p.m.)	b.m.e.p. (p.s.i.)	B.H.P.	Oil film thickness (inch)
1300	0	0	0.0005
950	36.1	1.47	0.0002
1330	106.0	6.00	0.0002

Oil film thicknesses given are the mean values of the ring-to-liner clearance during the engine cycle. As shown in the diagram below, this reduces to zero just after T.D.C.(firing stroke). In the last case (6.00 B.H.P.) an increase in clearance of 0.0003" amplitude is apparent immediately before T.D.C. (shown dotted).

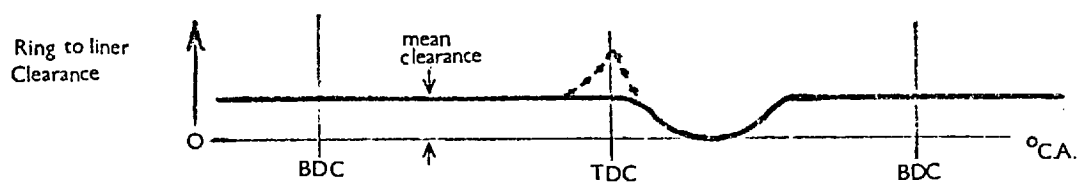


Table 2. - Temperature transient and oil-film thickness measurements.

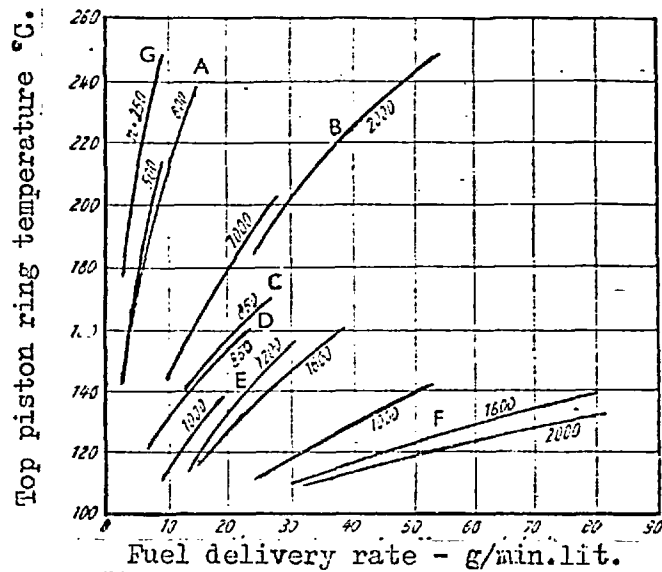


Fig. 1. Variation of top piston ring temperature with fuel delivery rate for a variety of diesel engine types and sizes.

Engine	Construction	Bore mm.	Stroke mm.	Cap. litre	Piston material
A	4-stroke Turbulence chamber	190	260	7.4	Alumin.
B	4-stroke Turbulence chamber	115	140	1.45	Alumin.
C	4-stroke Direct injection	152	203	3.7	Alumin.
D	4-stroke Pre-combustion chamber	145	200	3.3	Alumin.
E	4-stroke Direct injection	108	152	1.4	Alumin.
F	2-stroke, direct flow Direct injection	108	127	1.16	Cast Iron
G	2-stroke, cross-flow	480	700	110.	Cast Iron

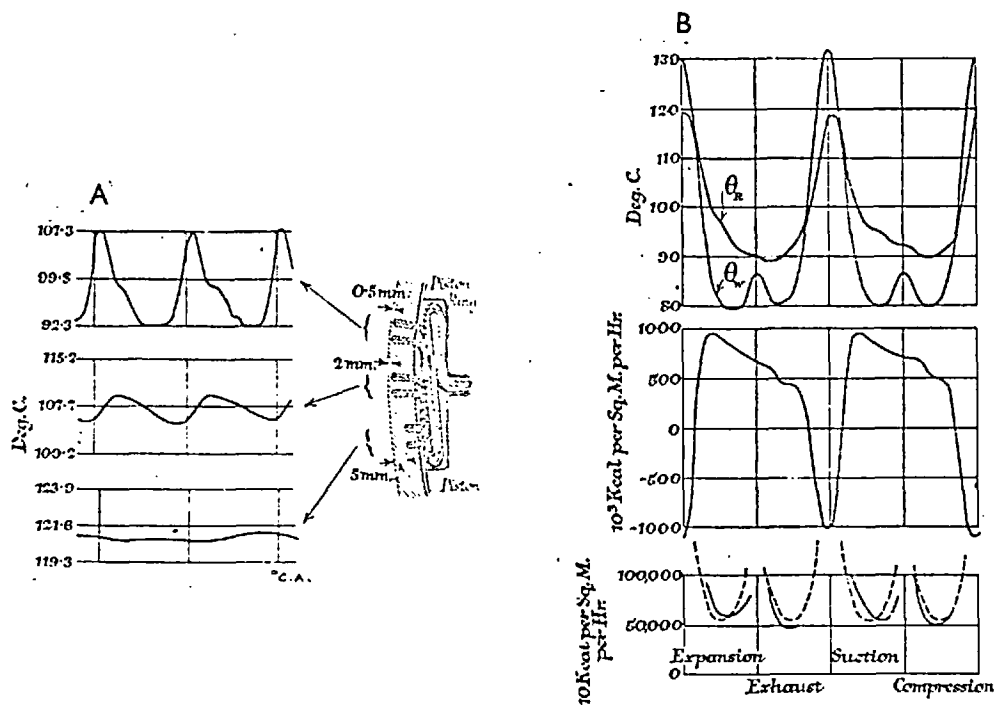


Fig. 2. - Cyclic variations in piston ring temperature as measured by Eichelberg.

A - Variation of piston ring temperature with crankshaft rotation at various depths from surface.

B - Heat flow through the ring as computed from the temperature measurements -A.

Engine data : 4-stroke diesel with no piston cooling.
 Bore = 230 mm.
 Stroke = 420 mm.
 Speed = 211 r.p.m.
 i.m.e.p. = 7.5 atn.

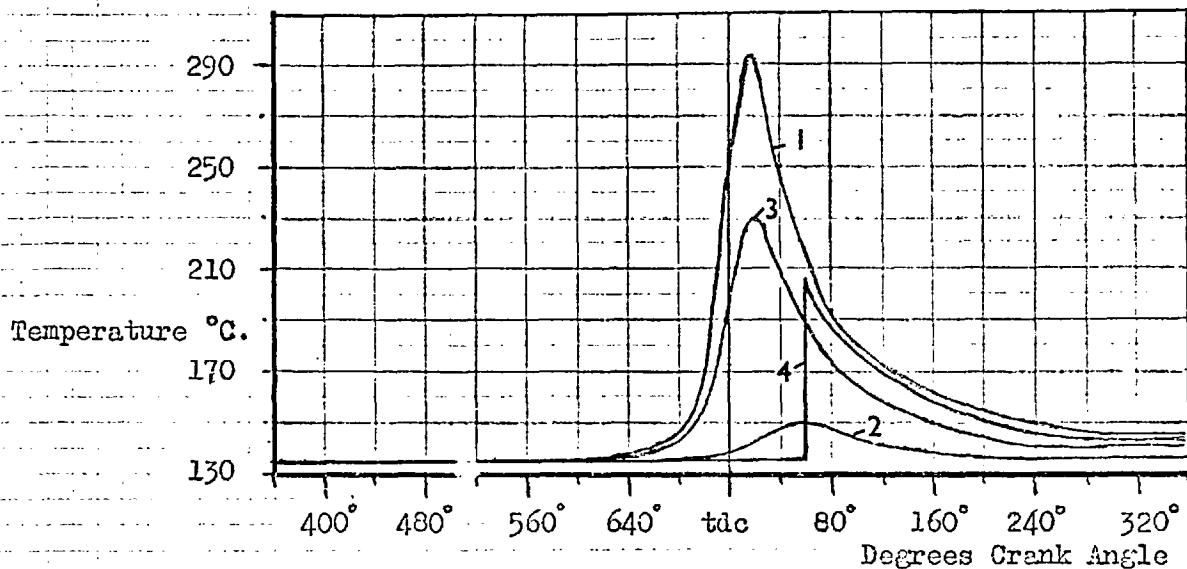
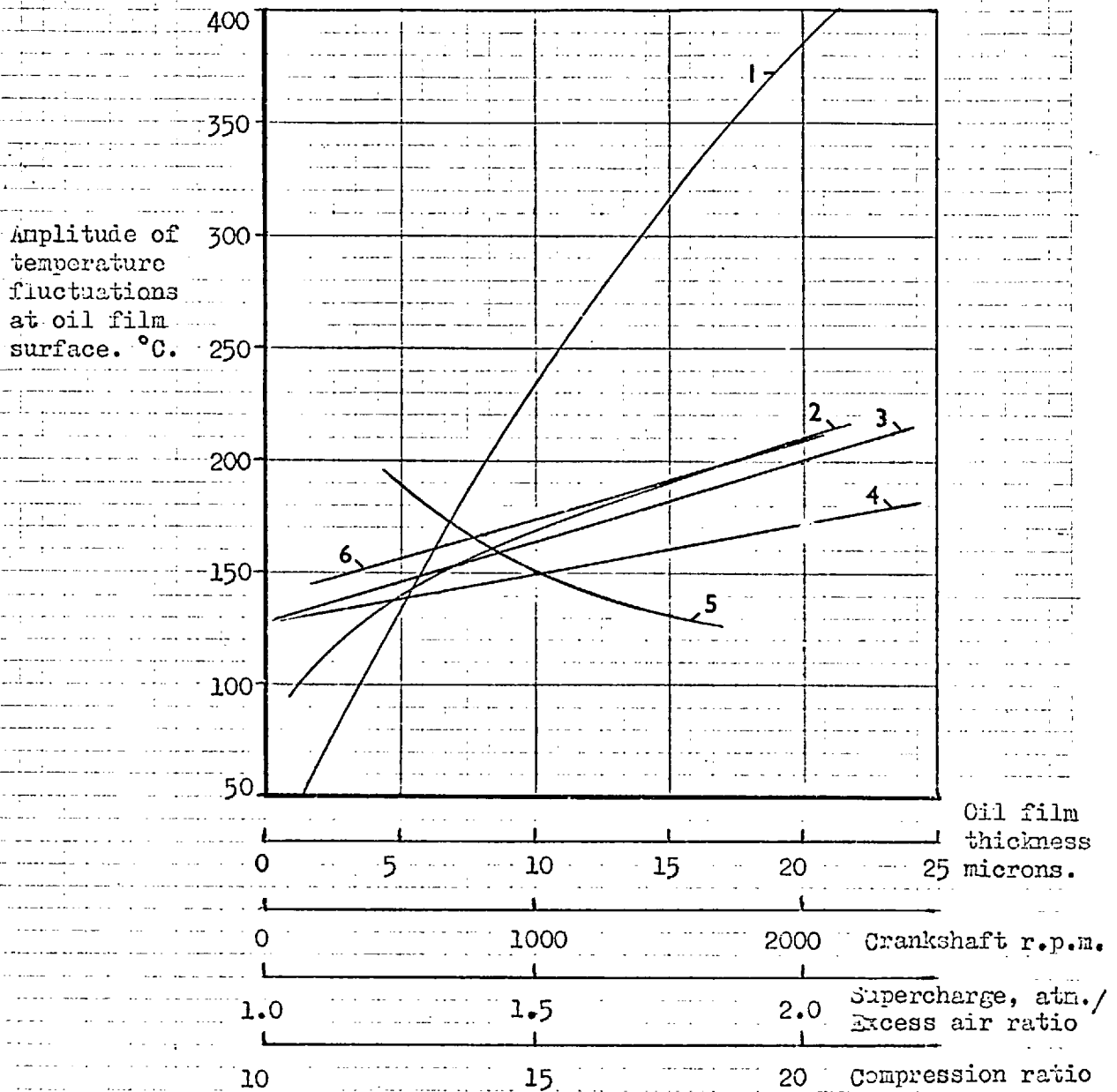


Fig. 3 - Theoretical surface temperatures (after Nepogod'ev & Podval'nyi)

- (1) - Oil film surface temperature on exposed portion of liner
- (2) - Liner metal surface temperature at point (1)
- (3) - Mean temperature of oil at point (1)
- (4) - Oil film surface temperature at portion of liner swept by piston at 120° of crankshaft revolution.

Four-stroke supercharged diesel engine
 300mm. bore ; 380 mm. stroke ; speed = 700 r.p.m.
 Oil film thickness = 6 micron.



- Key - 1 - Oil film thickness
 2 - Crankshaft r.p.m.
 3 - Supercharge pressure (without charge air cooling)
 4 - Supercharge pressure (with charge air cooling)
 5 - Excess air ratio
 6 - Compression ratio

Bore = 108 mm.

Results for two-stroke supercharged diesel engine - Stroke = 127 mm.

Figure 4. Factors affecting oil film temperature fluctuations.

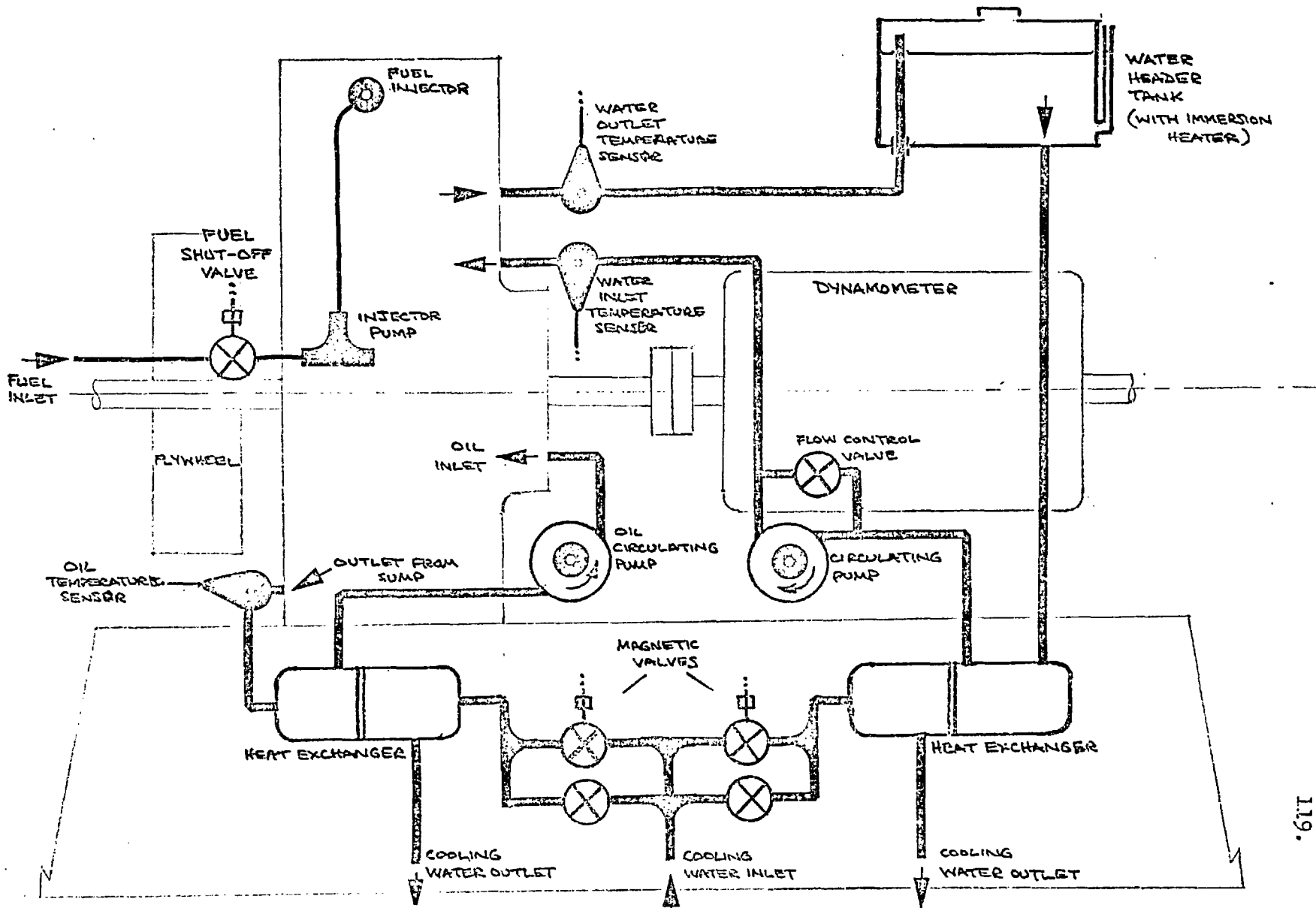


Fig. 5 - Fuel, Oil, and Water circuits of test-bed.

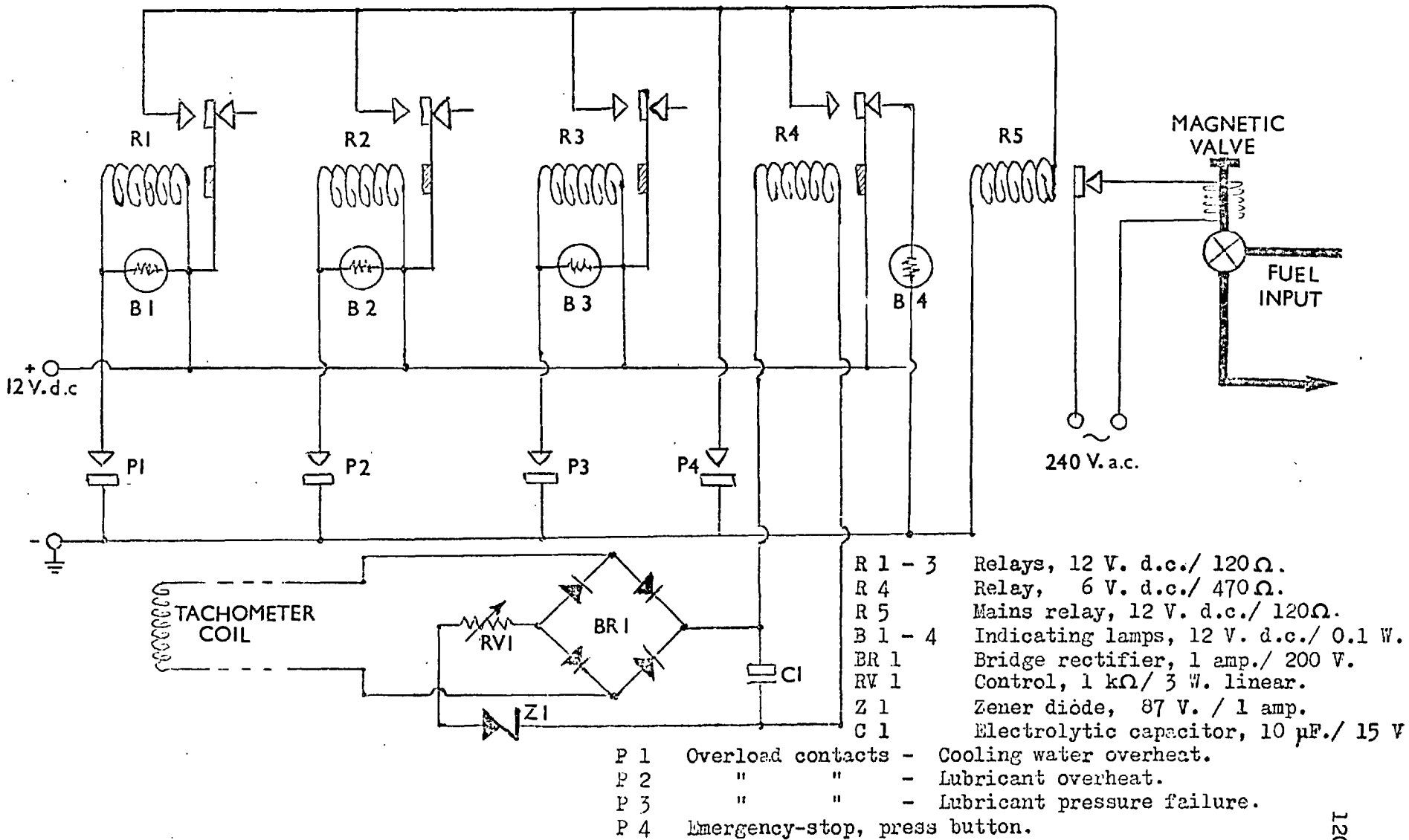


Fig. 6 - Overload protection circuits.

SCALE: APPROX. TWICE
FULL SIZE

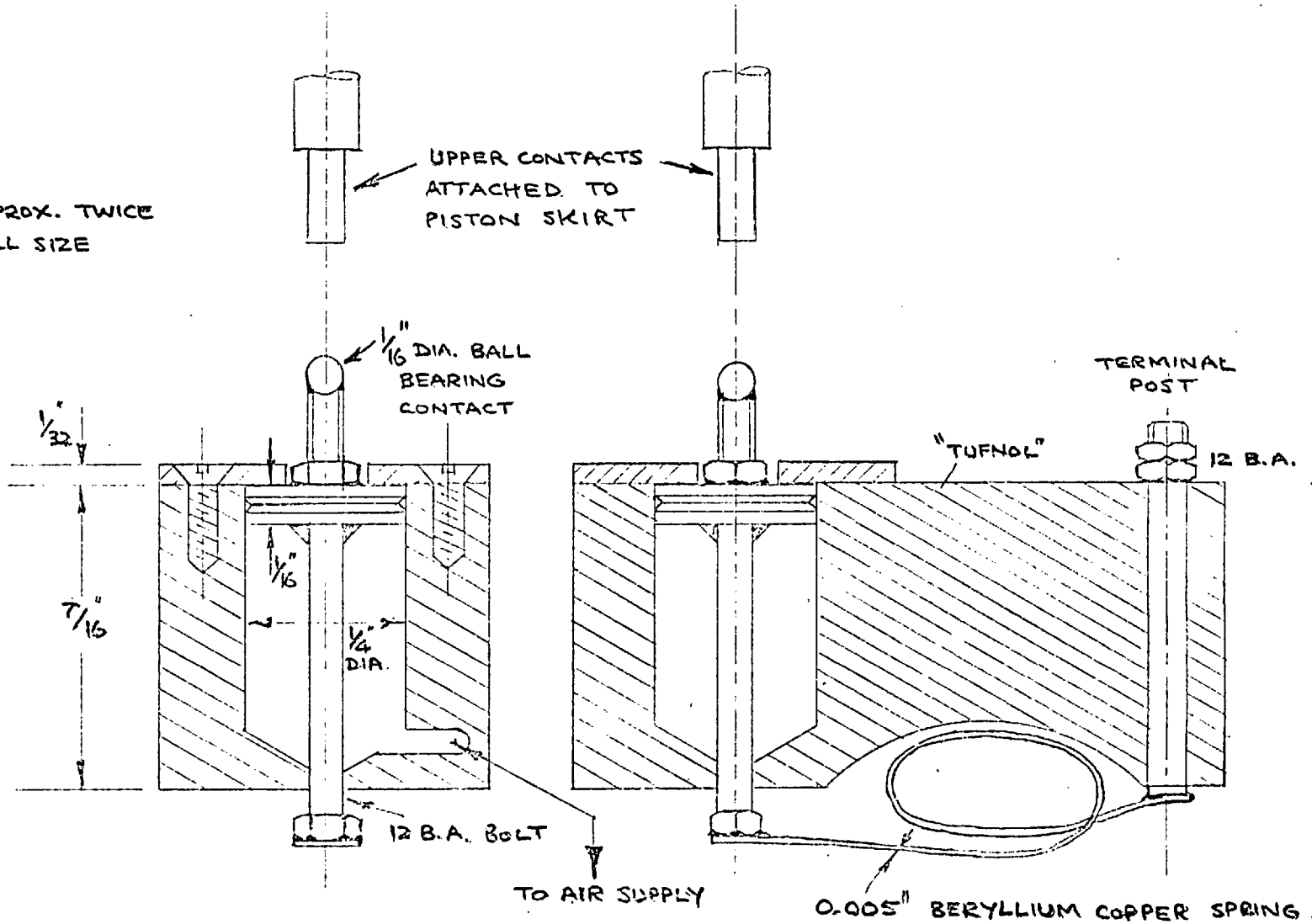
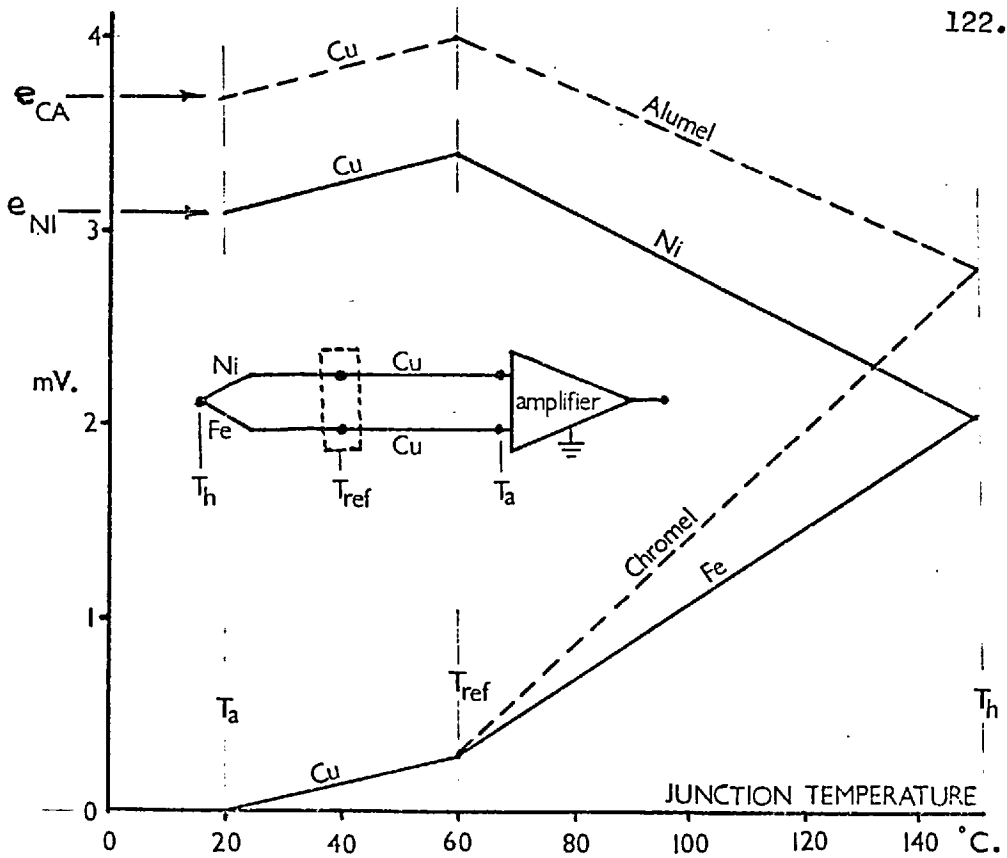


Fig. 7 - Compressed-air loaded piston contacts.



e_{CA} and e_{NI} are the output voltages from Chromel/Alumel and Nickel/Iron thermocouples respectively, where the hot junctions operate at $T_h = 150^\circ\text{C}$., the reference junctions are at $T_{ref} = 60^\circ\text{C}$., and the ambient temperature, $T_a = 20^\circ\text{C}$.. Thermojunction gradients, to a base of pure platinum, are given in the diagram below.

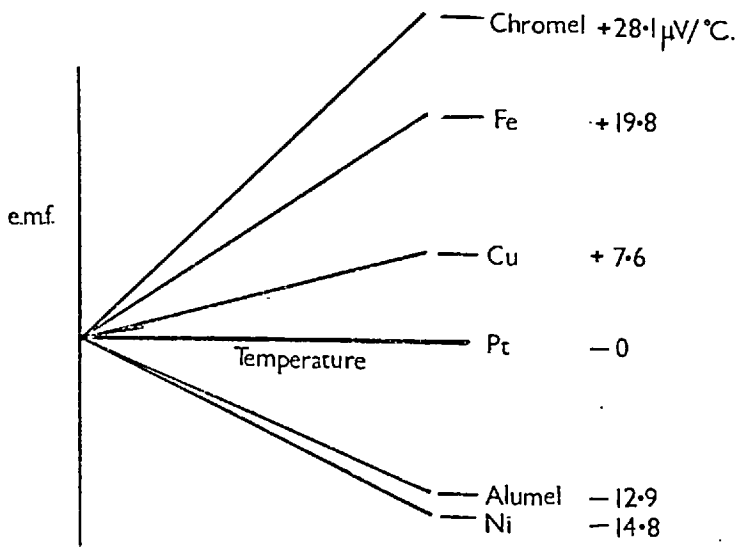
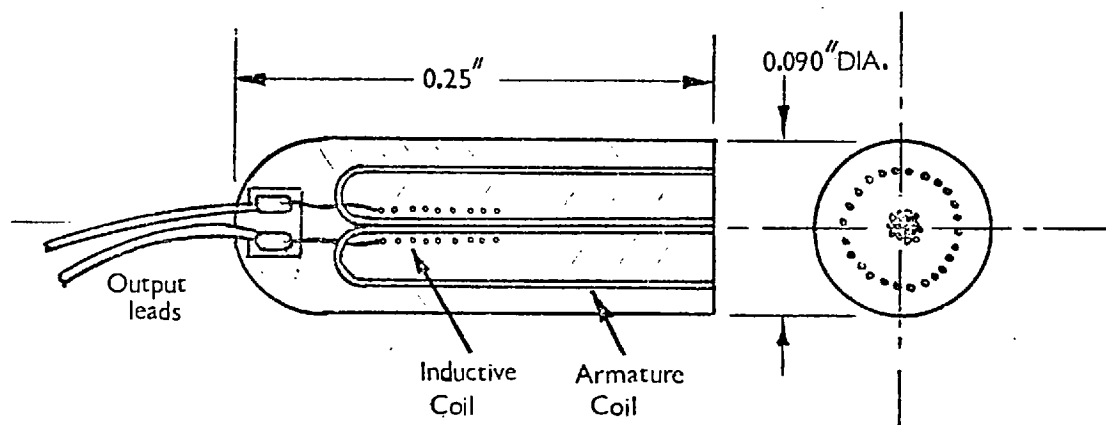


Fig. 8. Thin-film and bead thermocouple circuits.



Above - Section through vibration transducer (not to scale).

Below - Block diagram of complete electronics system.

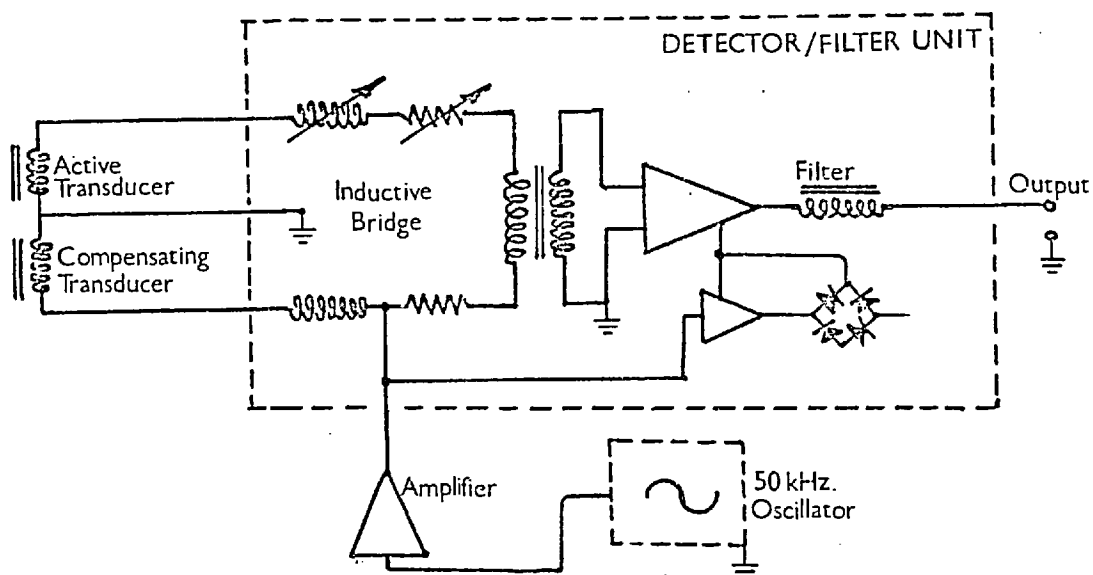
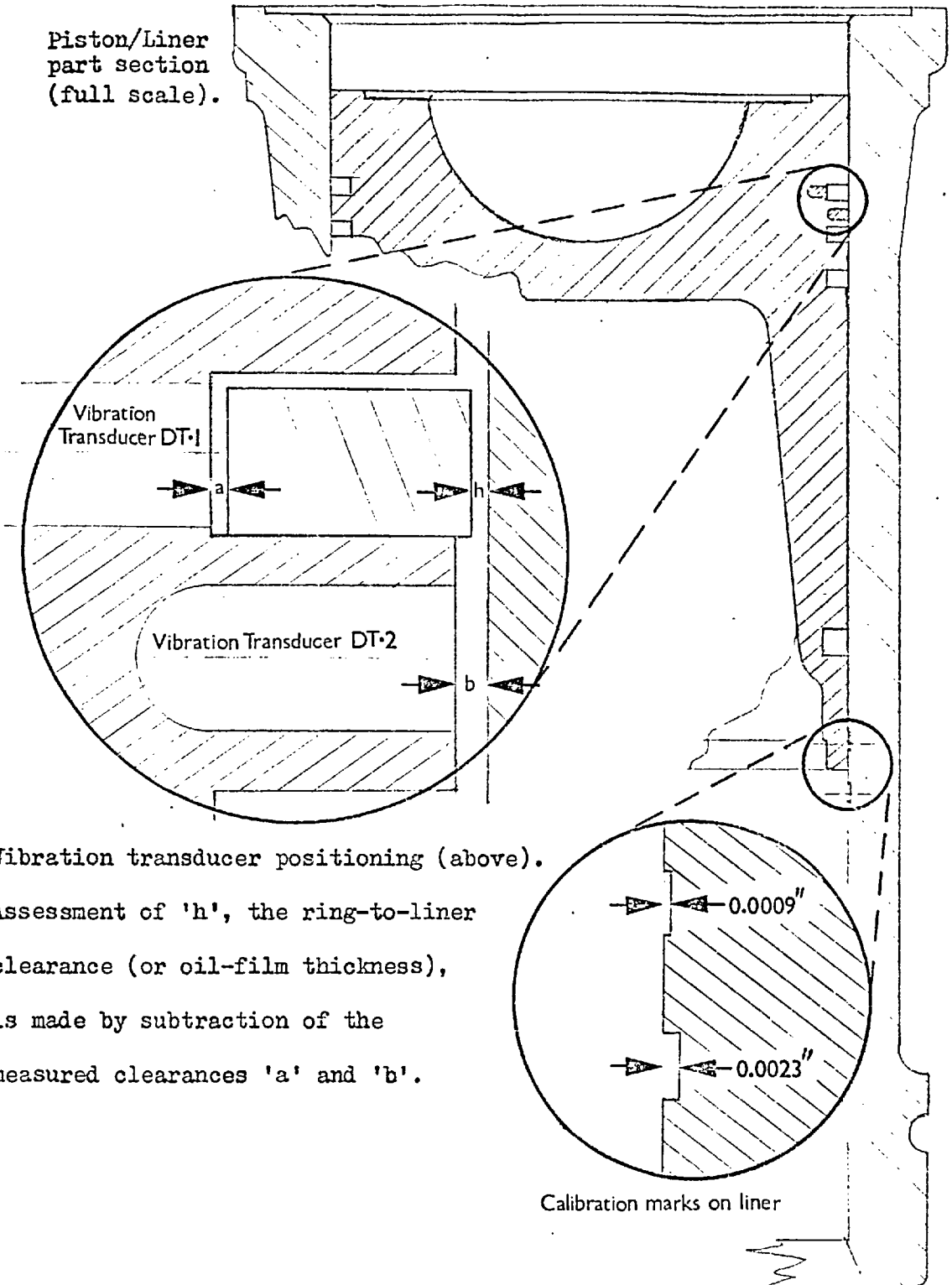


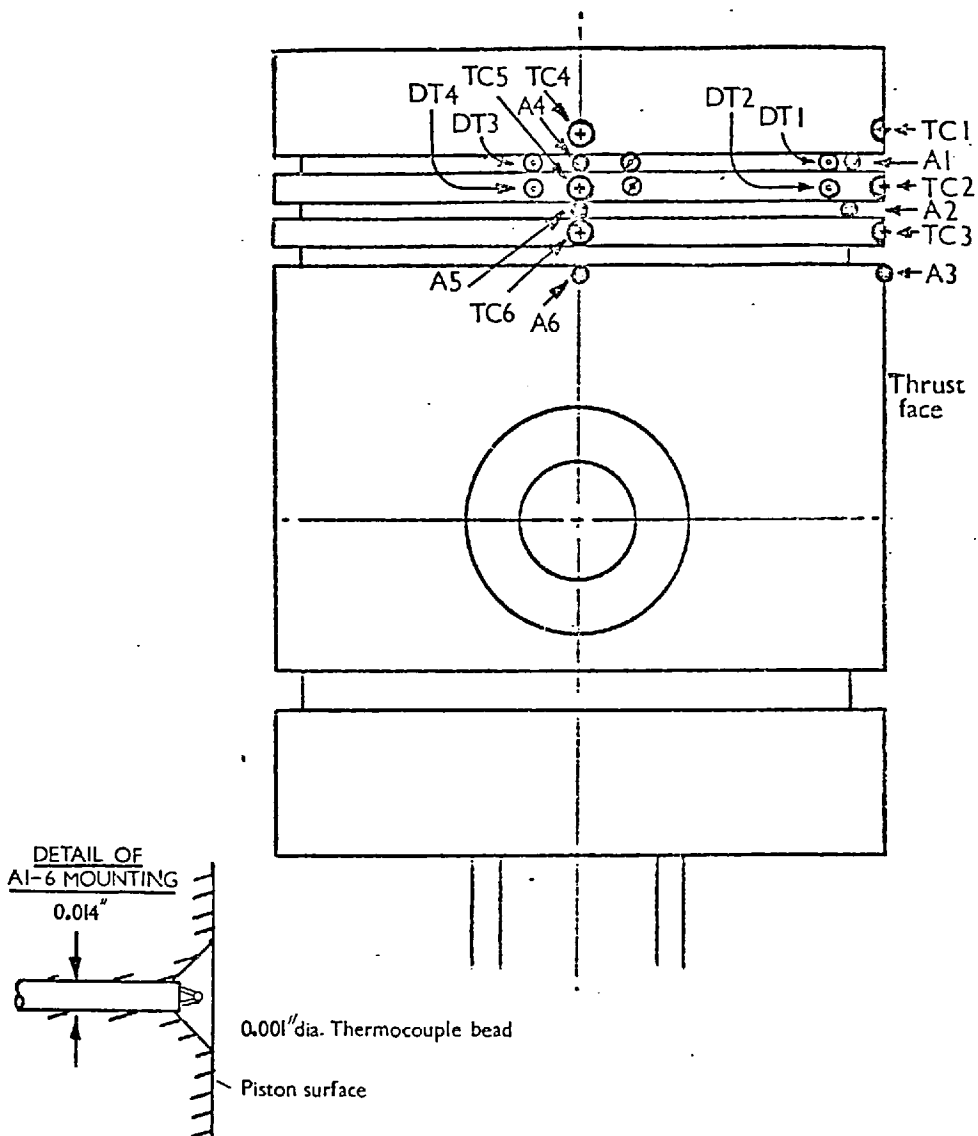
Fig. 9. - Vibration transducers and associated circuitry.

Piston/Liner
part section
(full scale).



Vibration transducer positioning (above).
Assessment of 'h', the ring-to-liner
clearance (or oil-film thickness),
is made by subtraction of the
measured clearances 'a' and 'b'.

Fig. 10. - Vibration transducer positioning and calibration markings
for measurement of oil-film thicknesses.



Identical instrument clusters positioned on thrust axis and one gudgeon-pin axis. The three transducer types are classified and symbolised as follows :

Thin-film thermocouples.... TC 1 - 6symbol ⊕

Bead thermocouples A 1 - 6symbol ⊙

Vibration transducers DT 1 - 4symbol ⊖

Compensating vibration transducerssymbol ⊗

All transducers fitted flush with piston surface except bead thermocouples which were recessed as shown in scrap-section above.

Fig. 11. - Piston instrumentation layout.

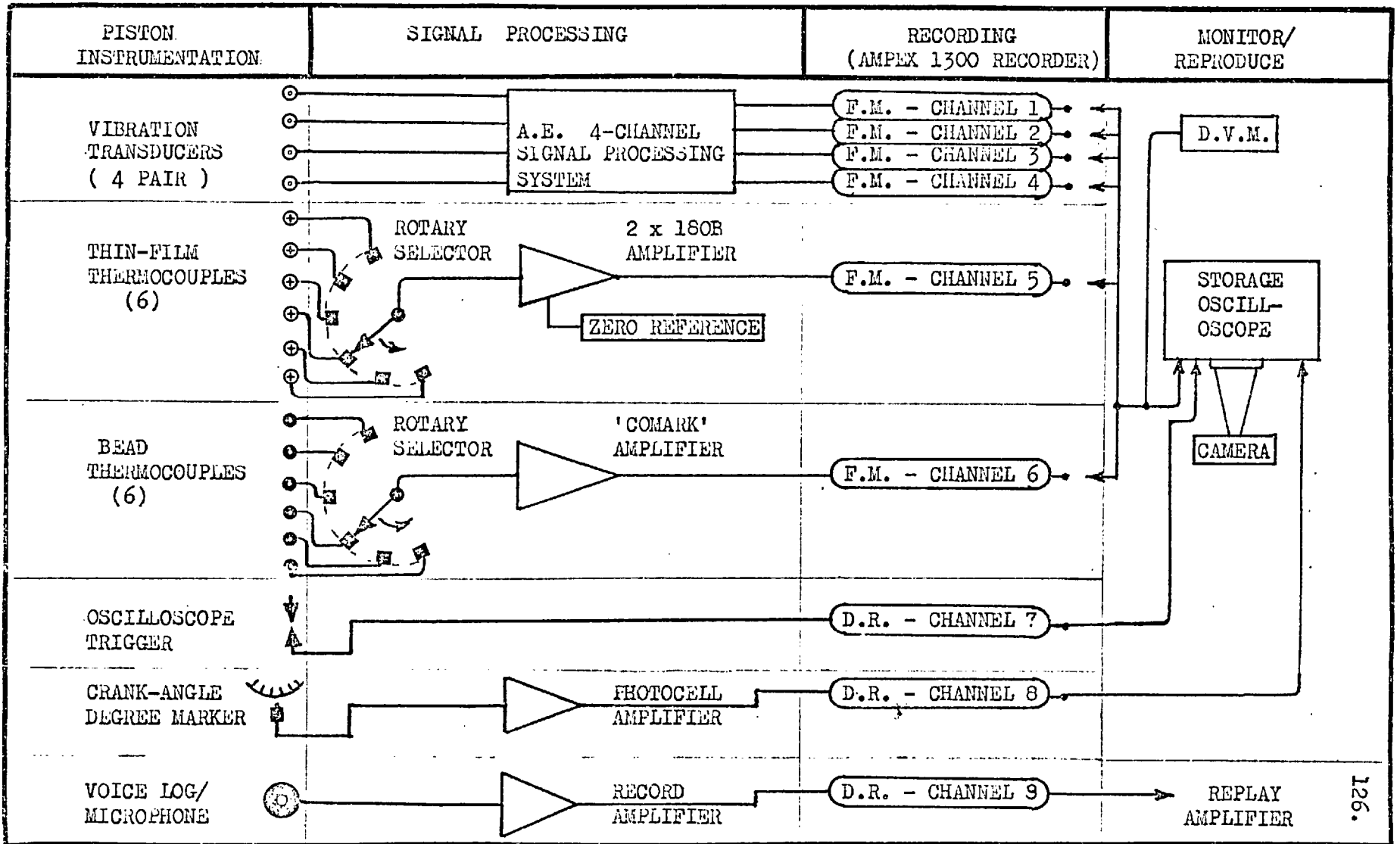


Fig. 12. - Data recording layout.

All oscilloscope records presented here are given in a fixed format for clarity, and a key to the symbols used is given below. For references to transducer code numbers please refer to Figure 11.

N = engine speed

B = b.m.e.p.

a

b

c ... references to individual oscilloscope traces.

d

etc.

V = vertical calibration of trace.

(1 div. corresponds to one large grid division).

S = horizontal (sweep-speed) calibration.

CA = crank-angle degree marker trace.... see below.

tdc = position of T.D.C. on firing stroke



(....) = information locating position of oscilloscope records on the data storage tapes.

The crank angle degree marker trace comprises a straight sweep trace broken by vertical markings at every 10° of crankshaft rotation, except at T.D.C. and B.D.C. where the markings are broken down to smaller subdivisions as below :-

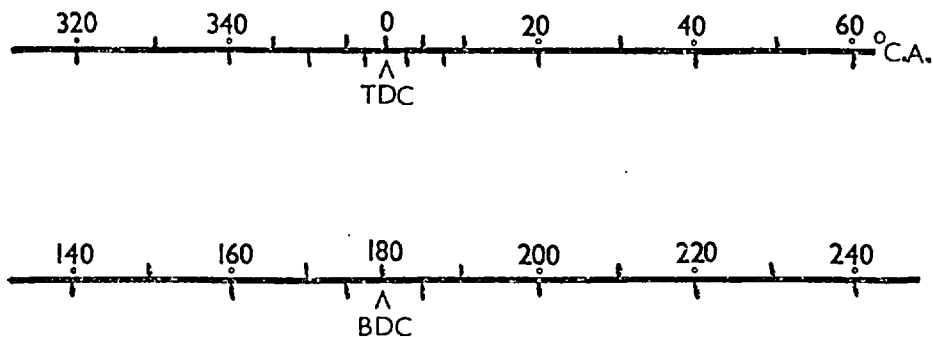


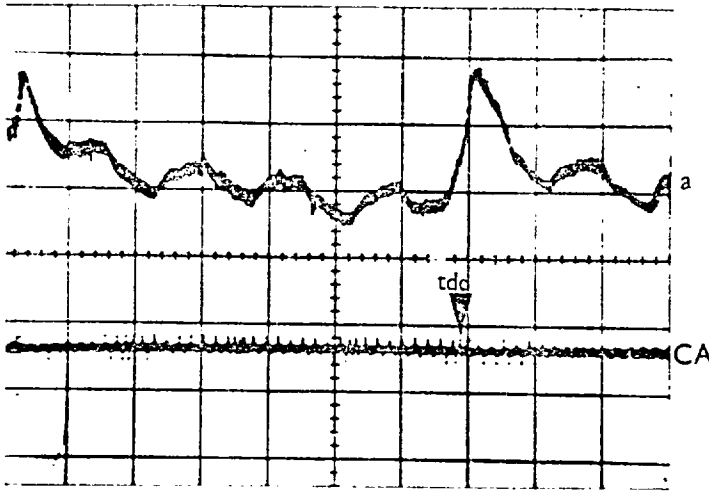
Fig. 13. Symbols used in the following oscilloscope records.

Top frame :-

a - thermocouple A1.
 V = 10°C./div.
 Mean temperature level
 = 184°C.
 S = uncalibrated

(tape C.742/11,15)

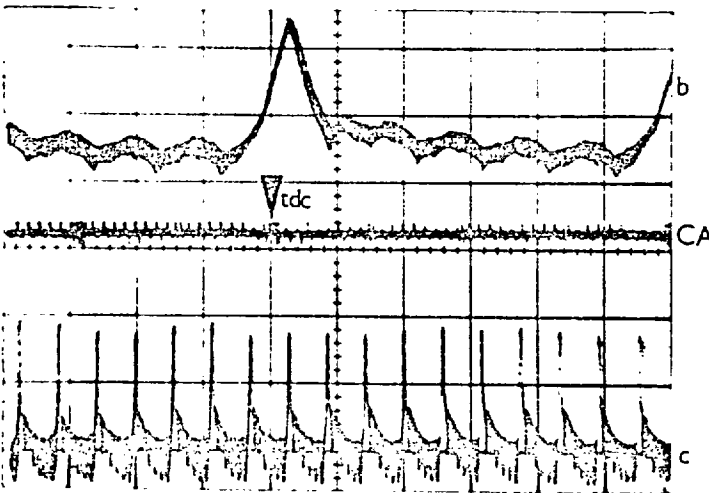
N = 1330 r.p.m.
 B = 106.0 p.s.i.

Centre frame :-

b and c - thermocouple A1.
 V (both traces) = 20°C./div.
 S (trace b) = 20 ms./div.
 S (trace c) = 0.2 s./div.

(tape B.540/8,1)

N = 1000 r.p.m.
 B = 49.3 p.s.i.

Bottom frame :-

d - thermocouple A1.
 e - " A2.
 f - " A3.
 g - " A4.
 h - " A5.
 j - " A6.

V (all traces) = 20°C./div.
 S = 0.2 s./div.

(tape B.1770/10,7)

N = 1050 r.p.m.
 B = 63.2 p.s.i.

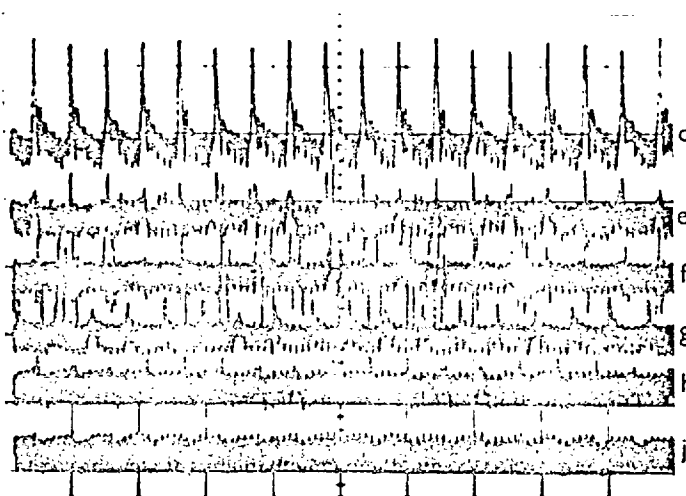
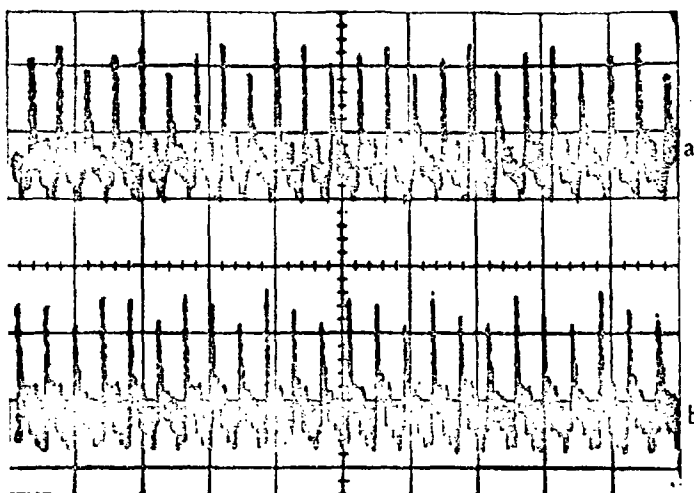


Fig.14. - Bead thermocouple records.



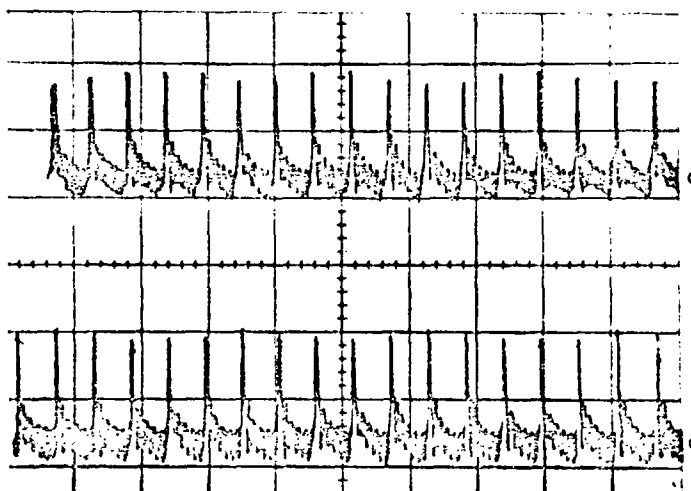
Top frame :-

a and b - thermocouple Al.

V = 10°C./div.
S = 0.2 s./div.

(tape C.439/11,12)

N = 1420 r.p.m.
B = 0 p.s.i.



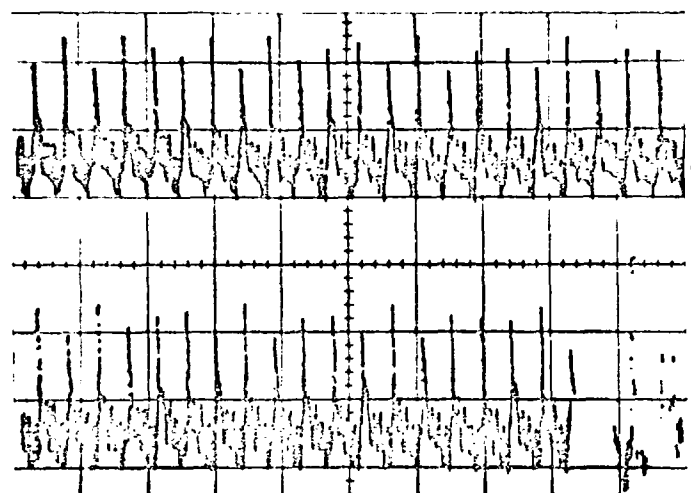
Centre frame :-

c and d - thermocouple Al.

V = 20°C./div.
S = 0.2 s./div.

(tape B.1720/10,6)

N = 1050 r.p.m.
B = 63.2 p.s.i.



Bottom frame :-

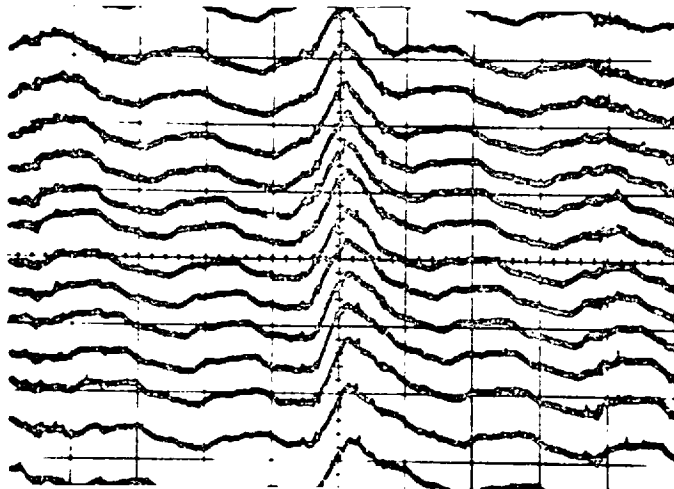
e and f - thermocouple Al.

V = 20°C./div.
S = 0.2 s./div.

(tape C.742/11,13)

N = 1330 r.p.m.
B = 106.0 p.s.i.

Fig. 15. - Multiple exposures of temperature peaks for statistical analysis.



Upper frame :-

Consecutive sweeps of thermocouple A1 recording.

$V = 20^{\circ}\text{C./div.}$

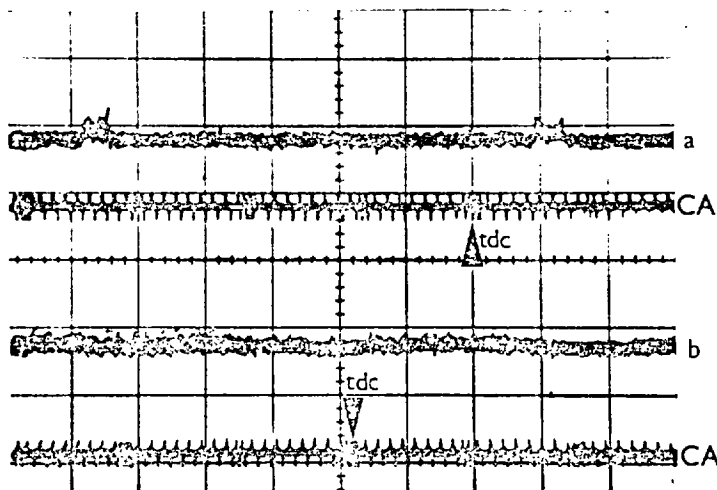
Mean temperature level
= 113°C.

$S = 10 \text{ ms./div.}$

(tape C.518/11,14)

$N = 1420 \text{ r.p.m.}$

$B = 0 \text{ p.s.i.}$



Lower frame :-

Film thermocouples :

a - thermocouple TC4.

b - thermocouple TC3.

$V = 3.0^{\circ}\text{C./div.}$

$S = \text{uncalibrated.}$

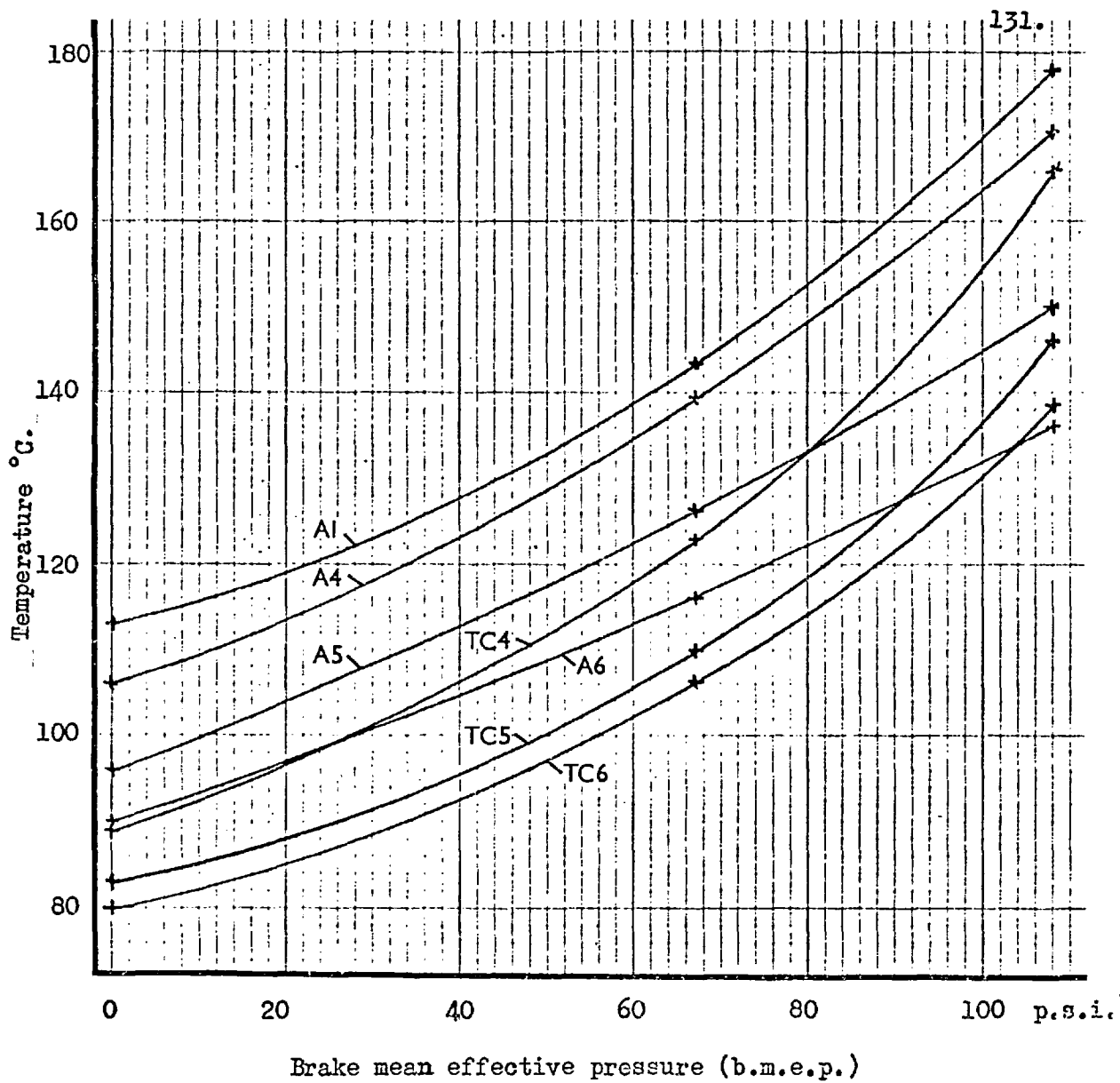
Mean temperature levels:

TC3 = 141.5°C.

TC4 = 165.5°C.

(tape C.1080/11,16)

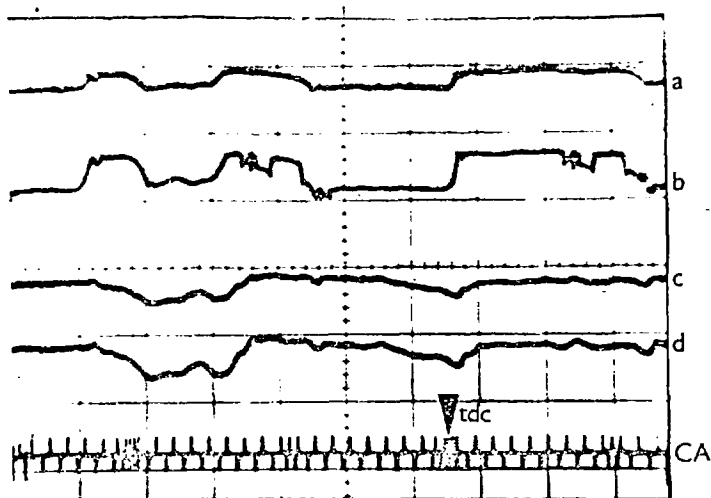
Fig. 16. - Records showing repeatability of results, and typical film thermocouple recordings.



Tranducer locations:

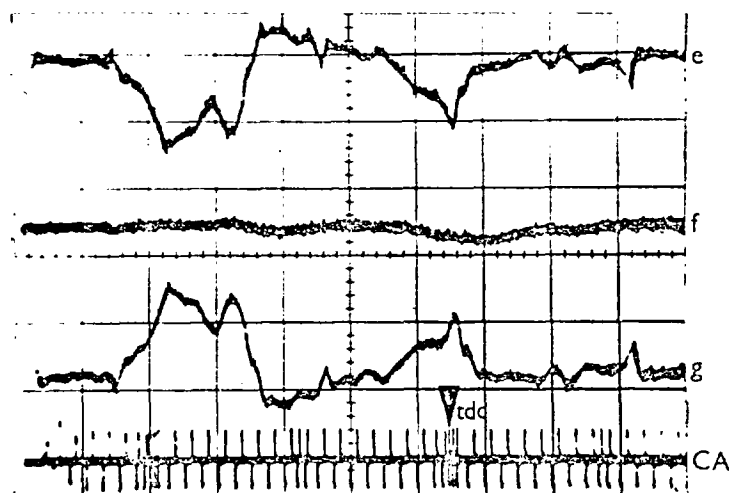
A1	- Thrust face	- behind top ring	- bead thermocouple.
A4	- G.P.axis	- " " "	- " "
A5	- "	- " 2nd. "	- " "
A6	- "	- below 3rd. "	- " "
TC4	- "	- above top ring	- film thermocouple.
TC5	- "	- between upper rings	" "
TC6	- "	- " lower "	- " "

Fig. 17. - Steady temperature levels as recorded over full range of engine power.

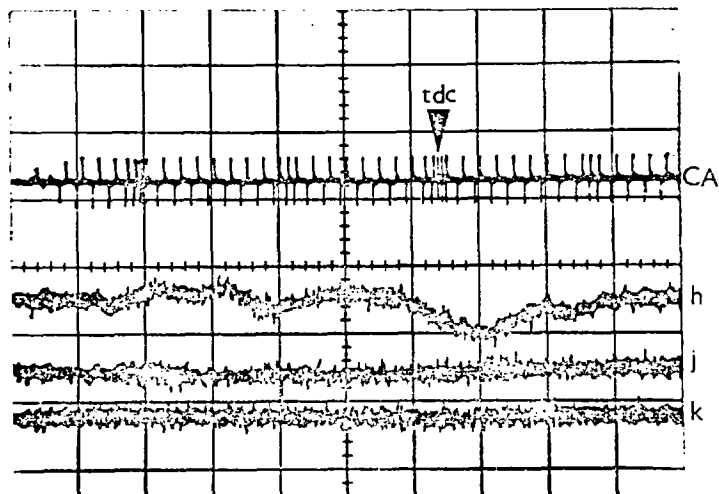
Top frame :-

- a - Thrust face, piston to ring clearance.
- b - Thrust face, piston to liner clearance.
- c - G.P. axis, piston to ring clearance.
- d - G.P. axis, piston to liner clearance.

Increase in clearance gives upward trace deflection.
 $V = \text{approx. } 0.01''/\text{div.}$ for traces a to d.

Centre frame :-

- e - trace 'c' amplified to $V = 0.0028''/\text{div.}$
- g - trace 'd' amplified, matched to same sensitivity as 'e', and inverted.
- f - electronic subtraction of signals (g - e).
 $V = 0.0028''/\text{div.}$

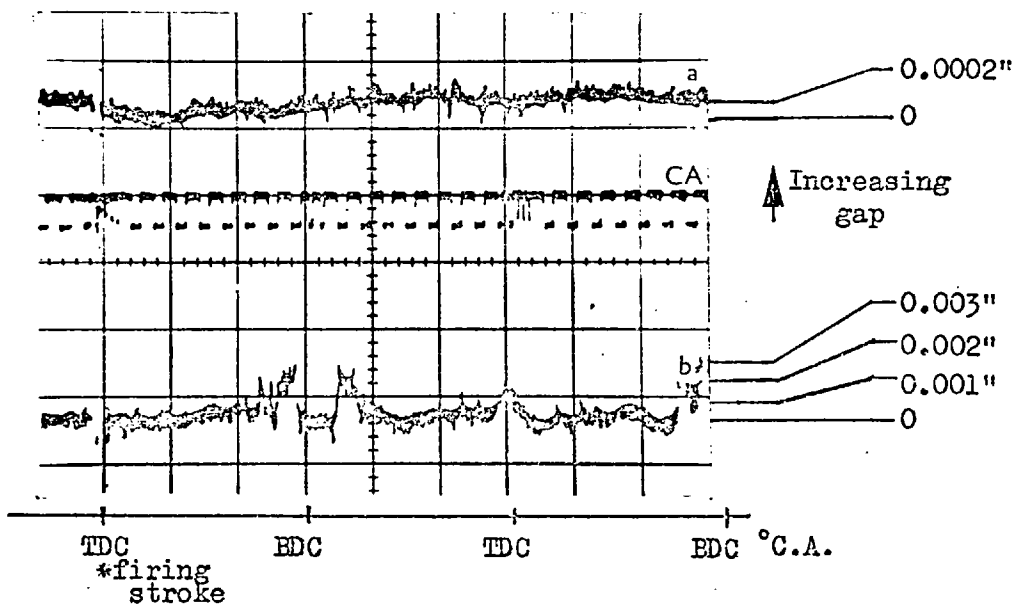
Bottom frame :-

- h - trace 'f' amplified to $V = 0.0011''/\text{div.}$
- j and k - zero reference traces at known temperature levels.

(tape C.300/11,1/D2/D5)

$N = 1300 \text{ r.p.m.}$
 $B = 0 \text{ p.s.i.}$
 $S = 10 \text{ ms./div.}$

Fig. 18. Subtraction of vibration signals to estimate oil-film thickness.



a - G.P. axis. Subtracted signal derived from vibration records showing oil film thickness between ring and liner. Vertical calibration as indicated.

b - Thrust axis. Record as for 'a' taken from transducers on thrust axis. The square pulses correspond to the calibration marks on the liner.

(tape A.216 / D6)

N = 950 r.p.m.

B = 36.1 b.m.e.p. (using Methane fuel)

S = 10 ms./div.

Fig. 19. Oil film thickness variation with engine crank-angle.

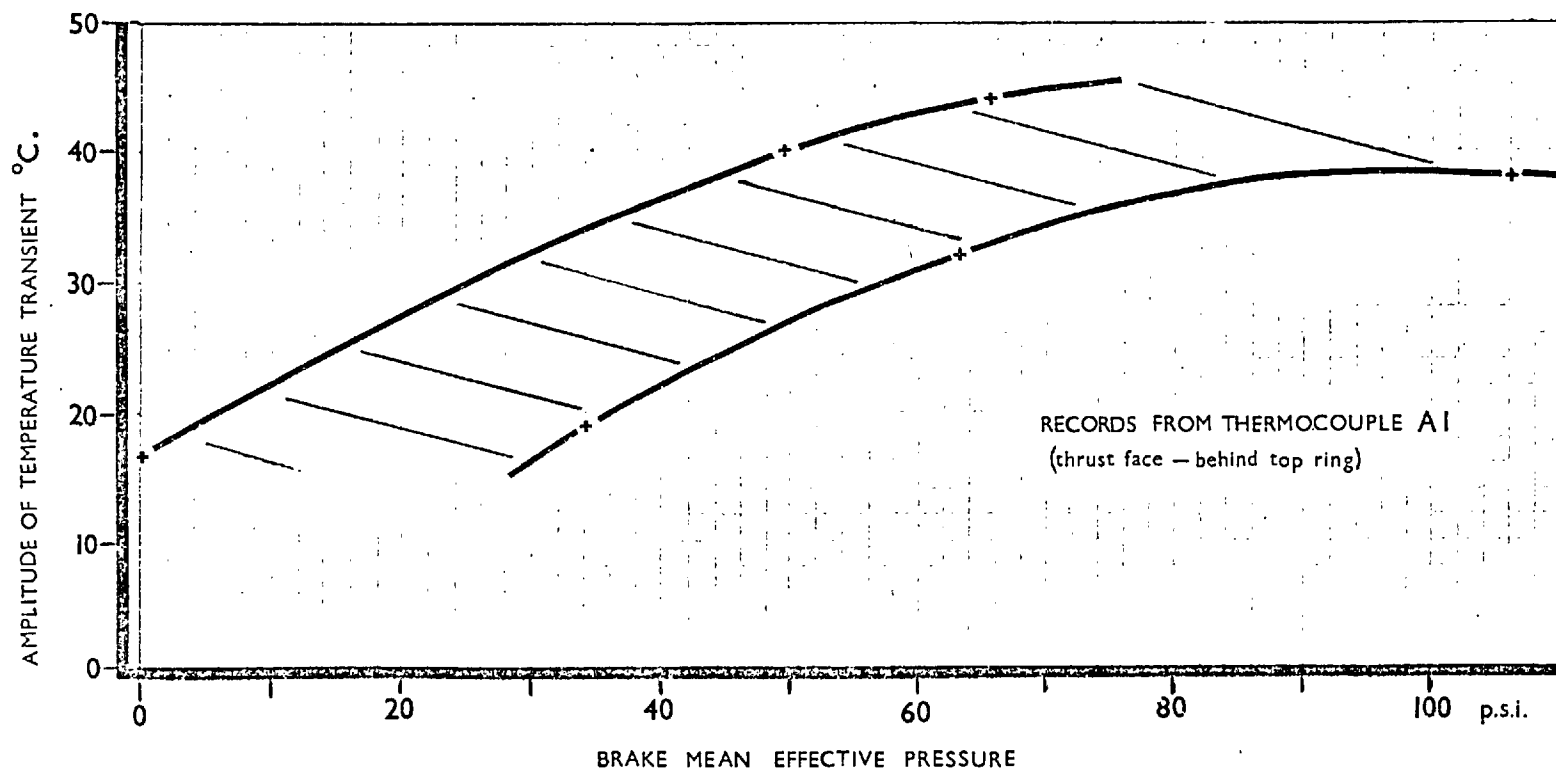


Fig. 20. - Amplitude of temperature transients as function of b.m.e.p.

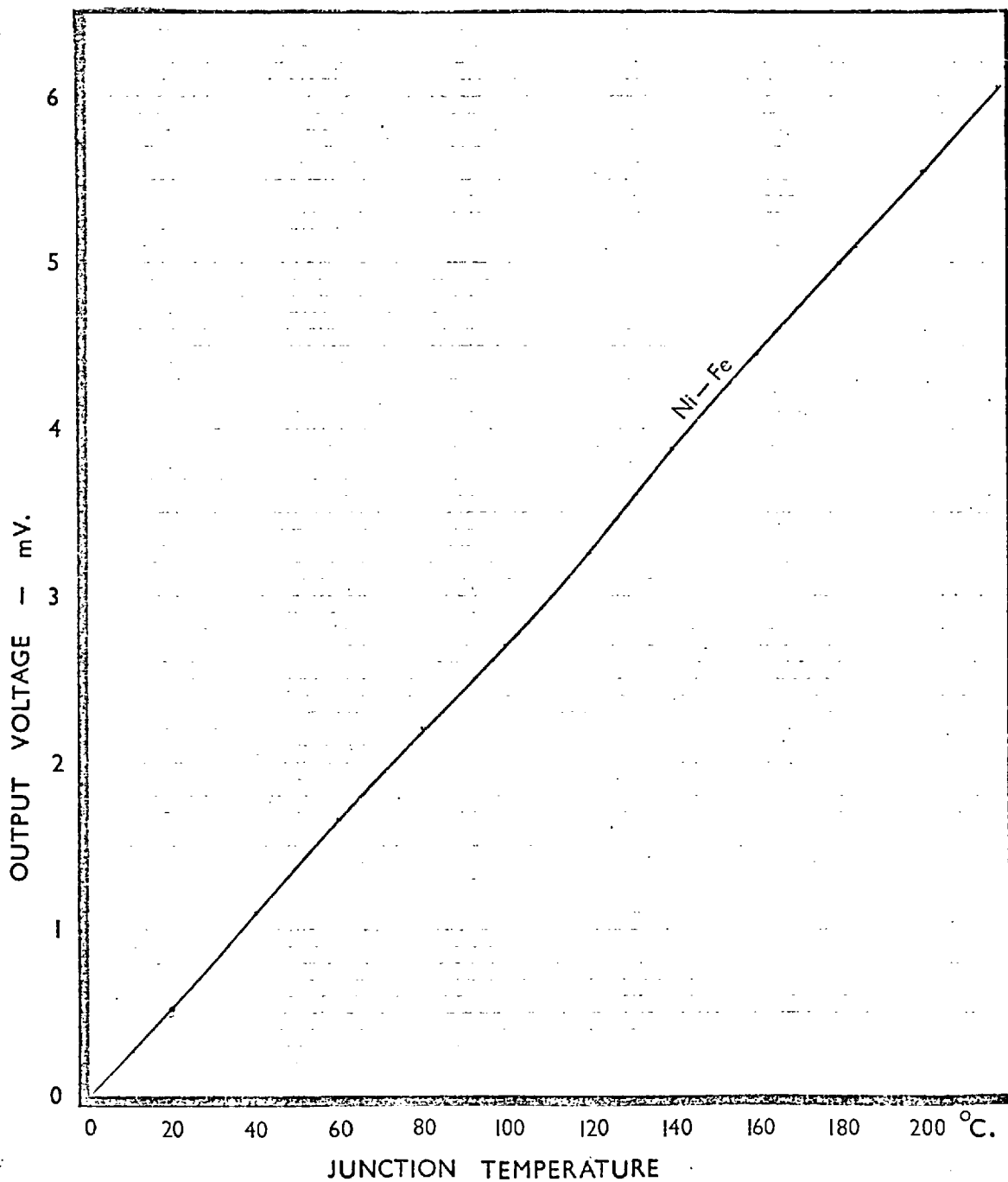
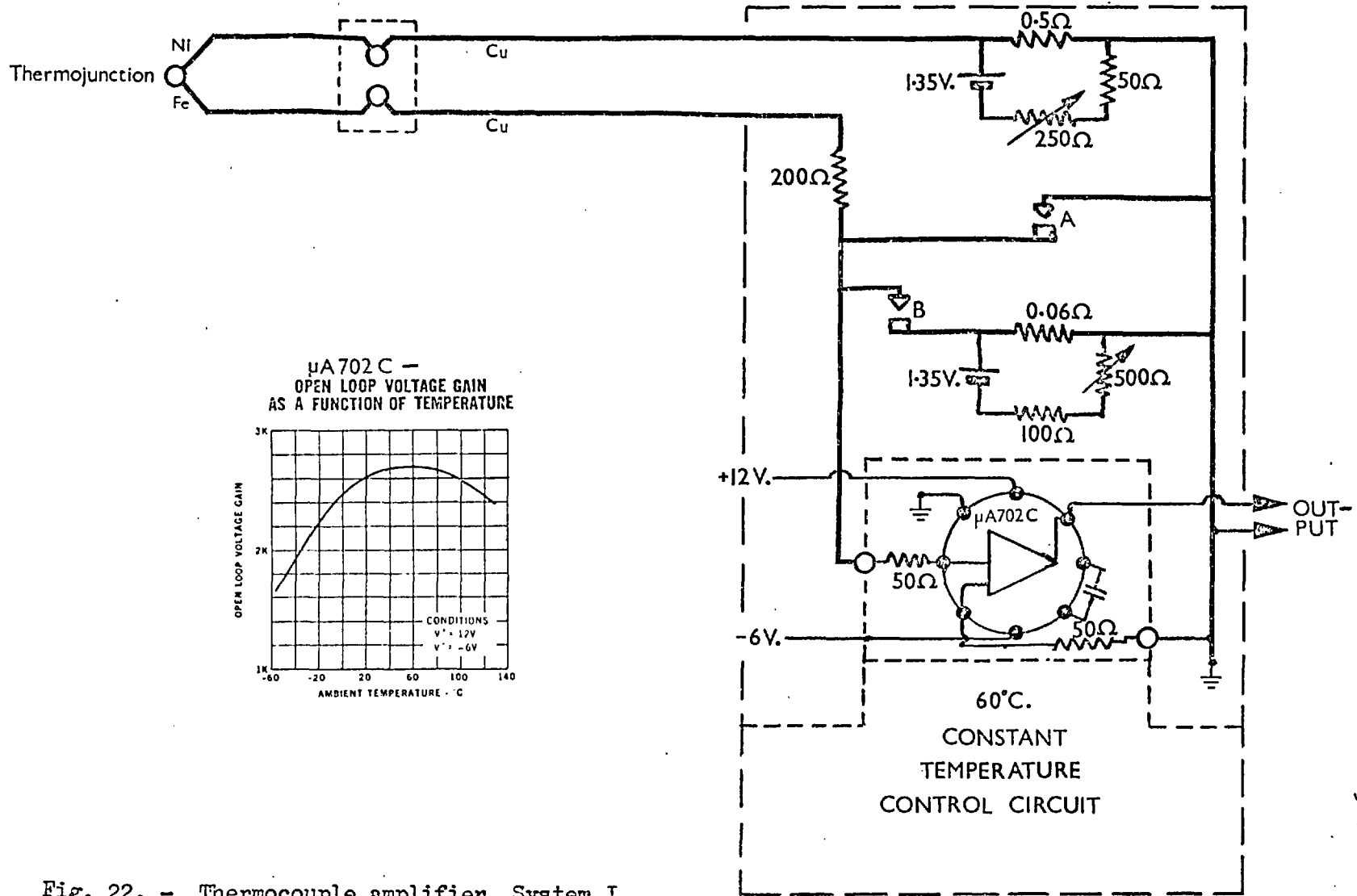


Fig. 21. - Calibration curve of nickel - iron thermocouples.



μA702C -
OPEN LOOP VOLTAGE GAIN
AS A FUNCTION OF TEMPERATURE

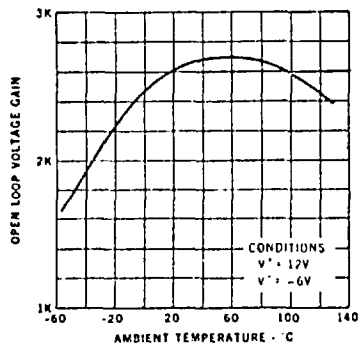
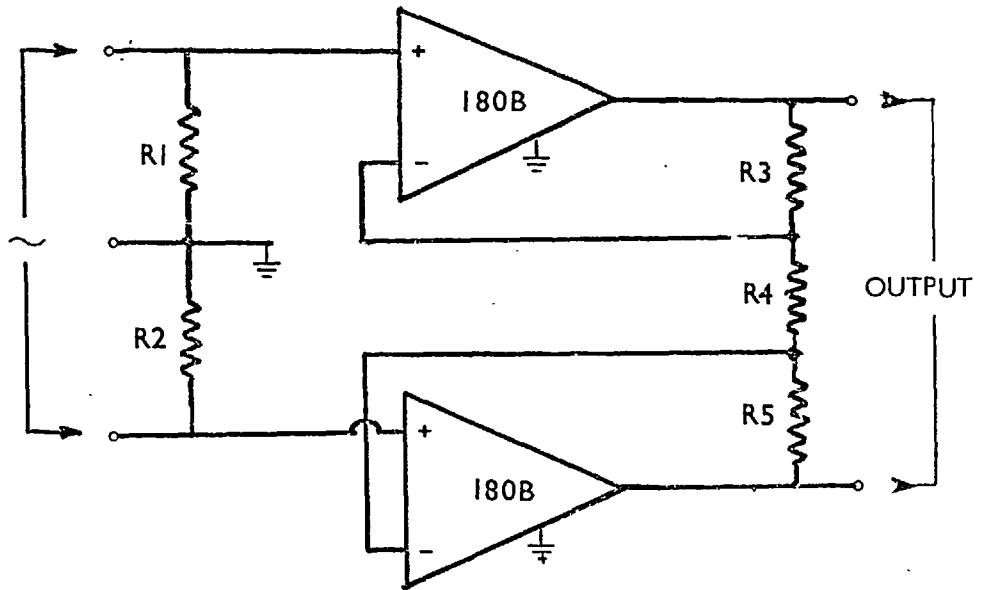


Fig. 22. - Thermocouple amplifier. System I.



$R1 = R2 = 10 \text{ M}\Omega.$
 $R3 = R5 = 3.9 \text{ k}\Omega.$
 $R4 = 56 \Omega.$

**180B
AMPLIFIER
CONSTRUCTION**

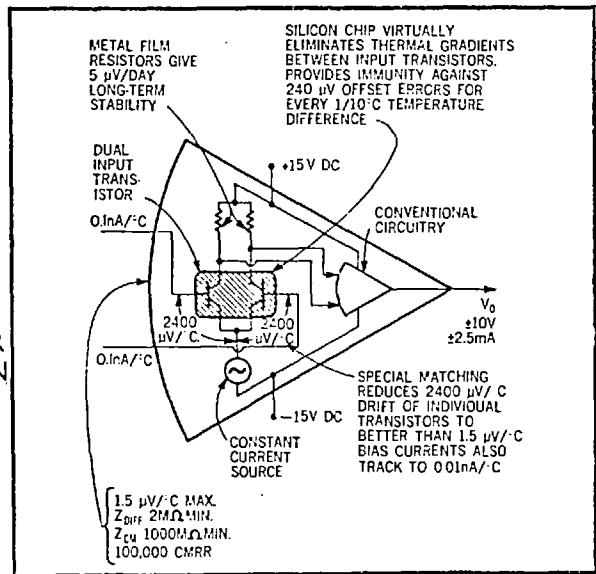
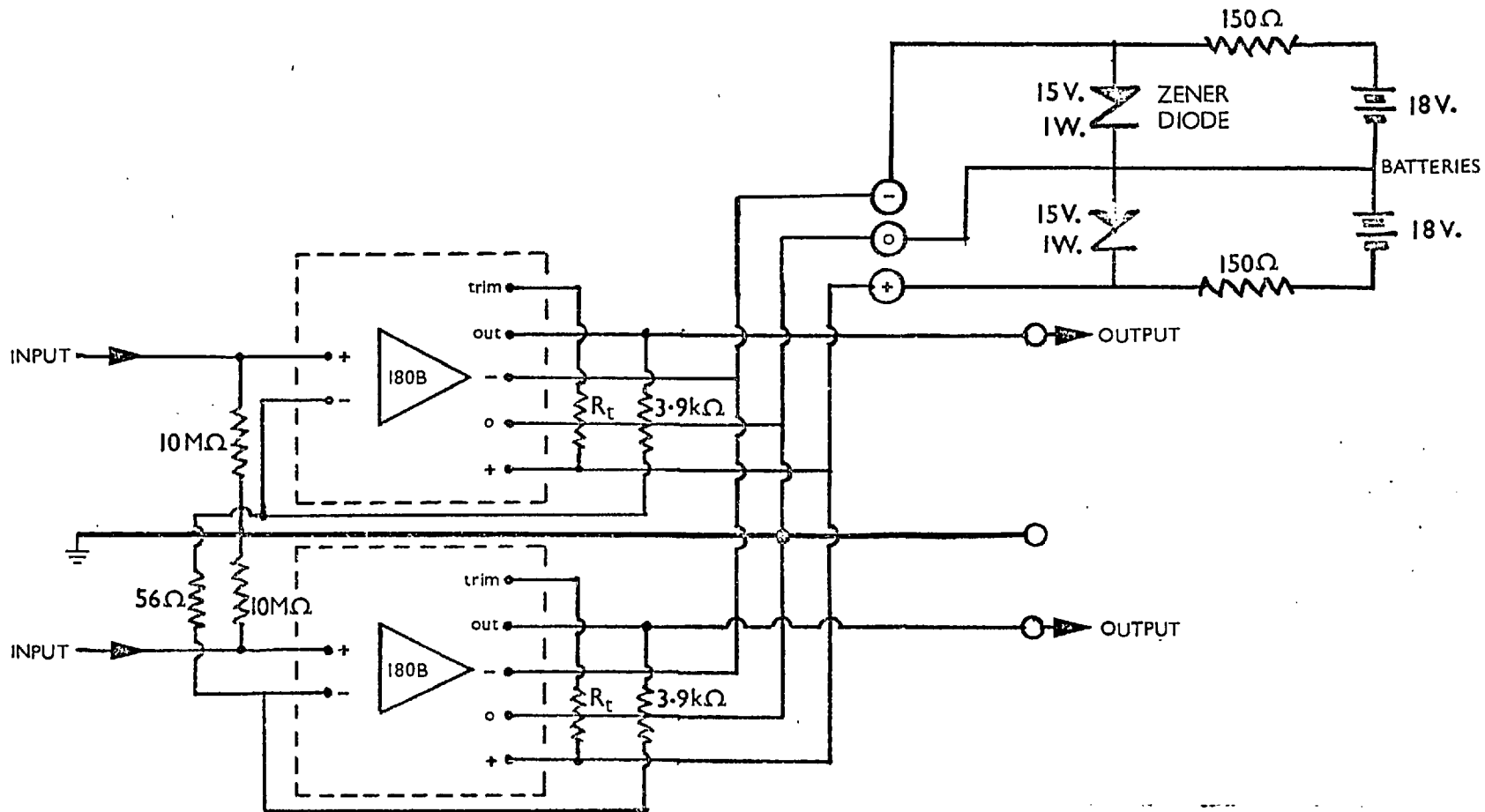


Fig. 23 - Thermocouple amplifier, System II.



R_t = selected resistor to balance amplifier input offset voltage.

Fig. 24. - Thermocouple amplifier, System II, circuit layout

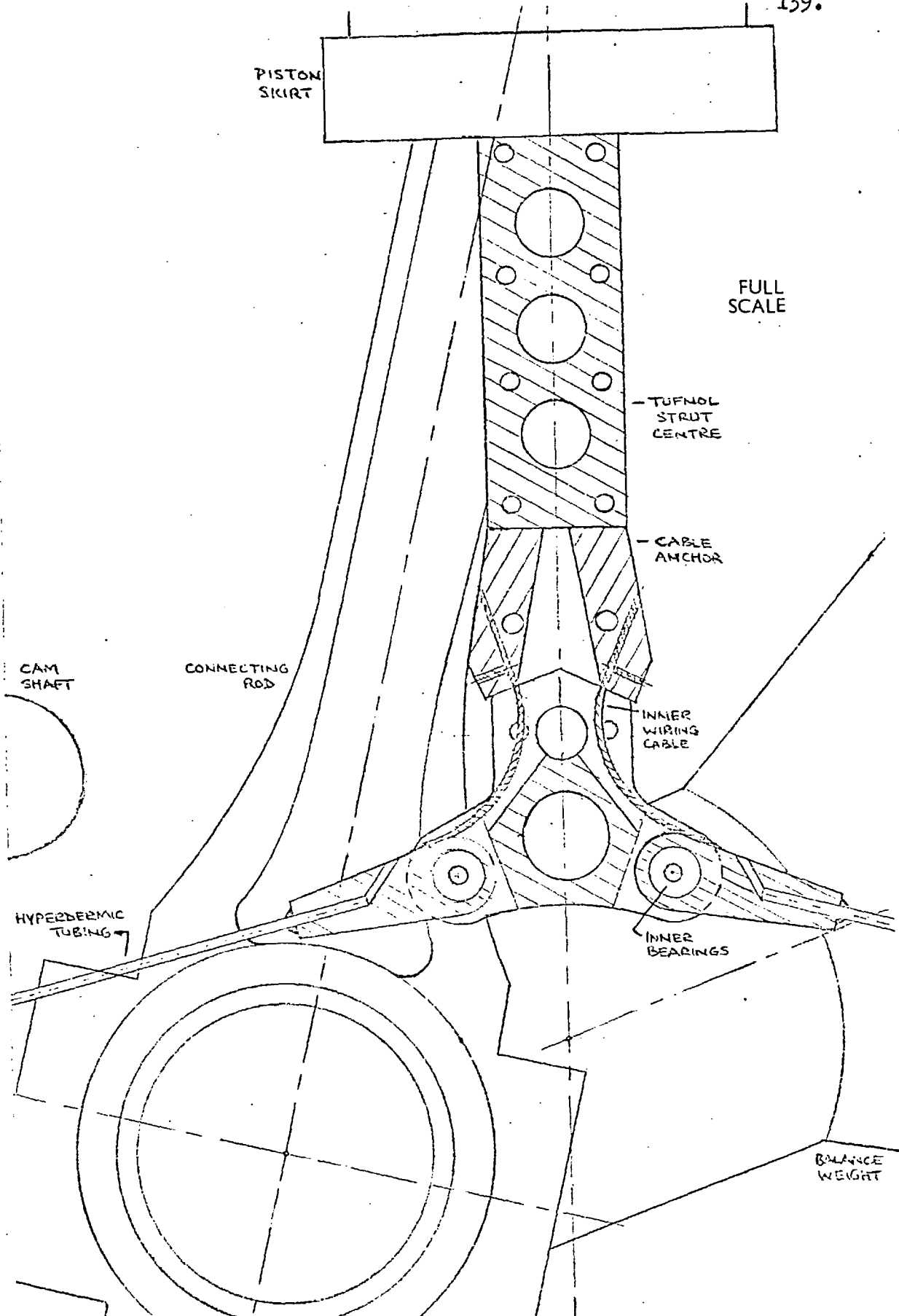


Fig. 25. - Piston linkage -- sectional view through piston strut.

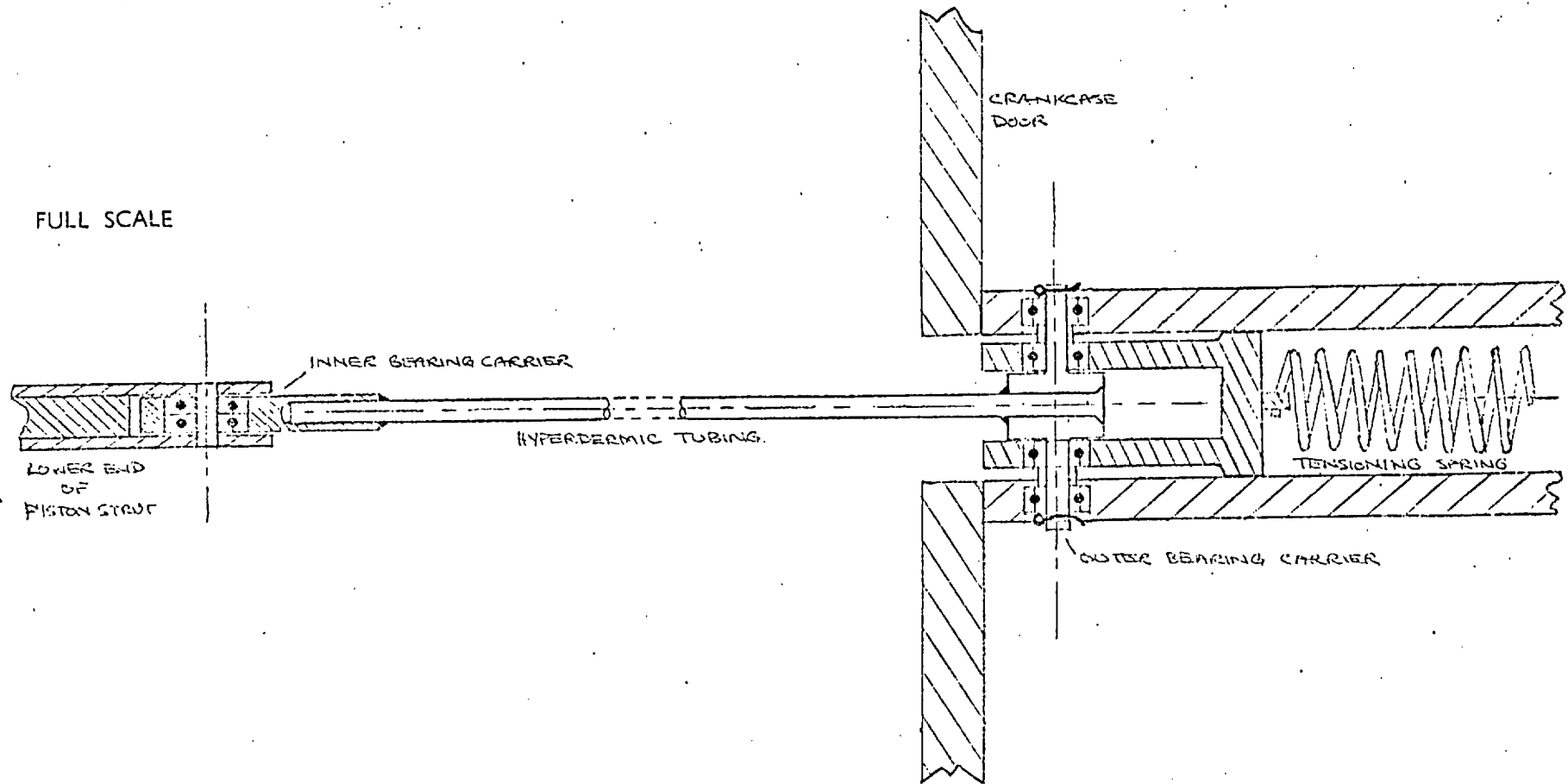


Fig. 26. - Piston linkage - connections to outer arms.

FULL SCALE

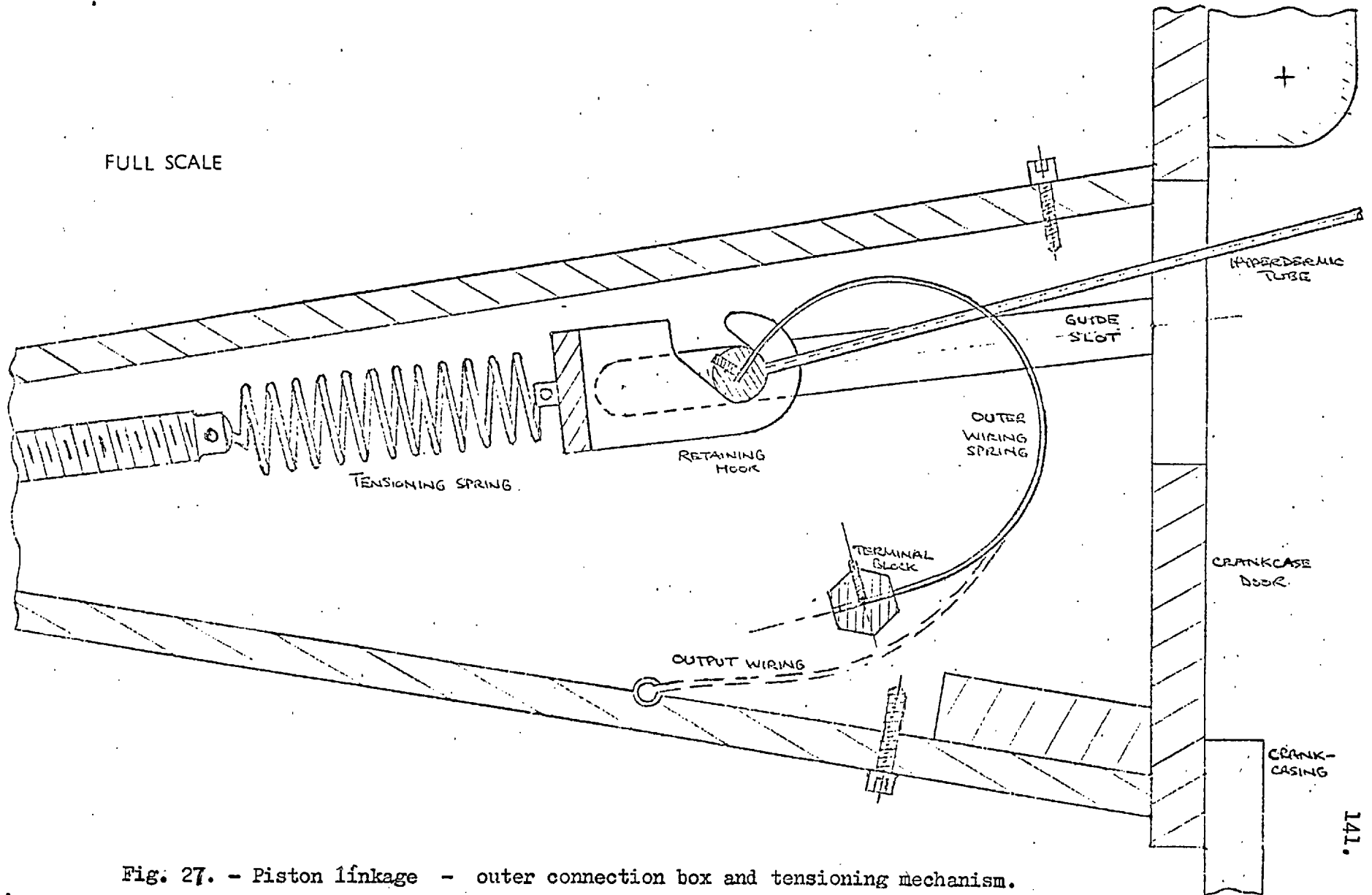


Fig. 27. - Piston linkage - outer connection box and tensioning mechanism.

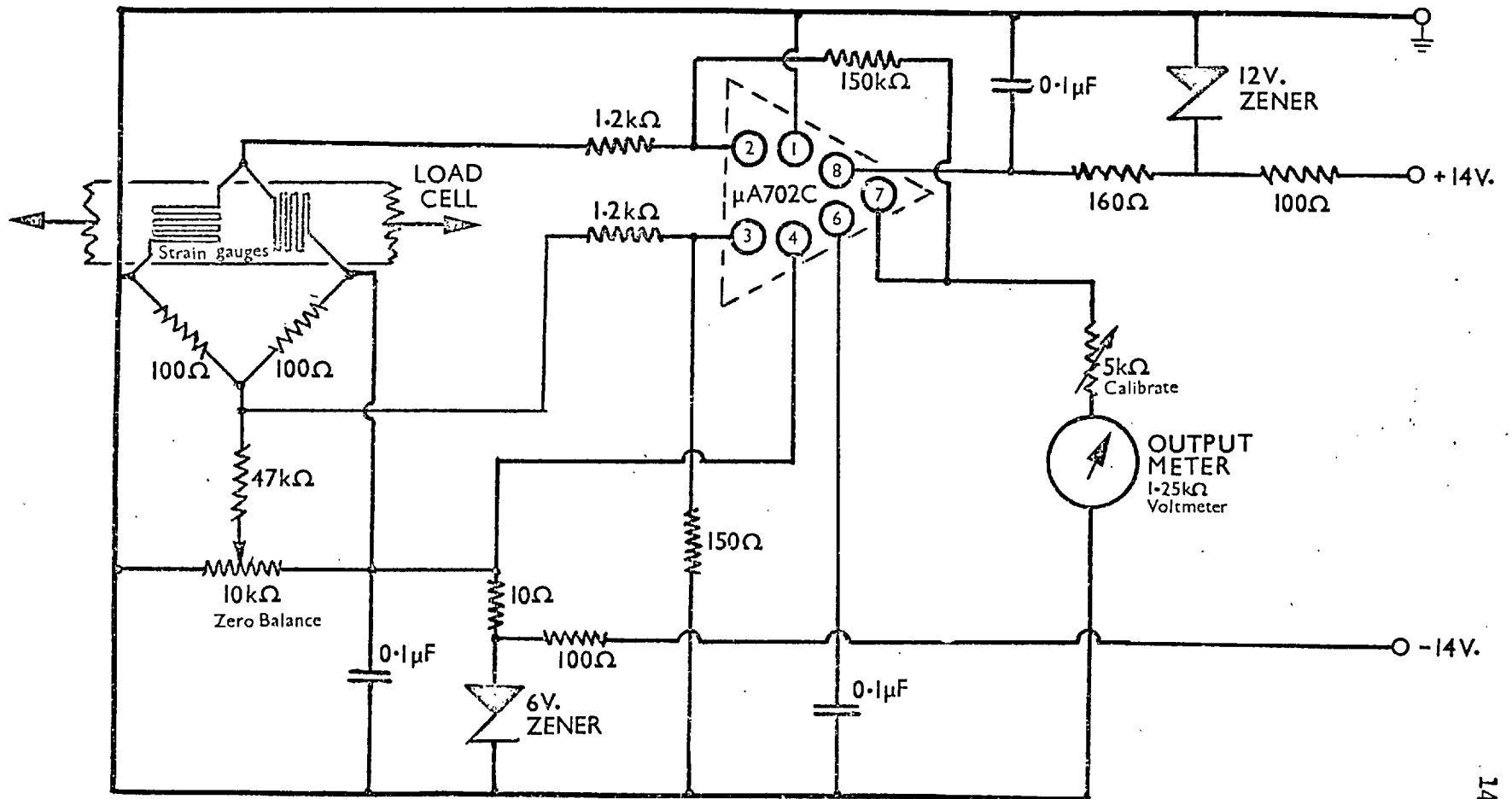
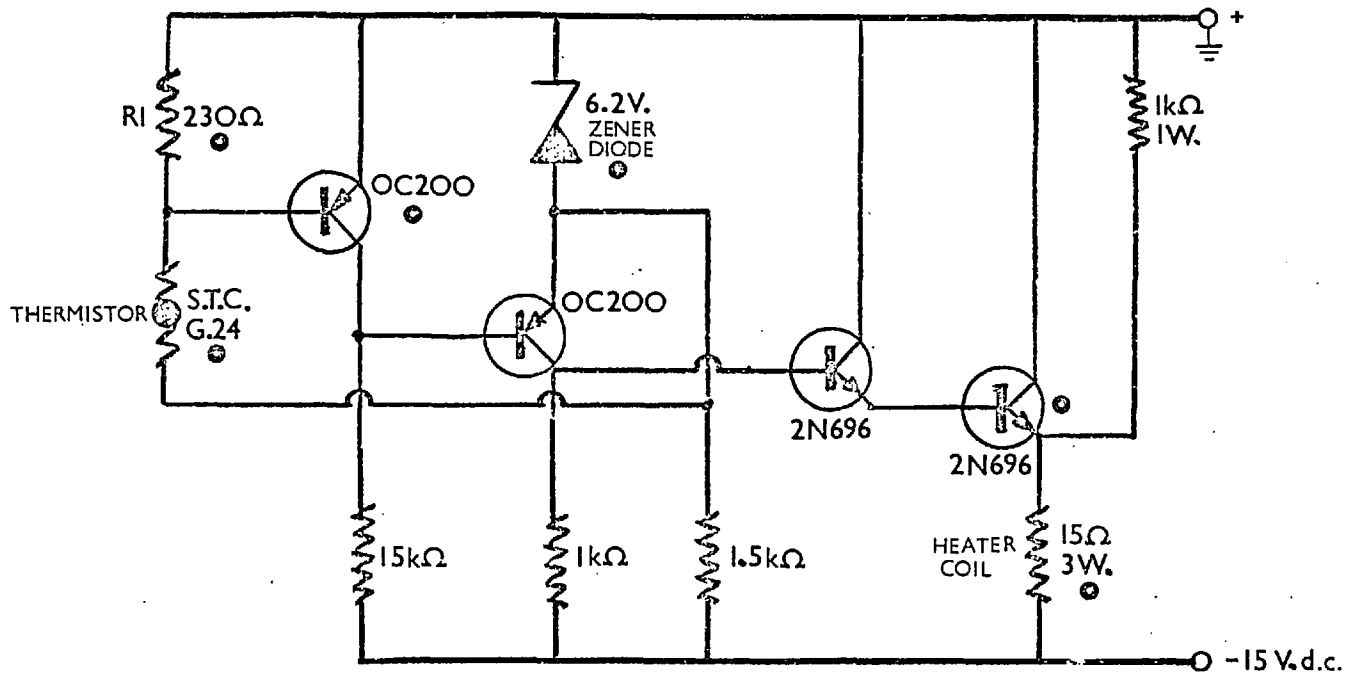


Fig. 28. - Dynamometer load cell circuit.

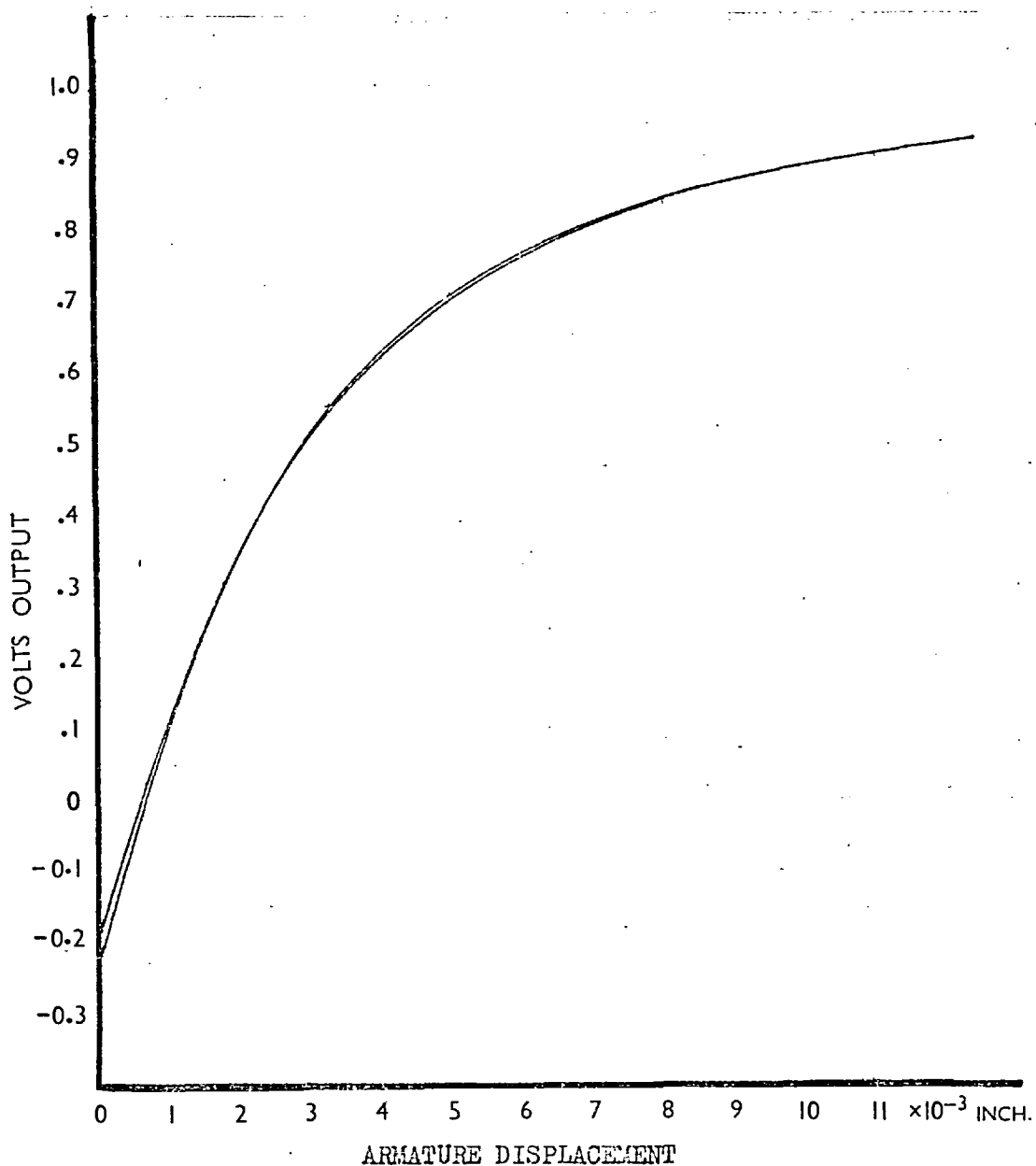


Resistor R1 presets the oven operating temperature, in this case to 58.0°C.

The 15 V. d.c. power supply is stabilised to better than $\pm 1\%$.

Components marked • are located within the controlled temperature block.

Fig. 29. - Thermocouple reference oven circuit.



Calibration curves of transducers DT1 and DT2.

Test conditions :

Carrier frequency - 50 kHz.

Armature material - segment of piston ring.

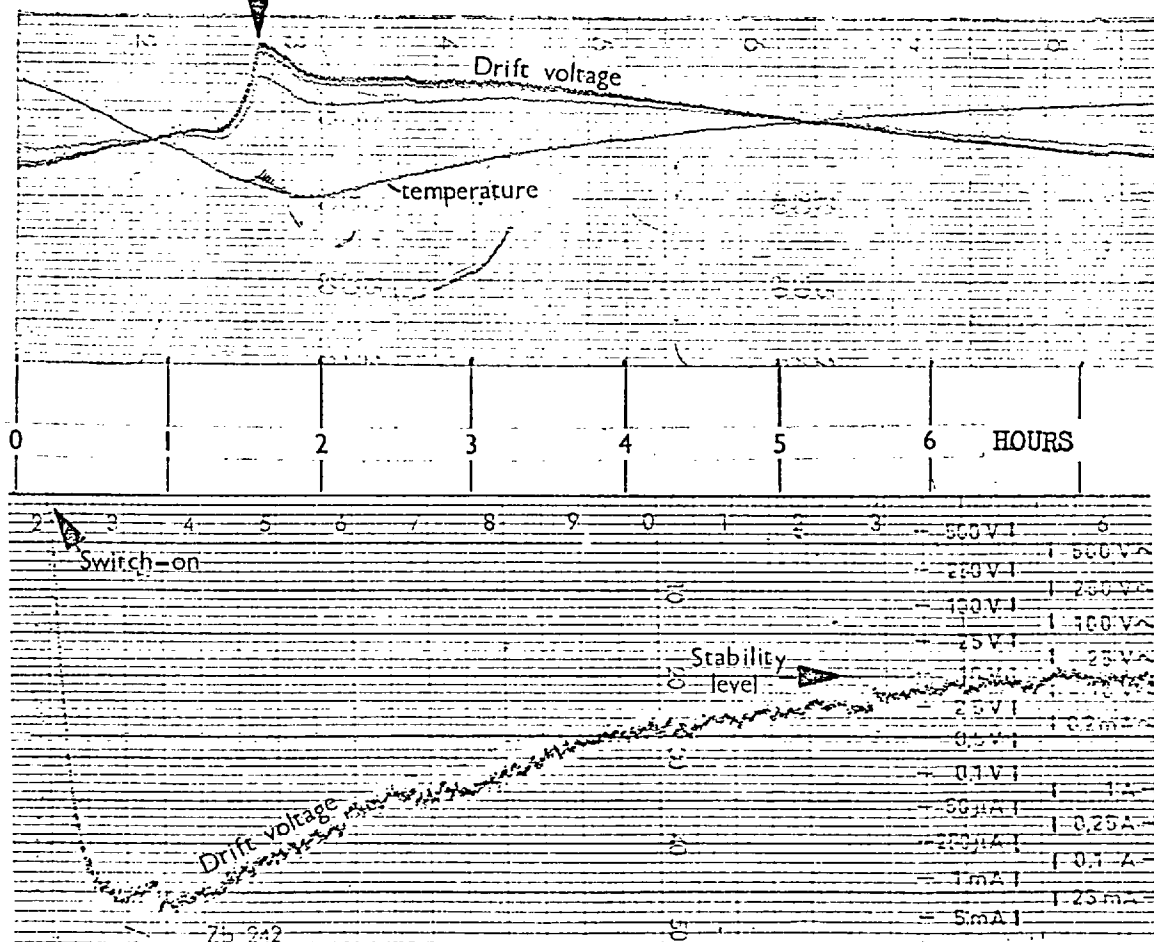
Calibration temperature - 20°C.

Fig. 30. - Typical calibration curves of A.E. vibration measuring system.

Thermal stability of transducers.

Test procedure - gradual heating of transducers with pre-set 0.005" gap in a silicon oil bath from ambient temperature to 148°C. over a period of 2 hours, followed by slow stirred cooling.

Maximum deviation of worst transducer = 2% of full output voltage.



Drift performance of transducers.

Test procedure - precision tracking of zero offset voltage from time of switching-on of electronics to time at which stability is achieved.

Peak drift (at one hour) = 0.26% of full output voltage.

Fig. 31. - Thermal and drift stability of A.E. measuring system.

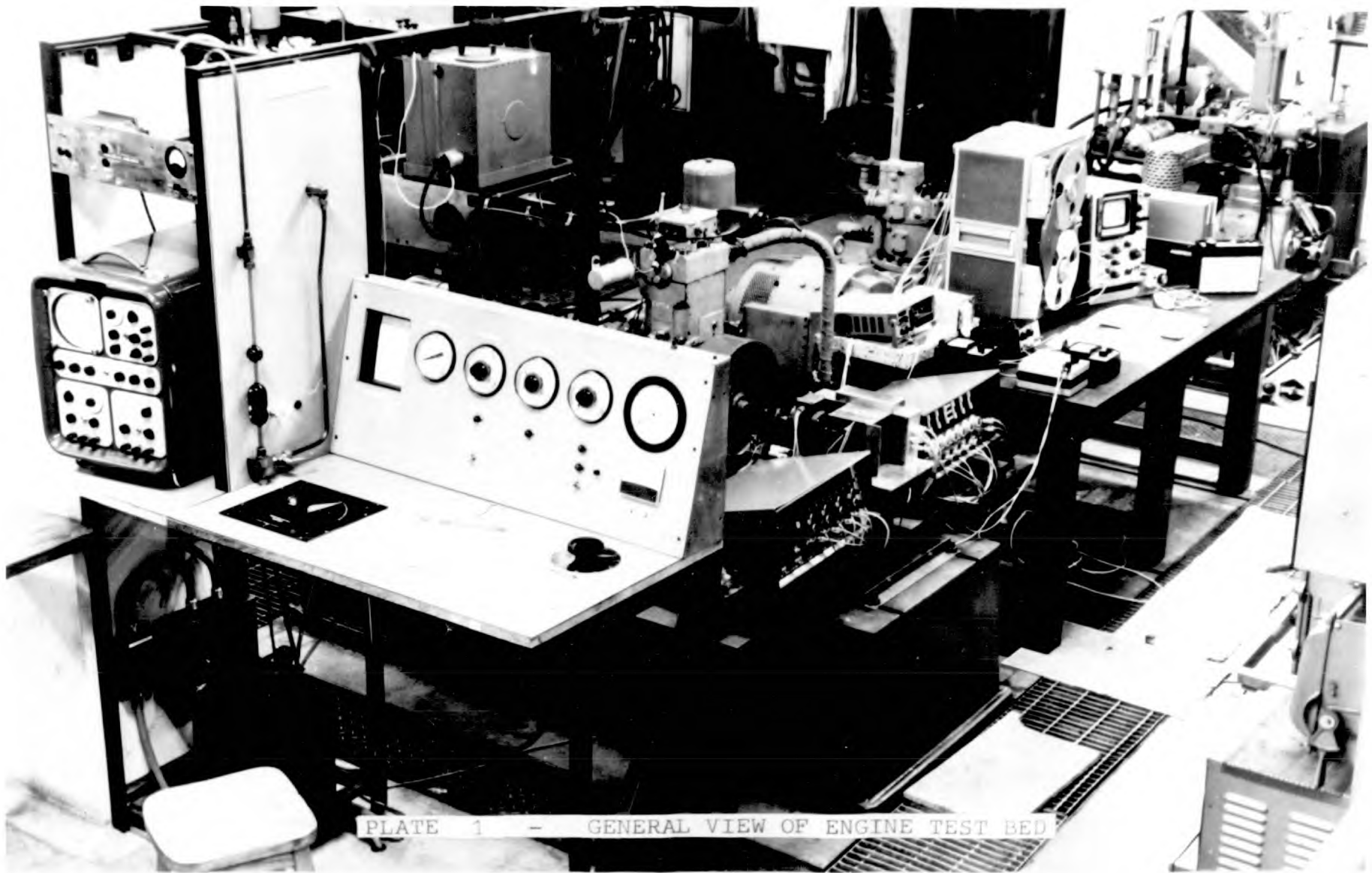


PLATE 1 - GENERAL VIEW OF ENGINE TEST BED

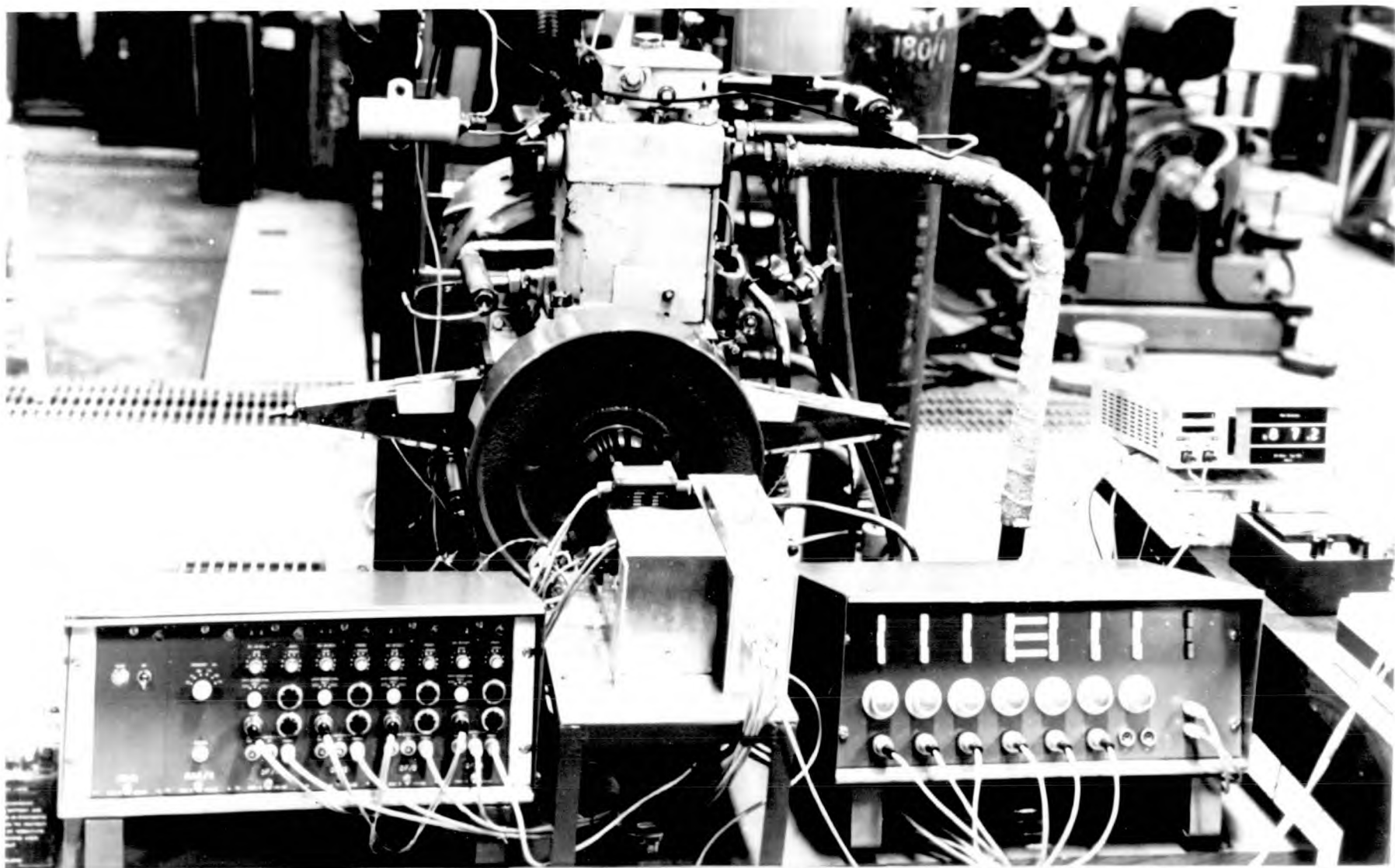


PLATE 2 - FRONT VIEW OF TEST BED SHOWING ROTARY SWITCHGEAR AND LINKAGE ATTACHEMENT BOXES

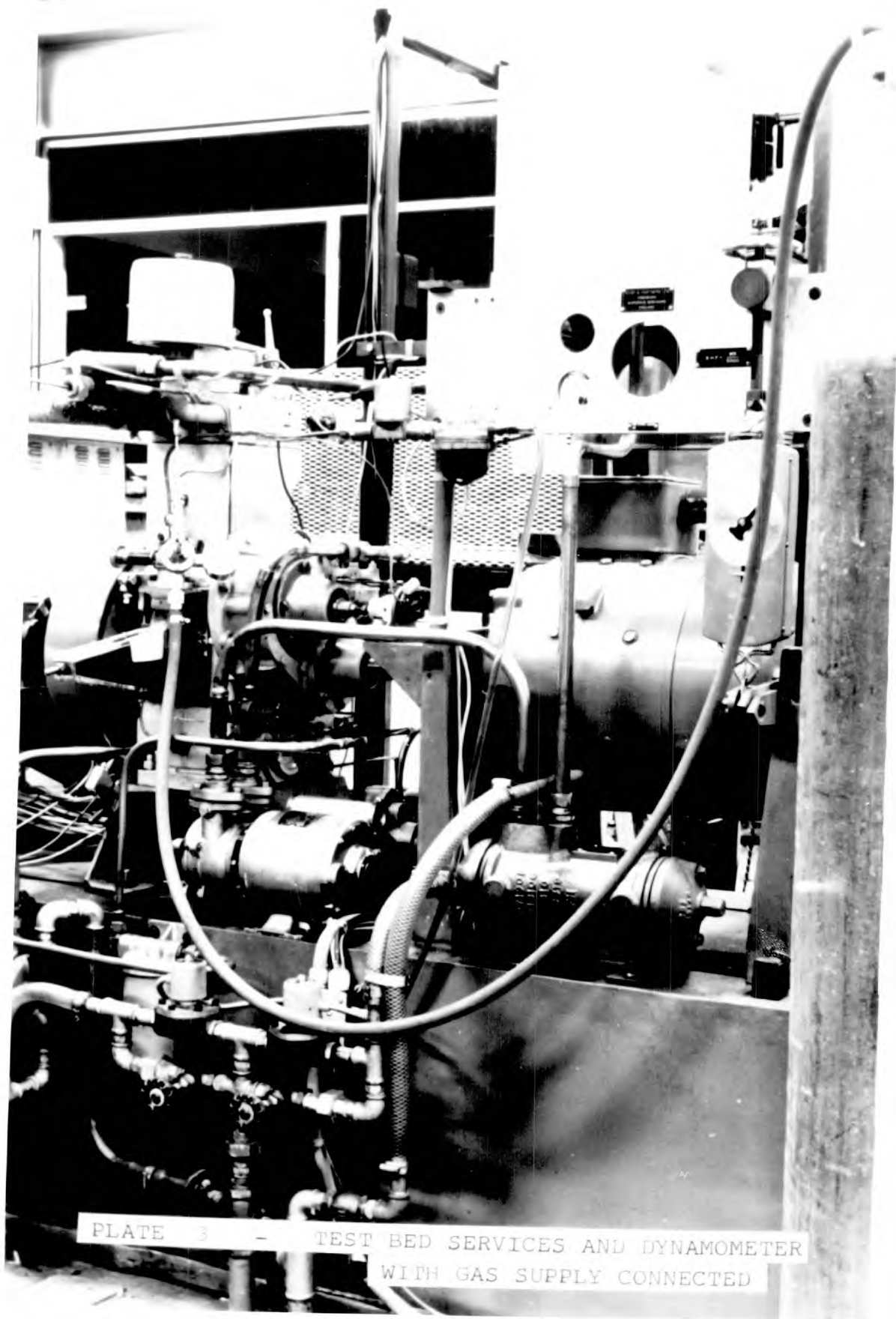


PLATE 3 - TEST BED SERVICES AND DYNAMOMETER
WITH GAS SUPPLY CONNECTED



PLATE 4 - INSTRUMENTATION & DATA RECORDING FACILITY.

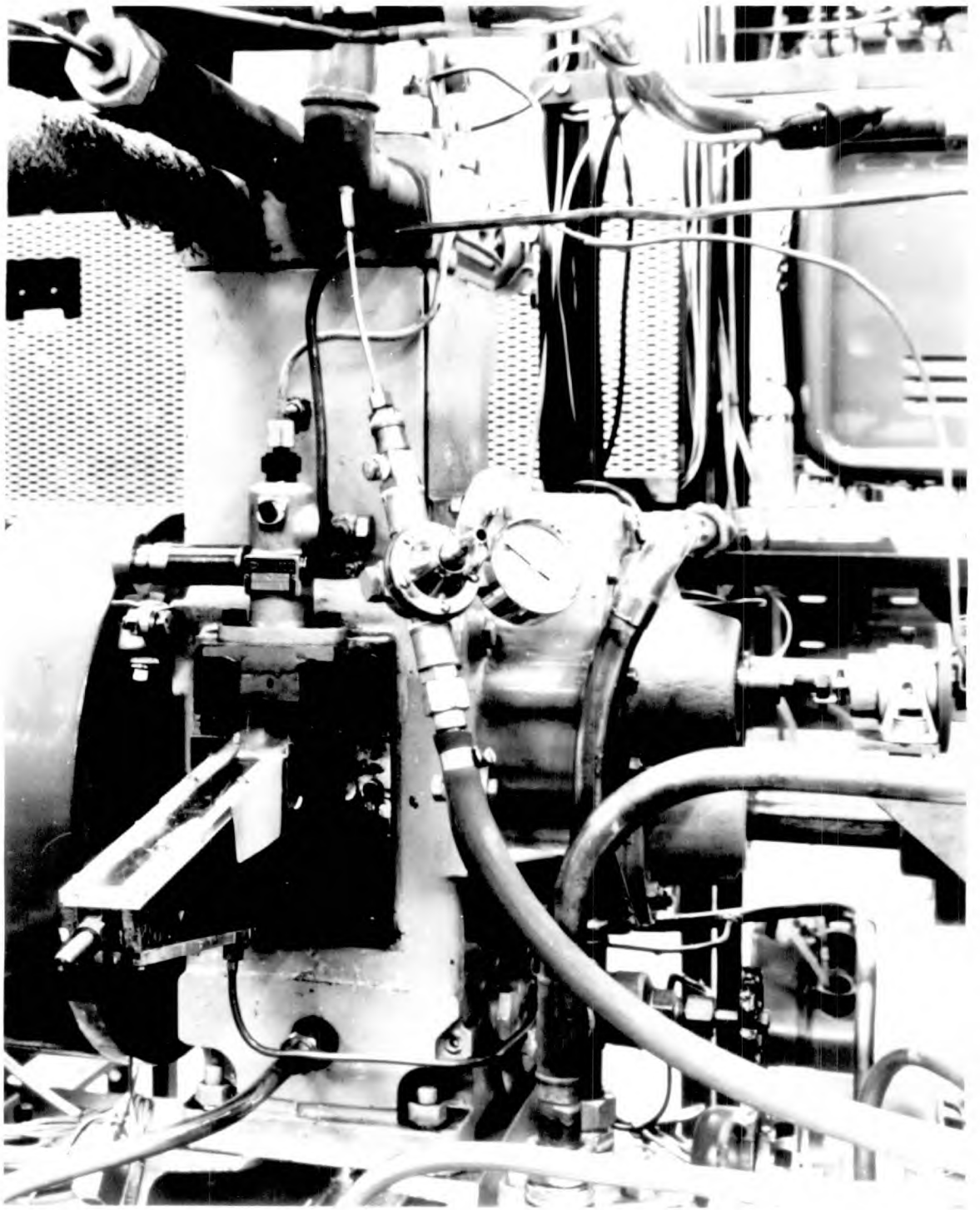


PLATE 5 — LINKAGE ATTACHMENT BOX , MODIFIED INJECTOR PUMP BRACKET ,
AND GAS SUPPLY REGULATOR .

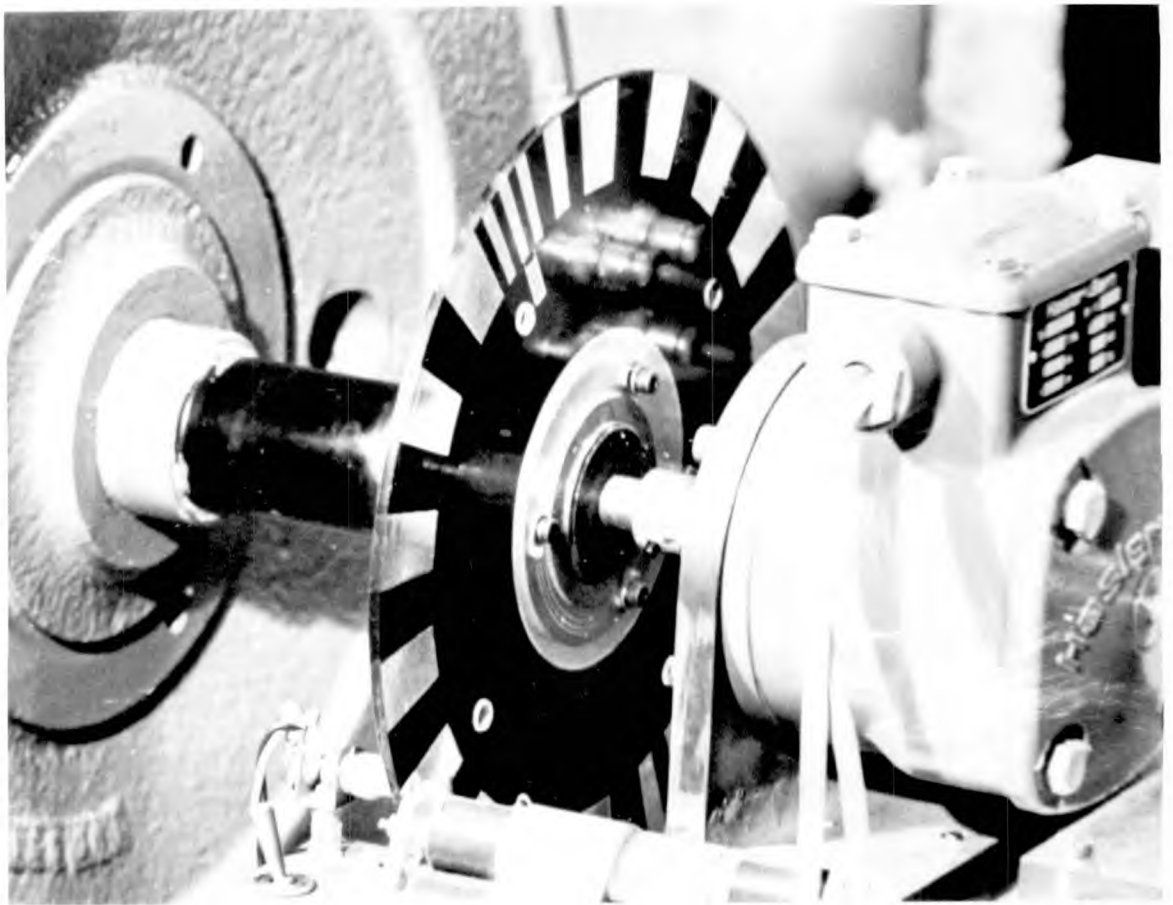
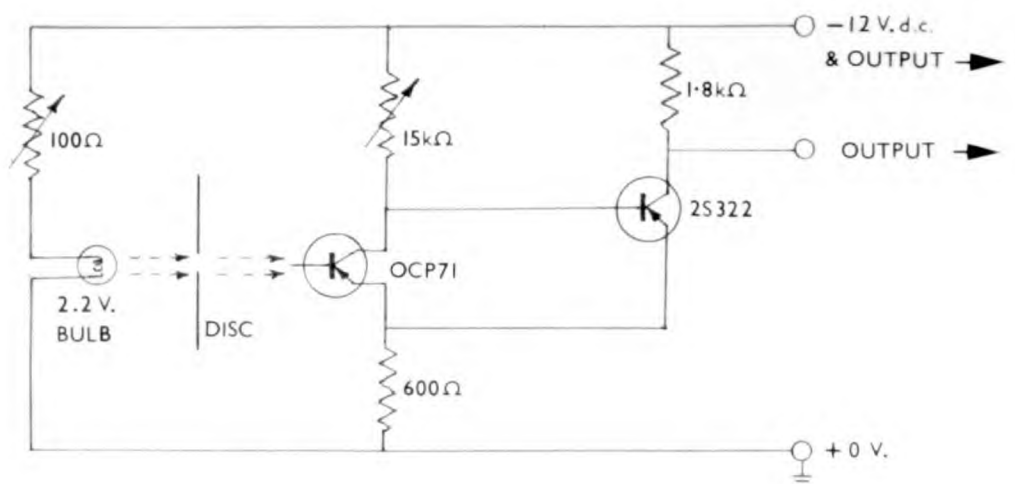


PLATE 6 — PHOTOELECTRIC DISC FOR CRANK-ANGLE DEGREE MARKER



PHOTOTRANSISTOR AND ILLUMINATION CIRCUITS

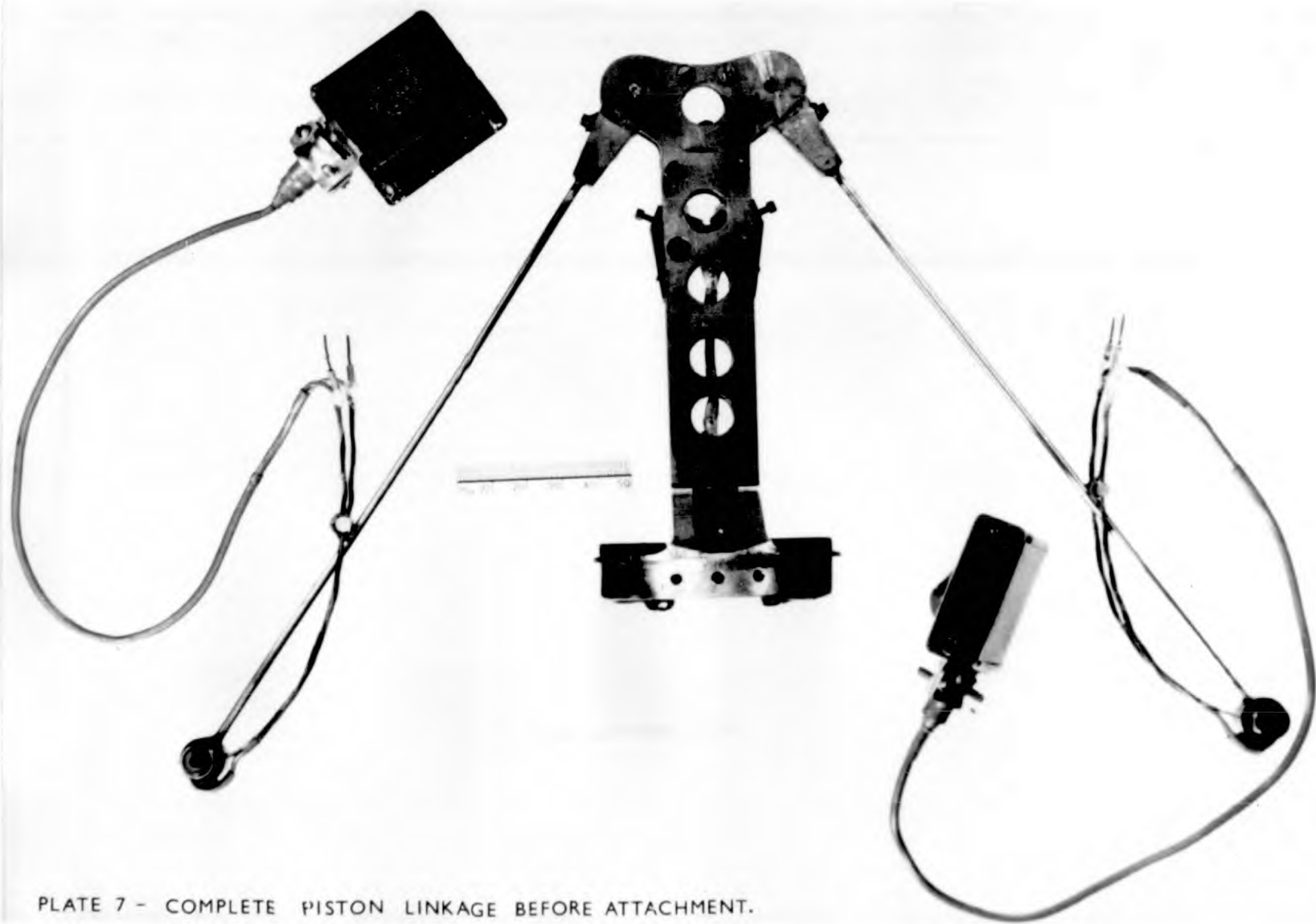


PLATE 7 - COMPLETE PISTON LINKAGE BEFORE ATTACHMENT.

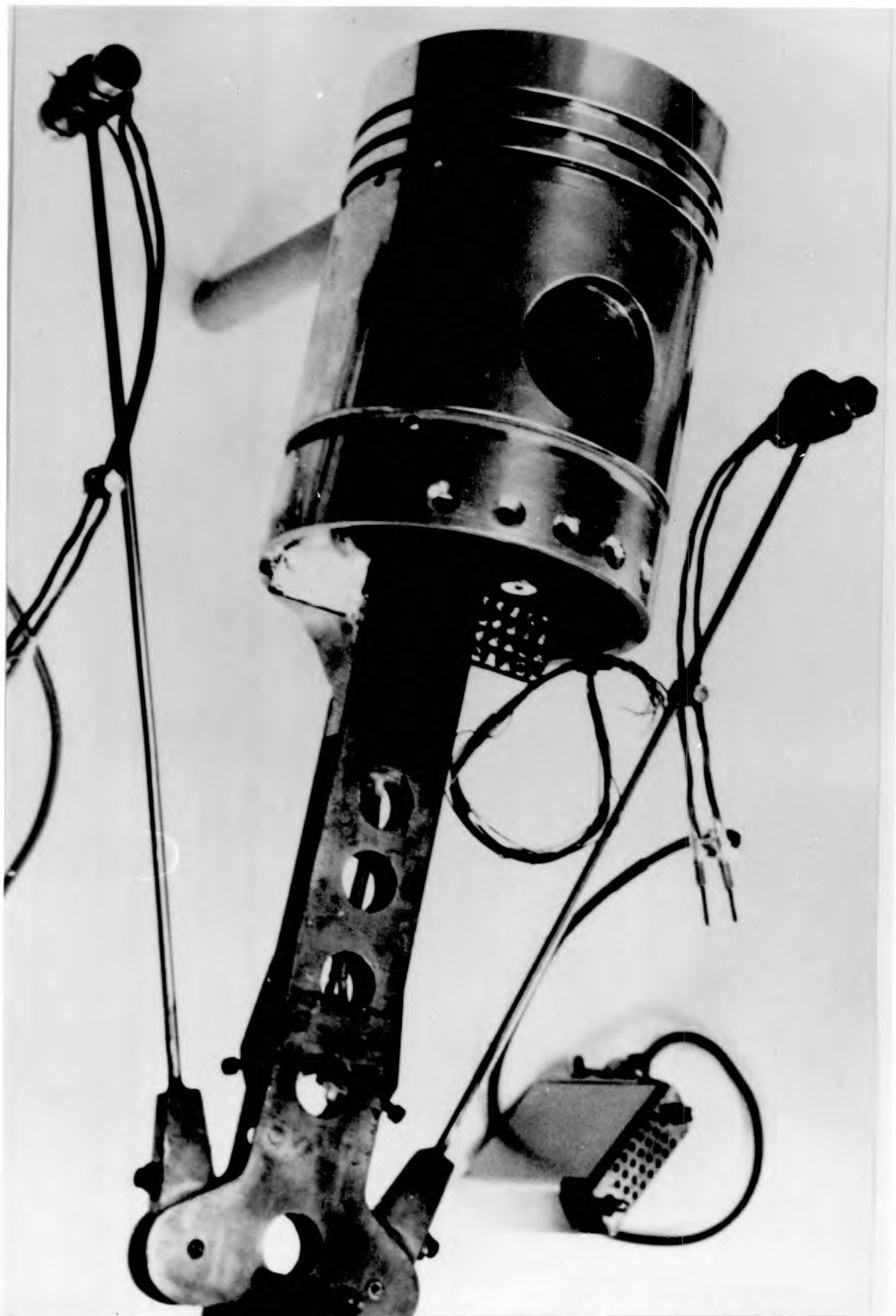


PLATE 8 - PARTIALLY WIRED PISTON AND LINKAGE
SHOWING ONE PATCHBOARD UNCOVERED

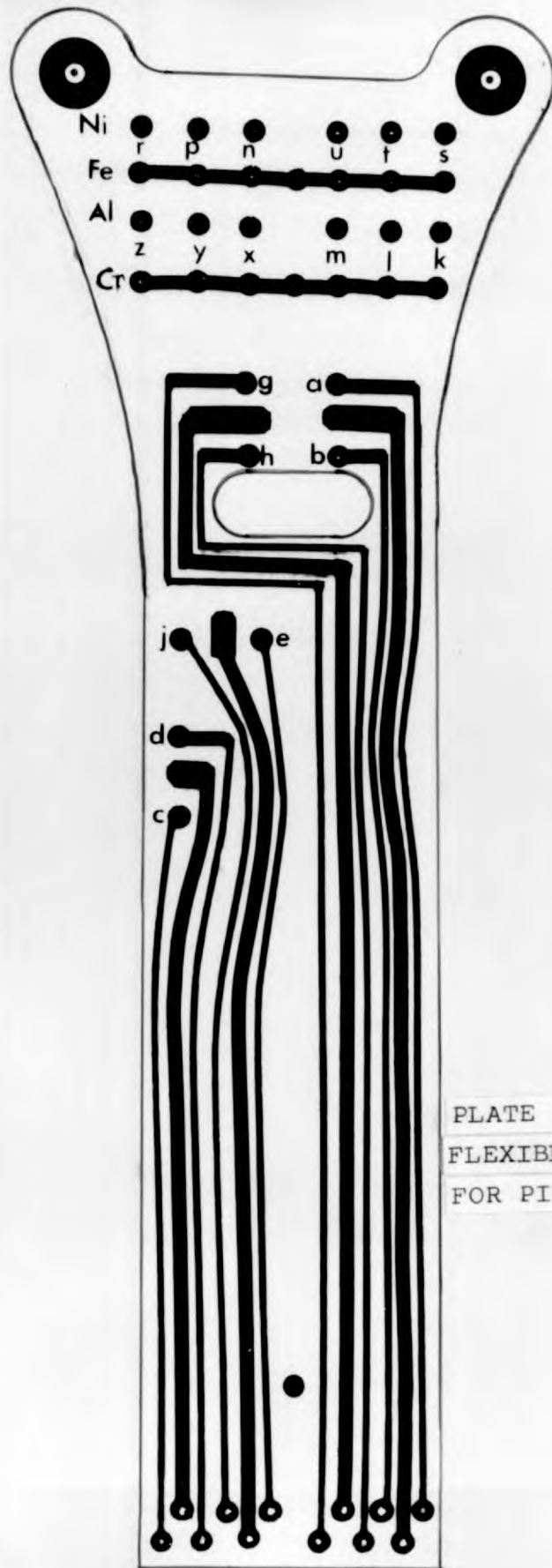
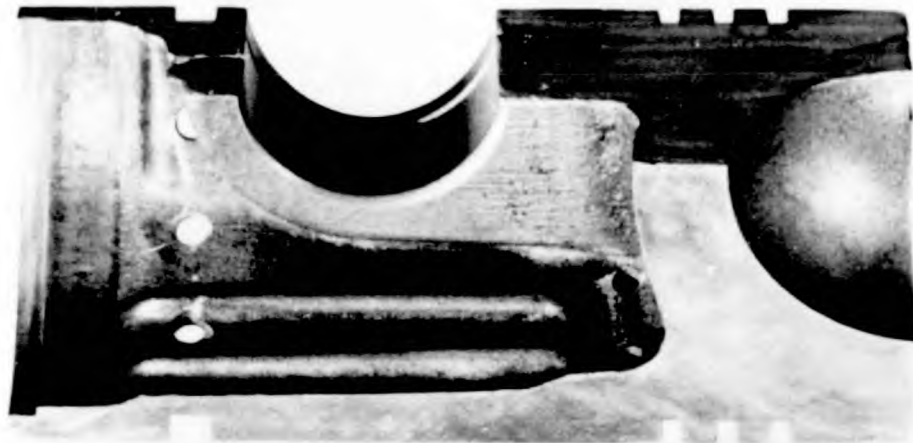


PLATE 9 -
FLEXIBLE PRINTED CIRCUIT
FOR PISTON WIRING



PLATE 10 - PARTIALLY WIRED PISTON WITH FLEXIBLE CIRCUIT AND SOME WIRING IN POSITION



Active



Compensating

PLATE 11 - DISPLACEMENT TRANSDUCERS SHOWN AGAINST SEGMENT OF PISTON

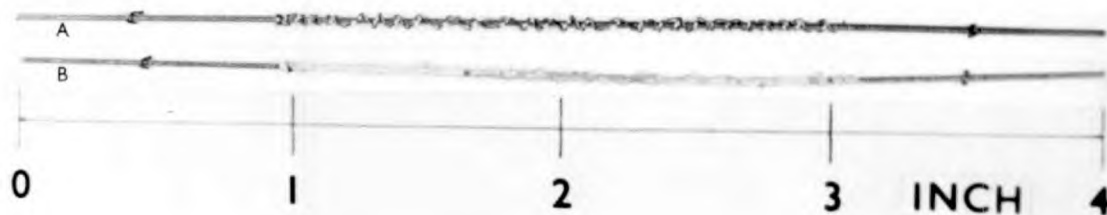
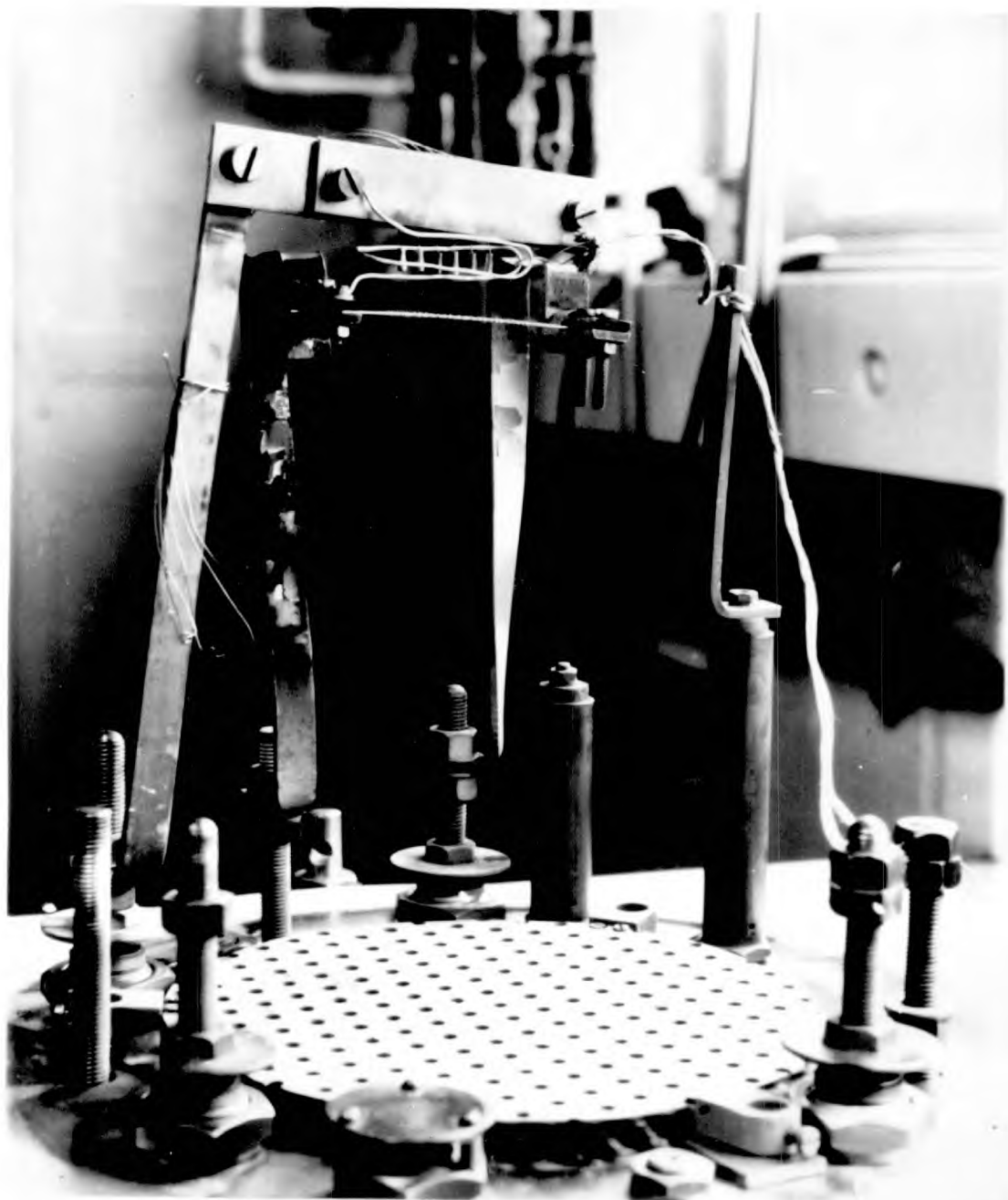


PLATE 12 — PLATING RIG FOR NICKEL COATING OF THIN-FILM THERMOCOUPLES.

A & B SHOW TYPICAL CHARGE-WIRES BEFORE AND AFTER THE EVAPORATION PROCESS.

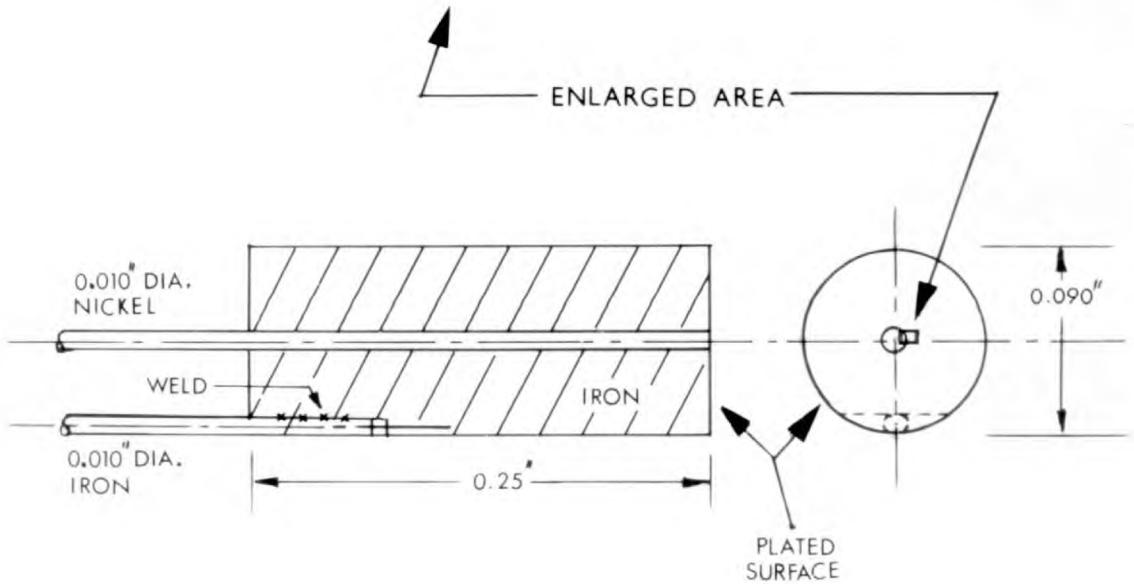
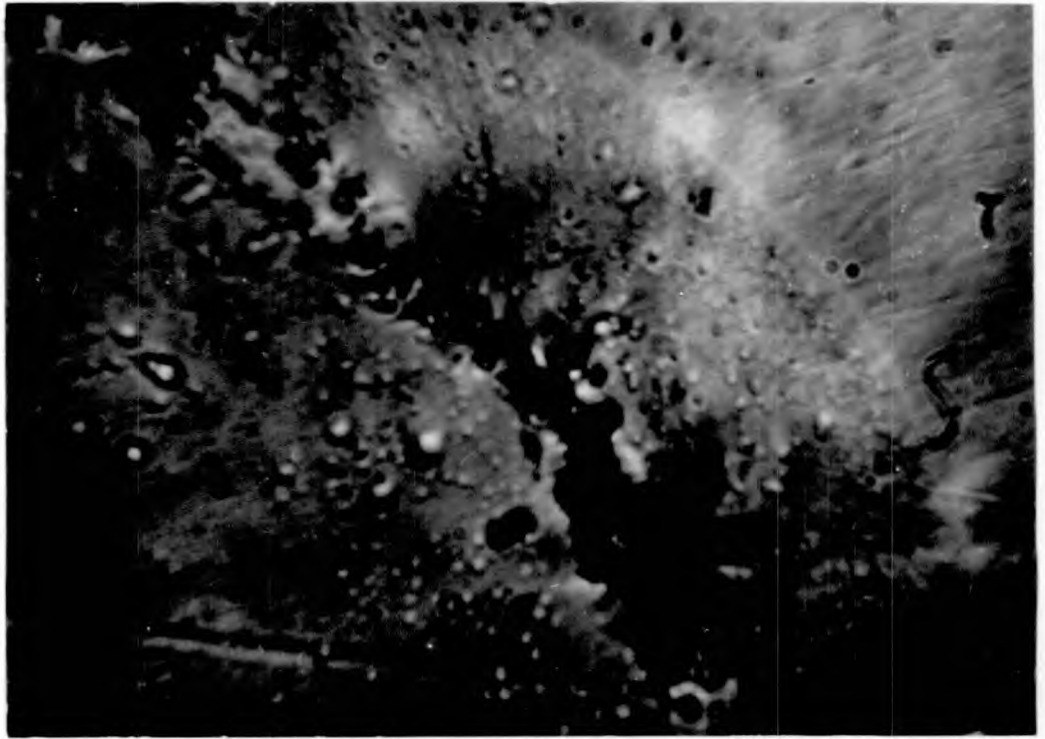
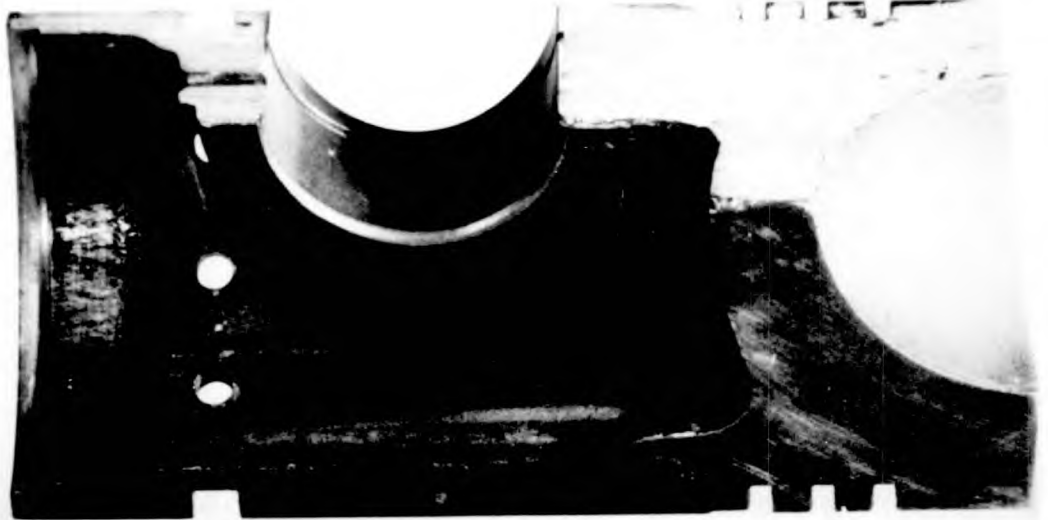
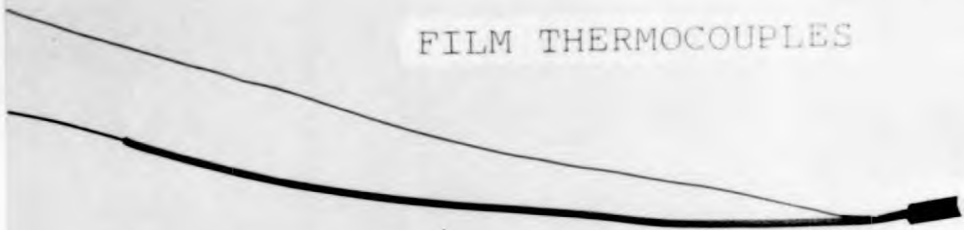


PLATE 13 - ENLARGEMENT OF NICKEL-COATED THERMOCOUPLE
FRONT SURFACE.



FILM THERMOCOUPLES



MINIATURE BEAD THERMOCOUPLES

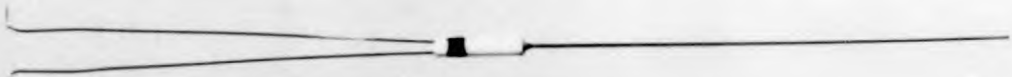


PLATE 14 - THIN-FILM AND BEAD THERMOCOUPLES
SHOWN AGAINST SEGMENT OF PISTON

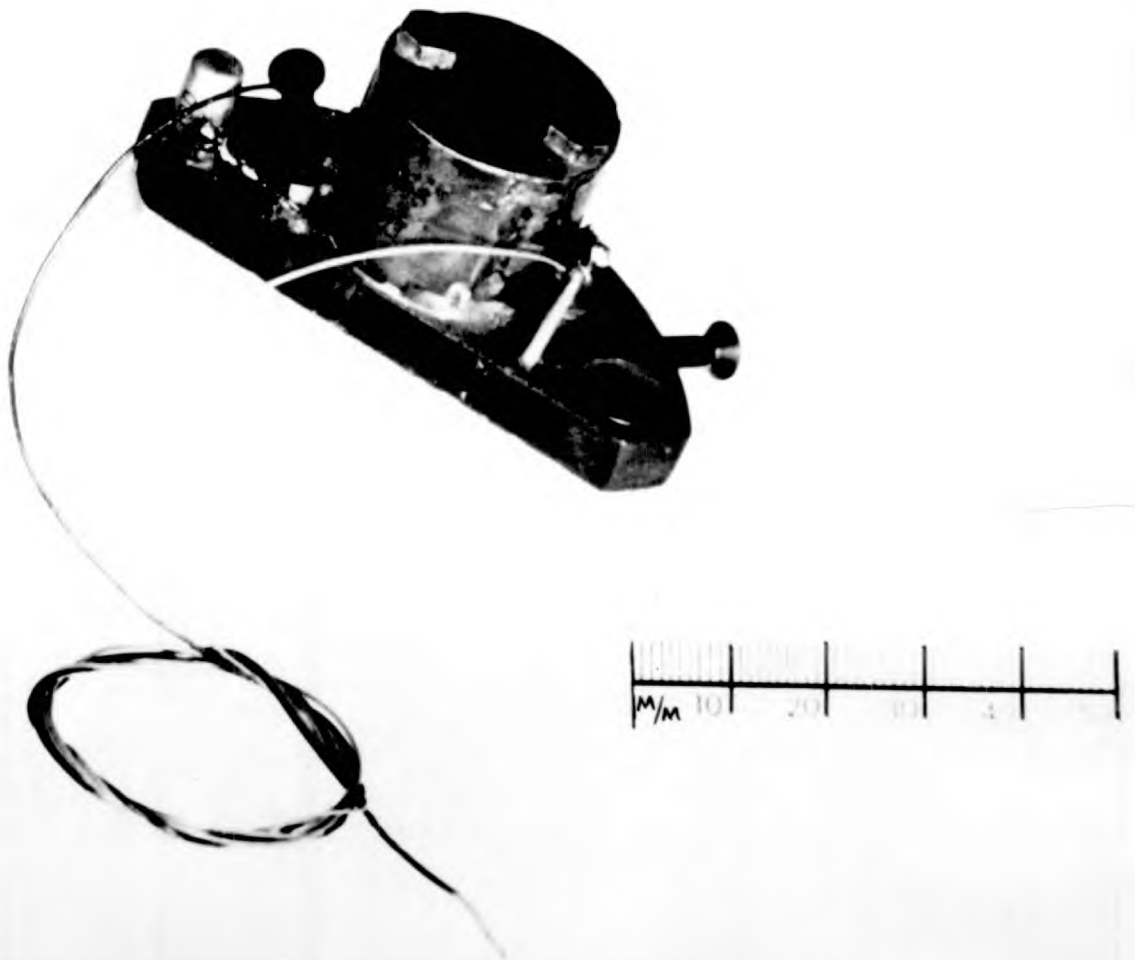
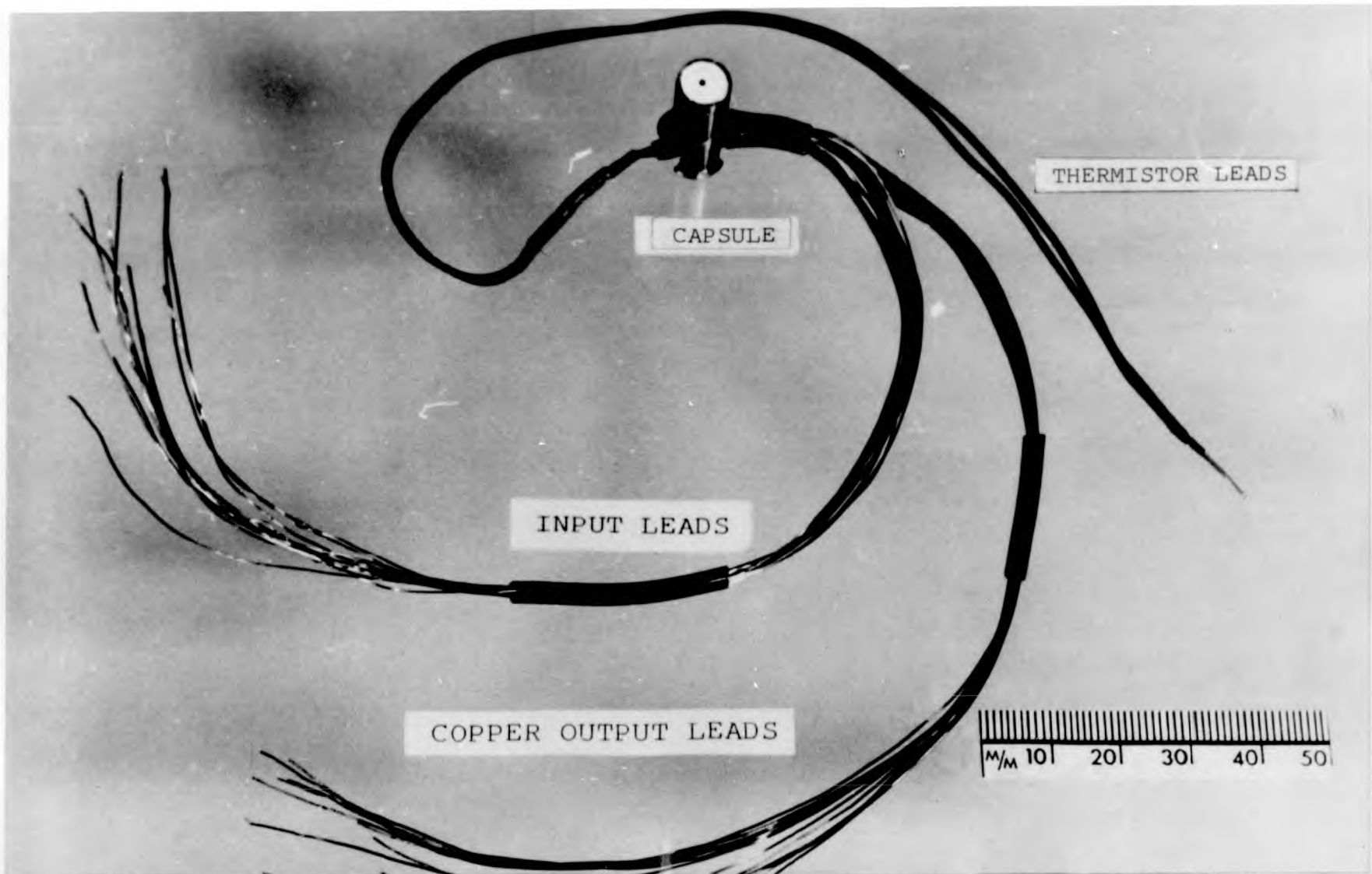


PLATE 15 - THERMOCOUPLE REFERENCE OVEN
BEFORE ASSEMBLY INTO POSITION



THERMISTOR LEADS

CAPSULE

INPUT LEADS

COPPER OUTPUT LEADS

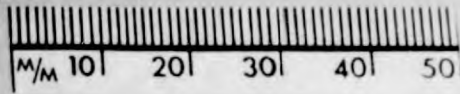


PLATE 16 - REFERENCE THERMOCOUPLE CAPSULE BEFORE ASSEMBLY INTO REFERENCE OVEN